AD_____

Award Number: DAMD17-02-1-0684

TITLE: Bone Sialoproteins and Breast Cancer Detection

PRINCIPAL INVESTIGATOR: Neal S. Fedarko, Ph.D.

CONTRACTING ORGANIZATION: Johns Hopkins University
Baltimore, MD 21205

REPORT DATE: July 2005

TYPE OF REPORT: Annual

PREPARED FOR: U.S. Army Medical Research and Materiel Command
Fort Detrick, Maryland 21702-5012

DISTRIBUTION STATEMENT: Approved for Public Release;
Distribution Unlimited

The views, opinions and/or findings contained in this report are those of the author(s) and should not be construed as an official Department of the Army position, policy or decision unless so designated by other documentation.

20060110 114

REPORT DOCUMENTATION PAGE

1. REPORT DATE	2. REPORT TYPE	3. DATES COVERED
01-07-2005	Annual	1 Jul 2004 – 30 Jun 2005

4. TITLE AND SUBTITLE

Bone Sialoproteins and Breast Cancer Detection

5a. CONTRACT NUMBER

5b. GRANT NUMBER
DAMD17-02-1-0684

5c. PROGRAM ELEMENT NUMBER

6. AUTHOR(S)

Neal S. Fedarko, Ph.D.

5d. PROJECT NUMBER

5e. TASK NUMBER

5f. WORK UNIT NUMBER

7. PERFORMING ORGANIZATION NAME(S) AND ADDRESS(ES)

Johns Hopkins University
Baltimore, MD 21205

8. PERFORMING ORGANIZATION REPORT NUMBER

9. SPONSORING / MONITORING AGENCY NAME(S) AND ADDRESS(ES)
U.S. Army Medical Research and Materiel Command
Fort Detrick, Maryland 21702-5012

10. SPONSOR/MONITOR'S ACRONYM(S)

11. SPONSOR/MONITOR'S REPORT NUMBER(S)

12. DISTRIBUTION / AVAILABILITY STATEMENT
Approved for Public Release; Distribution Unlimited

13. SUPPLEMENTARY NOTES

14. ABSTRACT

We have been studying a family of proteins that we have termed SIBLINGs for Small Integrin Binding LIgand N-linked Glycoproteins, that share similar structural domains, human chromosomal location, normal synthesis by skeletal tissue, and abnormal expression by neoplasms . The goal of our research is to test whether SIBLINGs might be informative markers for breast cancer detection. To accomplish this goal we have developed competitive enzyme-linked immunosorbent assays (ELISAs) for the SIBLINGs bone sialoprotein (BSP), osteopontin (OPN), dentin matrix protein-1 (DMP1), dentin sialophosphoprotein (DSPP) and matrix extracellular phosphoglycoprotein (MEPE). Sandwich-based ELISA assays have also been developed. When the competitive ELISAs were used to screen SIBLING protein levels, BSP and OPN exhibited the highest degree of sensitivity and specificity for the detection of breast cancer. Microarray analysis of normal and breast cancer-derived mRNA samples found a similar elevated levels of elevated SIBLING expression. Technical aspects of the immunoassays are being refined to improve throughput and reproducibility. These results suggest that SIBLINGs may have utility as serum-based markers for breast cancer detection.

15. SUBJECT TERMS
Biomarkers, immunoassay, detection, receiver operating, characteristics (ROC), sensitivity, specificity, detection

16. SECURITY CLASSIFICATION OF:			17. LIMITATION OF ABSTRACT	18. NUMBER OF PAGES	19a. NAME OF RESPONSIBLE PERSON
a. REPORT U	**b. ABSTRACT** U	**c. THIS PAGE** U	UU	56	19b. TELEPHONE NUMBER (include area code)

Table of Contents

Introduction

Tumor progression involves modulation of cell adhesion, differentiation, division, apoptosis, angiogenesis as well as migration and metastasis. We have been studying a gene family we term SIBLINGs (for Small Integrin-Binding Ligand N-linked Glycoproteins) that are induced by certain neoplasms. Members of the SIBLING family include bone sialoprotein (BSP), osteopontin (OPN), dentin matrix protein (DMP1), dentin sialophosphoprotein (DSPP), and matrix extracellular phosphoglycoprotein (MEPE). Our published work has shown that BSP and OPN are extended and flexible in solution (such lack of ordered structure is shared by a number proteins that have multiple binding partners) [1]. SIBLINGs can bind integrins including $\alpha_V\beta_3$ via their RGD sequence [2-4]. OPN and DMP1 can also bind CD44 (via an amino terminal domain) [5-7]. SIBLINGs can bind to complement Factor H and sequester it to the cell surface thereby regulating complement-mediated cell lysis [7, 8]. More recently we have shown that SIBLINGs can bind to and modulate the activity of specific MMPs [9]. It is our hypothesis that SIBLINGs promote breast cancer progression through neoplastic expression of SIBLINGs that bind to and modulate the activity of specific MMPs. MMPs play multiple roles in tumor progression including: angiogenesis; processing and presentation of certain growth factors; and metastasis. We further hypothesize that SIBLINGs are biologically plausible surrogate endpoint markers for cancer detection.

The goal of the current research is to develop SIBLINGs as serum measures for use in breast cancer detection, by determining the distribution of their serum levels in a breast cancer patient population before and after treatment, a large normal (cancer-free) population, and a patient population at risk for developing breast cancer. Serum levels of gene family members in normal and breast cancer patients will be used to establish the sensitivity, specificity and predictive value of these markers in breast cancer. In patients with defined breast cancer, serum levels will be correlated with stage, prognosis and response to treatment. This research will determine whether serum SIBLING levels have high sensitivity (low false negative rate) and high specificity (low false positive rate), can be analyzed in a general laboratory setting (does not require highly specialized procedures/equipment), and enable early detection.

Body

Overview:

As of the end of the third year of this grant, almost all Tasks have been completed. We have yet to be unblinded as to staging (TNM scores) and outcome data for the subjects from whom the serum samples were derived, hence Task 2c (analyzing for clinical correlation between serum SIBLING levels and cancer stage, prognosis, tumor burden and response to treatment) has not been completed. The refinement of the immunoassay methodology (Task 3 - migration to sandwich-based assays) has been expanded to include streamlining sample preparation/extraction (see below). A no cost extension was requested and granted to enable additional time and effort to be applied to completing Task 3 so that all data from the immunoassays (competitive and sandwich-based ELISAs) will be locked down prior to unblinding and completion of Task 2c. Three papers were published during the current reporting period and are included in the Appendix.

During the current reporting period and on the strength of data generated from our studies of SIBLING biology, the P.I. successfully applied for sponsored funding for a study examining potential racial differences in the SIBLING expression pattern in African American versus Caucasian women. The P.I. also successfully applied for funding from the Department of Defense to develop the SIBLING DSPP as a biomarker for prostate cancer progression.

Original Statement of Work:

The tasks outlined in the original Statement of Work for the first year were to:

Task 1. To complete development of competitive ELISA for the SIBLINGs DMP1 and MEPE (Months 1 – 6):
    a. Develop adenovirus expression vector for expressing recombinant human MEPE.
    b. Perform checkerboard assays to determine optimum antigen coating and antibody concentrations for MEPE and DMP1.
    c. Determine precision and yield of these new assays.

Task 2. To determine the distribution of serum SIBLING (BSP, OPN, DMP1 and MEPE) levels in serum obtained from normal donors and breast cancer patients (Months 7 - 24).
    a. Measure BSP, OPN, DMP1 and MEPE in a normal population, breast cancer patients and a population at risk for breast cancer.
    b. Determine sensitivity and specificity and perform ROC analysis.
    c. Test for clinical correlation between serum SIBLING levels and cancer stage, prognosis, tumor burden and response to treatment.

Task 3. To refine the existing competitive ELISA assay systems to more rapid sandwich-based assay systems and verify previous results (Months 24 – 36).
    a. Screen monoclonal antibodies for utility in OPN, DMP1 and MEPE assays.
    b. Employ checkerboard assays to define optimum capture antibody coating, second antibody concentration and incubation time.
    c. Re-analyze normal and breast cancer patient sera using the new sandwich based assays.

Progress:

In the previous annual report we gave the results of the competitive assays for BSP, OPN, DMP1 and DSPP in large number of serum samples from normal and breast cancer subjects. Intrinsic to our study design is that the laboratory is blinded to staging data on the subjects from whom the breast cancer serum samples were drawn. The plan is to complete the "refined" immunoassay measures (sandwich ELISAs as well as alternative sample preparation/extraction), "lock down" the raw data and results and only then will the study be unblinded in terms of staging, and the association of SIBLING levels and tumor stage assessed.

A number of issues arose in the past year concerning the current immunoassays. One issue is that stability tests over the past year revealed a change occurred in microtiter plate chemistries. We have had to switch microtiter plate manufacturer's (from Greiner Bio-One high binding plates to Costar ELISA/RIA high binding plates. This was necessitated by a change in Greiner's manufacturing process that altered the surface charge/properties of their plates that adversely effected SIBLING protein binding. We re-screened a number of manufacturer's 96

well plates to obtain binding profiles and standard curves closes to those obtained with the "old" plates.

A second issue arises from the nature of the serum sample preparation prior to the immunoassay. Because SIBLINGs are bound in blood/serum/plasma to complement Factor H (very abundant at ~ 0.5 mg/ml), to detect the SIBLINGs we need to disrupt the complex. The complex is disrupted through a combination of chaotropic agents, heating and reduction so that sample clean-up prior to the immunoassay is required. We have been investigating alternative methods of sample preparation and clean-up for their yield and speed (the current standard method uses dithiothreitol reduction in a chaotropic buffer followed by strong anion exchange chromatography to remove reducing agent and chaotropic buffer. We have been developing an alternative method of disruption of the SIBLING serum complex. This method involves displacement of the SIBLING through the preteatment of serum with a buffer containing sialic acid and mucin. The advantage of such an approach is that after a brief pretreatment, the serum can be taken directly to either the competitive ELISA or the sandwich-based assay.

Summary of Research

During the course of developing and testing the immunoassay for the SIBLING MEPE, novel observation were made on its levels, distribution as well as physiological correlations. In the paper by Jain et al. (Appendix I, [10]), we have shown that a) significant levels of MEPE in the serum of normal humans can be measured, (b) a clear age-related decrease in serum MEPE levels, (c) a positive correlation between MEPE and phosphorus, a inverse correlation with parathyroid hormone, and (d) a significant positive correlation with total hip and neck bone mineral density. While this study demonstrates the association of serum MEPE levels with serum phosphate, PTH and bone mineral density, it does not address causality. In the very least, the results suggest that MEPE may be an interesting marker of normal human bone and mineral metabolism.

Given what we now know about SIBLING and MMP biology, experiments were designed to address whether biologically and physiologically relevant complexes of SIBLING + MMP + cell surface receptor could be measured (Appendix II, [11]). Studies were performed to demonstrate that BSP interacted with MMP-2 and cell-surface integrin $\alpha_v\beta_3$ to form a trimolecular complex as shown by immunoprecipitation, flow cytometry, and *in situ* hybridization. Enhanced invasiveness of breast cancer cells by BSP addition was shown to require $\alpha_v\beta_3$ and MMP-2 and the formation of the trimolecular complex at the membrane surface [11].

The expression levels of five SIBLING gene family members – BSP, OPN, DMP1, MEPE, and DSPP as well as certain MMPs were determined using cancer profiling arrays containing normalized cDNA from both tumor and corresponding normal tissues from 241 individual patients representing 9 distinct cancer types (Appendix III, [12]). Significantly elevated expression levels were observed for BSP in cancer of the breast, colon, stomach, rectum, thyroid and kidney; OPN in cancer of the breast, uterus, colon, ovary, lung, rectum, and thyroid; DMP1 in cancer of the breast, uterus, colon and lung; DSPP in breast and lung cancer. The degree of correlation between a SIBLING and its partner MMP was found to be significant within a given cancer type (e.g. BSP and MMP-2 in colon cancer, OPN and MMP-3 in ovarian cancer; DMP1 and MMP-9 in lung cancer). The expression levels of SIBLINGs were distinct

within subtypes of cancer (e.g. breast ductal tumors compared to lobular tumors). SIBLING expression increased with cancer stage for breast, colon, lung and rectal cancer [12].

The biological and biochemical consequences of SIBLING modulation of MMP activity were investigated by measuring the effect of BSP on the inhibition kinetics of MMP-2 by TIMP2 or by a small molecular weight inhibitor illomastat (Appendix IV, [13]). In this study, the hypothesis that BSP acts biologically to lessen the effectiveness of MMP inhibitors was investigated. Solution and solid phase binding assays were carried out demonstrating that binding between recombinant BSP and latent as well as active MMP-2 does not require the hemopexin domain. BSP binding restored activity to hemopexin-deleted MMP-2 inhibited by tissue inhibitor of matrix metalloproteinase-2 (TIMP2) when activity was measured using both natural, large macromolecular substrates and synthetic, small molecular weight, freely diffusable substrates. BSP effects on TIMP2 inhibition of wild type active MMP-2 were quantified by varying small molecular weight substrate concentrations at different fixed inhibitor concentrations, and solving a general linear mixed inhibition rate equation with a global curve fitting program. The results indicate an ~ 20-fold increase in the competitive inhibition constant and an ~ 10-fold increase in uncompetitive inhibition constant for the MMP-2+BSP complex. To address whether the failure of clinical trials of MMP inhibitors may be explained at least in part by the activity of BSP, the effect of BSP binding to MMP-2 on inhibition by a small molecular weight drug (illomastat) was similarly determined. An over 10-fold increase in K_I was observed [13].

The ability of BSP to modulate MMP inhibitor action in an *in vitro* angiogenesis model system was tested. The *in vitro* model of angiogenesis utilized human umbilical vein endothelial cells (HUVECs) co-cultured with normal adult human diploid dermal fibroblasts. The endothelial cells form small islands amongst the fibroblasts, proliferate, and migrate through the co-culture matrix to form thread-like tubule structures. These cord-like structures join up to form a network of anastomosing tubules. These linked tubules produce endothelial cell-specific components such as PECAM-1 (CD31) that can be stained immunohistochemically and quantified. When human umbilical vein endothelial cells were treated with either nM TIMP2 or illomastat, the degree of tubule formation was reduced while the addition of equimolar BSP restored vessel formation. [13]. The observed effects of BSP (stimulating basal tubule formation and restoring formation to TIMP2- or illomastat-inhibited cultures) was consistent with BSP modulating MMP-2 activity. Profiling MMP-2 levels and activity in the *in vitro* system (by zymography and fluorescent substrate assays) demonstrated changes with BSP treatment. Thus, BSP has biochemical and biological plausibility to be playing an active role in tumor progression *in vivo*. BSP is induced by multiple neoplasms *in vivo* and its modulation of MMP inhibition might contribute to the relative lack of efficacy seen in the recent clinical trials of MMP inhibitors in numerous cancers [13].

Key Research Accomplishments

- Assay Development:

  - Competitive ELISAs
    - ✓ implemented for BSP, OPN, DMP1, DSPP and MEPE.

  - Indirect sandwich-based ELISAs
    - ✓ implemented for BSP, OPN, DMP1, and DSPP.

  - Alternative serum processing
    - ✓ Replacing sample reduction & column chromatography with "displacement reagent" treatment of serum.

- Assay Application:

  - Competitive ELISAs of normal and breast cancer sera completed

- Submitted Manuscripts

  - Jain, A., Fisher, L.W. and N.S. Fedarko. (2005) Bone Sialoprotein Binding To Matrix Metalloproteinase-2 Alters Enzyme Inhibition Kinetics. J. Biol. Chem.

- Meeting Abstracts

  - Jain, A., Fisher, L.W. and N.S. Fedarko Small Integrin Binding Ligand N-Linked Glycoproteins (SIBLINGs) Bind and Activate Matrix Metalloproteinases. Era of Hope 2005 Department of Defense Breast Cancer Research Program Meeting. June 9th, 2005, Philadelphia, PA (Appendix V)

  - Jain, A., Fisher, L.W. and N.S. Fedarko. Small Integrin Binding Ligand N-Linked Glycoprotein (SIBLING) Gene Family Expression In Breast Cancer. Era of Hope 2005 Department of Defense Breast Cancer Research Program Meeting. June9[th], 2005, Philadelphia, PA (Appendix VI)

  - Fedarko, N.S., Fisher, L.W. and A. Jain. Small Integrin Binding Ligand N-Linked Glycoproteins Modulate Matrix Metalloproteinases and Angiogenesis. Era of Hope 2005 Department of Defense Breast Cancer Research Program Meeting. June 9th, 2005, Philadelphia, PA (Appendix VII)

Reportable Outcomes

- Publications

    ➢ Jain, A., Fedarko, N.S., Collins, M.T., Gelman, R., Ankrom, M.A., Tayback, M., and L.W. Fisher. (2004) Serum levels of matrix extracellular phosphoglycoprotein (MEPE) in normal humans correlate with serum phosphorus, parathyroid hormone and bone mineral density. J. Clin. Endo. Metab.89(8):4158-4161.

    ➢ Karadag, A., Ogburke K.U.E. , Fedarko, N.S., and L.W. Fisher. (2004) Bone sialoprotein promotes invasion by osteotropic cancer cells in vitro by bridging MMP-2 to $\alpha V\beta 3$ integrin. J. Natl. Cancer Inst. 96:956-965.

    ➢ Fisher, L.W., Jain, A., Tayback, M., and N.S. Fedarko. (2004) Small Integrin Binding Ligand N-Linked Glycoprotein (SIBLING) gene family expression in different cancers. Clin. Cancer Res. 10(24): 10:8501-8511.

- Invited Presentations:

    ➢ "The SIBLING gene family promotes tumor progression." 2004-2005 Johns Hopkins University Oncology Translational Research Conference, November 3rd, 2004, Baltimore, MD.

    ➢ "SIBLING modulation of matrix metalloproteinases and tumor progression." 2nd National Meeting of the American Society for Matrix Biology. November 12, 2004, San Diego, CA.

    ➢ "What do bone proteins have to do with tumor progression?" The Sidney Kimmel Comprehensive Cancer Center At Johns Hopkins Longrifles Seminar Series, March 2nd, 2005, Baltimore MD.

- Funding Applied For

    ➢ NCI, NIH 1 R01 CA113865. "Small integrin-binding proteins and tumor progression."

- Funding Received

    ➢ Howard/Hopkins Partnership in Cancer ,NCI Minority Institution/Cancer Center Partnership, "Molecular Analysis of Co-Expression of Matrix Metalloproteinases and SIBLINGs in African American –vs- Caucasian Women."
    Agnes A. Day, Ph. D. (Howard University P.I.) & Neal S. Fedarko, Ph. D. (Johns Hopkins University P.I.)

    ➢ DOD/CDMRP. HSRRB No. a-13026 (Proposal No. PC040013), "Prostate Cancer Progression and Serum SIBLING (Small Integrin Binding N-linked Glycoprotein) Levels."

Conclusions

Summary. The development of competitive ELISAs and sandwich-based ELISAs to measure serum levels of SIBLING gene family members has been a necessary requirement in order to evaluate the utility of these potential markers in breast cancer detection. These assays have been developed and implemented. As reported previously, serum levels of SIBLINGs were found to be elevated in most breast cancer subjects. The final refinement of the assay system (improving sample processing/disrupting the SIBLING-Factor H complex in serum) and reanalysis of samples by ELISA will be completed by early Fall of 2005, enabling the completion of the statistical analysis and clinical correlation between serum SIBLING levels and cancer stage, prognosis, tumor burden and response to treatment.

What we will have learned. There currently does not exist a serum marker that can be used to detect breast cancer at an early stage. Because of evolving knowledge concerning both the biological actions of SIBLINGs (modulating MMPs) and their serum levels and tumor tissue expression, members of the SIBLING gene family hold promise as biomarkers for early cancer detection. The completion of the research described in this progress report and in the original grant application will enable the utility of these breast cancer biomarkers to be defined. Once completed, the groundwork will be laid for subsequent clinical trials of these biomarkers. A further byproduct of the research conducted so far, is an expansion of our understanding of the basic biology involved in tumor progression, identification of novel alternative methods of MMP activation and of potential pathways for therapeutic intervention.

References

1. Fisher, L.W., Torchia, D.A., Fohr, B., Young, M.F., and Fedarko, N.S., *The solution structures of two SIBLING proteins, bone sialoprotein and osteopontin, by NMR.* Biochem. Bophys. Res. Comm., 2001. 280: p. 460-465.

2. Wu, Y., Denhardt, D.T., and Rittling, S.R., *Osteopontin is required for full expression of the transformed phenotype by the ras oncogene.* Br J Cancer, 2000. 83(2): p. 156-63.

3. Takano, S., Tsuboi, K., Tomono, Y., Mitsui, Y., and Nose, T., *Tissue factor, osteopontin, alphavbeta3 integrin expression in microvasculature of gliomas associated with vascular endothelial growth factor expression.* Br J Cancer, 2000. 82(12): p. 1967-73.

4. Tuck, A.B., Elliott, B.E., Hota, C., Tremblay, E., and Chambers, A.F., *Osteopontin-induced, integrin-dependent migration of human mammary epithelial cells involves activation of the hepatocyte growth factor receptor (Met).* J Cell Biochem, 2000. 78(3): p. 465-75.

5. Ue, T., Yokozaki, H., Kitadai, Y., Yamamoto, S., Yasui, W., Ishikawa, T., and Tahara, E., *Co-expression of osteopontin and CD44v9 in gastric cancer.* Int J Cancer, 1998. 79(2): p. 127-32.

6. Zohar, R., Suzuki, N., Suzuki, K., Arora, P., Glogauer, M., McCulloch, C.A., and Sodek, J., *Intracellular osteopontin is an integral component of the CD44-ERM complex involved in cell migration.* J Cell Physiol, 2000. 184(1): p. 118-30.

7. Jain, A., Karadag, A., Fohr, B., Fisher, L.W., and Fedarko, N.S., *Three SIBLINGs (small integrin-binding ligand, N-linked glycoproteins) enhance factor H's cofactor activity enabling MCP-like cellular evasion of complement-mediated attack.* J Biol Chem, 2002. 277(16): p. 13700-8.

8. Fedarko, N.S., Fohr, B., Gehron Robey, P., Young, M.F., and Fisher, L.W., *Factor H*

binding to bone sialoprotein and osteopontin enables molecular cloaking of tumor cells from complement-mediated attack. J. Biol. Chem., 2000. 275: p. 16666-16672.

9.   Fedarko, N.S., Jain, A., Karadag, A., and Fisher, L.W., *Three small integrin binding ligand N-linked glycoproteins (SIBLINGs) bind and activate specific matrix metalloproteinases.* Faseb J, 2004. 18(6): p. 734-6.

10.   Jain, A., Fedarko, N.S., Collins, M.T., Gelman, R., Ankrom, M.A., Tayback, M., and Fisher, L.W., *Serum levels of matrix extracellular phosphoglycoprotein (MEPE) in normal humans correlate with serum phosphorus, parathyroid hormone and bone mineral density.* J. Clin. Endo. Metab., 2004. 89(8): p. 4158-4161.

11.   Karadag, A., Ogbureke, K.U., Fedarko, N.S., and Fisher, L.W., *Bone sialoprotein, matrix metalloproteinase 2, and alpha(v)beta3 integrin in osteotropic cancer cell invasion.* J Natl Cancer Inst, 2004. 96(12): p. 956-65.

12.   Fisher, L.W., Jain, A., Tayback, M., and Fedarko, N.S., *Small Integrin Binding LIgand N-linked Glycoprotein (SIBLING) gene family expression in different cancers.* Clin. Can. Res, 2004. 10(24): p. 8501-8511.

13.   Jain, A., Fisher, L.W., and Fedarko, N.S., *Bone sialoprotein binding to matrix metalloproteinase-2 alters enzyme inhibition kinetics. .* J. Biol. Chem., 2005. submitted.

Appendices

Appendix I. Jain, A., Fedarko, N.S., Collins, M.T., Gelman, R., Ankrom, M.A., Tayback, M., and L.W. Fisher. (2004) Serum levels of matrix extracellular phosphoglycoprotein (MEPE) in normal humans correlate with serum phosphorus, parathyroid hormone and bone mineral density. J. Clin. Endo. Metab.89(8):4158-4161.

Appendix II. Karadag, A., Ogburke K.U.E., Fedarko, N.S., and L.W. Fisher. (2004) Bone sialoprotein promotes invasion by osteotropic cancer cells in vitro by bridging MMP-2 to $\alpha_v\beta_3$ integrin. J. Natl. Cancer Inst. 96:956-965.

Appendix III. Fisher, L.W., Jain, A., Tayback, M., and N.S. Fedarko. (2004) Small Integrin Binding Ligand N-Linked Glycoprotein (SIBLING) gene family expression in different cancers. Clin. Cancer Res. 10(24): 10:8501-8511.

Appendix IV. Jain, A., Fisher, L.W., and N.S. Fedarko. (2005) Bone Sialoprotein Binding To Matrix Metalloproteinase-2 Alters Enzyme Inhibition Kinetics. J. Biol. Chem. Submitted.

Appendix V. Jain, A., Fisher, L.W. and N.S. Fedarko Small Integrin Binding Ligand N-Linked Glycoproteins (SIBLINGs) Bind and Activate Matrix Metalloproteinases. 2005 Era of Hope Meeting. Philadelphia, PA.

Appendix VI . Jain, A., Fisher, L.W. and N.S. Fedarko. Small Integrin Binding Ligand N-Linked Glycoprotein (SIBLING) Gene Family Expression In Breast Cancer. 2005 Era of Hope Meeting. Philadelphia, PA.

Appendix VII . Fedarko, N.S., Fisher, L.W. and A. Jain. Small Integrin Binding Ligand N-Linked Glycoproteins Modulate Matrix Metalloproteinases and Angiogenesis. 2005 Era of Hope Meeting. Philadelphia, PA.

APPENDIX I

Serum Levels of Matrix Extracellular Phosphoglycoprotein (MEPE) in Normal Humans Correlate with Serum Phosphorus, Parathyroid Hormone and Bone Mineral Density.

A. JAIN, N.S. FEDARKO, M.T. COLLINS, R. GELMAN, M.A. ANKROM, M. TAYBACK AND L.W. FISHER

Division of Geriatric Medicine, Department of Medicine, Johns Hopkins University, Baltimore, MD 21224 (A.J., N.S.F., M.A.A.); General Clinical Research Center, Johns Hopkins Bayview Medical Center, Baltimore, MD 21224 (N.S.F., R.G., M.T.); Craniofacial and Skeletal Diseases Branch, National Institute of Dental and Craniofacial Research, National Institutes of Health, DHHS, Bethesda, MD 20892 (M.T.C., L.W.F.).

ABSTRACT. Matrix extracellular phosphoglyco-protein (MEPE), a member of the Small Integrin Binding Ligand N-linked Glycoprotein (SIBLING) family, is primarily expressed in normal bone and has been proposed as a phosphaturic factor because of high expression and secretion in oncogenic hypophosphatemic osteomalacia tumors. In order to begin to address the role of MEPE in normal human physiology, we developed a competitive ELISA to measure serum levels of MEPE. The ELISA was used to characterize the distribution pattern in a population consisting of 114 normal adult subjects. The mean value of MEPE was 476 ± 247 ng/ml and levels decreased significantly with increasing age. MEPE levels were also significantly correlated with serum phosphorus and parathyroid hormone (PTH). In addition, MEPE levels correlated significantly with measures of bone mineral density in the femoral neck and total hip in a subset of 60 elderly subjects. The results are consistent with MEPE being involved in phosphate and bone metabolism in a normal population.

Introduction

Matrix extracellular phosphoglycoprotein (MEPE), is a member of the SIBLING gene family (1, 2). Other family members include bone sialoprotein (BSP), osteopontin (OPN), dentin matrix protein-1 (DMP1), and dentin sialophosphoprotein. The family shares the RGD integrin-binding motif, several conserved phosphorylation and N-glycosylation sites, a common gene structure and chromosomal localization (4q21).

Normal MEPE expression has been described primarily in bone marrow, brain (3) and bone (4), while tumors which cause hypophosphatemic osteomalacia exhibit high expression and secretion (3). MEPE has consistently been linked with mineralization and bone formation associated with bone mineral (3-6). Whether MEPE plays a role as a positive or negative regulator of bone formation in humans remains unclear. The current study was undertaken to determine the distribution of MEPE in normal donors and to correlate the values with other biomarkers of bone metabolism as well as measures of bone mineral density (BMD).

Methods

Subjects. Sera from clinically defined normal patients were obtained under IRB approved protocols from a commercial serum bank (East Coast Biologicals, Inc., North Burwick, ME) as well as from the Johns Hopkins Bayview Medical Center General Clinical Research Center (JHBMC). The JHBMC normal group was obtained from an existing serum bank using samples from which all patient identifiers were removed.

Cloning and expression of MEPE. The last exon of human MEPE constitutes 95% of the mature protein as defined by Rowe et al. (3). The last exon was amplified by PCR from human genomic DNA using a 5' oligonucleotide with a NdeI restriction site engineered in (AGTACCCATATGAAAGACAATA-TTGGTTTTCACCAT) and a 3' oligonucleotide with a BamHI site (CTGATGGGATCCCTAGTCACCAT-CGCTCTCAC). The ~1.5 kbp PCR product was gel purified, digested with NdeI plus BamHI, ligated into pET15b expression vector (Novagen, Madison, WI) digested with the same restriction enzymes. After transfection into BL-21 (DE3) E. coli cells, a high expression colony was selected and used to produce the MEPE protein by stimulation with IPTG. The MEPE protein in the apparent inclusion bodies was purified in 6 M urea on a HisBind resin column (Novagen) following the manufacturer's instructions. The eluted fraction was dialyzed exhaustively against 0.1 M ammonium acetate at 4°C and freeze-dried. Four ~200 µg aliquots of the highly purified MEPE were injected into a New Zealand white rabbit to make antiserum LF-155.

Serum sample preparation and competitive ELISA procedure. The SIBLINGs BSP, OPN and DMP1 are complexed with complement Factor H in human serum (7, 8). We have developed competitive ELISAs for measuring the BSP and OPN that requires disruption of the serum complex between the SIBLING and complement Factor H (9). For the current study, serum samples for use in ELISA analyses were processed in a chaotropic buffer exactly as described (9). The MEPE competitive ELISA developed utilized the same plates, buffers, and protein standard concentrations, secondary antibody concentrations, as well as substrate color reagents as

previously described (9). The only changes to the ELISA steps were that plates were coated with 10 ng/well recombinant MEPE and the primary antibody, LF-155, was employed at a 1:200,000 dilution.

Western blotting. Samples diluted in gel sample buffer were resolved by Tris/glycine SDS 12% polyacrylamide gels (Invitrogen, Inc., Carlsbad, CA) and transferred to nitrocellulose following standard conditions (10). Nitrocellulose membranes were rinsed with Tris-buffered saline-Tween (TBS-Tween, 0.05 M Tris-HCl, pH 7.5, 0.15 M NaCl containing 0.05% Tween 20). After a 1 h incubation in TBS-Tween + 5% non-fat powdered milk at room temperature, a 1:20,000 primary antibody (polyclonal antibody LF-155) was incubated overnight at 4 °C. The blot was washed in TBS-Tween four times for 5 min with TBS-Tween and then HRP-conjugated goat anti-rabbit IgG (1:2,000) in TBS-Tween + 5% milk was added and incubated for 2 h at room temperature. After washing, enhanced chemiluminescence reagents were employed for signal detection (Pierce Chemical Co., Chicago, IL) with x-ray film.

DEXA measurements. BMD was measured in the hip, spine and proximal femur using the Hologic QDR 1000 scanner (Hologic Corp., Waltham MA). The precision of this machine is 1.8% ± 0.05%. Mean values for total hip and spine were obtained, as were BMD values for neck and trochanter in the left proximal femur.

Serum and urine biochemical measures. Blood samples were drawn in the morning after an overnight fast. Serum bone biochemical measurements included bone-specific alkaline phosphatase (Hybritech, San Diego, CA), osteocalcin (Immunotopics, San Clemente, CA), procollagen type 1 carboxy-terminal propeptide (DiaSorin Stillwater, MN), intact PTH (Nichols Institute, San Juan Capistrano, CA), and 25 hydroxy vitamin D (DiaSorin). The excretion of deoxypyridinoline crosslinks (Quidel Corp. San Diego, CA) and cross-linked amino-terminal telopeptides (OSTEX International, Seattle, WA) were assayed in 2-hour, second-void morning urine specimens. The values for cross-links were normalized to urinary creatinine assayed using the Jaffe Rate method and a Beckman Creatinine Analyzer 2 (11). Serum inorganic phosphorus was measured using standard clinical methods (12). The performance characteristics of the immmunoassays as carried out in our laboratory are given in Table I.

Results

Previous work has demonstrated that the SIBLINGs BSP, DMP1 and OPN were bound to complement Factor H in serum (7, 8). Disruption of the serum complex required heating in a chaotropic buffer containing reducing agent, followed by a column step to clean up the sample (9). The same disruption procedure was used on serum samples from elderly and young adult donors and MEPE was detected by western blot. Immunoreactive bands shifted in migration with reduction and younger donors appeared to have more MEPE present (Fig. 1a and b). The amount of MEPE present in sera from 114 different normal subjects was analyzed. A reproducible standard curve profile combining 34 different analyses performed over the past two years was obtained (Fig. 1c). MEPE values quantified by ELISA paralleled semi-quantitative results obtained from western blots (Fig/ 1c, inset).
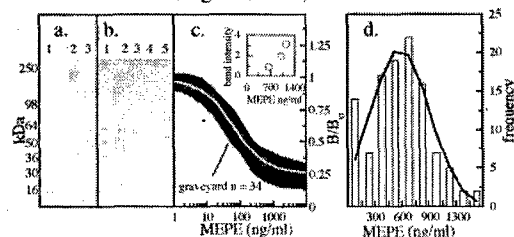

Figure 1. MEPE is present in human serum. (a) Unreduced (lane 2) and reduced (lane 3) serum samples from normal donors were analyzed for the presence of MEPE by western blot. Molecular weight standards were run in lane 1. (b) Samples derived from different age donors analyzed by western blot. Lane 1, standards; lanes 2, 3 & 4 contained 60, 24 and 78-year-old normal donor serum, lane 5, recombinant MEPE (lacking glycosylation). (c) Competitive ELISA profile; inset, representative correlation of western blot band intensity with ELISA results. (d) The distribution of MEPE (bars) in 114 normal subjects. Solid line represents the normal Gaussian distribution.

Addition of recombinant MEPE to serum samples prior to reduction, column chromatography and competitive ELISA yielded an average recovery of 88 % based on three different trials. The inter-assay coefficient of variance for repetitive measurements on the same serum sample was 19.4% (n = 6), while the intra-assay coefficient of variance was 12.6% (n = 12). The major source of this variance was tracked to the column chromatography step. Repeated measures of post-reduction and column samples gave rise to a coefficient of variance of 7.9%. The measure of MEPE levels in normal subject-derived sera revealed a distribution with a slight hook at the low end (Fig. 1d).

When MEPE levels were plotted versus the age of the subject, the reason for the low end hook to the distribution of normal values became apparent. MEPE exhibited a significant age-related decrease in level, (Fig. 2a). The population analyzed possessed a sufficient number of subjects > 60 years of age, where MEPE levels are 1/2 to 1/3 those of younger adults, to account for the increased distribution at low MEPE levels. Serum measures of markers of bone metabolism were also performed on normal subjects. Comparing MEPE levels with serum values of bone-specific alkaline phosphatase, procollagen type I carboxy-terminal propeptide, 25-hydroxy vitamin D, osteocalcin, and urine levels of collagen cross-link markers revealed no significant correlation (data not shown).

Table I. Immunoassay Performance and Study Population Characteristics.

Analyte	mean ± s.d.	units	range	%CV intra-assay	%CV inter-assay
bone-specific alkaline phosphatase	11.2 ± 4.2	ng/ml	5.0 – 28	5.49	5.83
deoxypyridinoline crosslinks	5.1 ± 2.0	nM/mM Cr	1.7 – 13	6.00	4.16
N-terminal telopeptides	31.3 ± 13.3	BCE/mM Cr	5.2 – 64.2	8.25	4.00
osteocalcin	5.2 ± 1.9	ng/ml	2.1 – 10.2	4.55	6.10
procollagen type I C-terminal propeptide	133.9 ± 45	ng/ml	10.7 – 289	2.24	4.38
intact parathyroid hormone	33.7 ± 14.5	pg/ml	3.2 – 94.2	2.40	5.95
25-hydroxy vitamin D	34.5 ± 9.3	ng/ml	14.6 – 62.6	5.19	7.90
MEPE	476.0 ± 247	ng/ml	19.0 – 1269	12.60	19.40
study population	male (n = 64)	60 ± 20	years	21 - 87	
	female (n = 54)	55 ± 12	years	35 - 62	
	BMD group (n = 60)	65 ± 11	years	50 - 82	

Because MEPE has been proposed to play a role in phosphate metabolism, we next investigated serum levels of PTH and inorganic phosphorus. Using a third generation commercial intact PTH assay, the PTH levels were found to be significantly negatively correlated with serum MEPE values (Fig. 2b). The serum levels of intact PTH showed no correlation with donor age (data not shown), suggesting that the association of MEPE and PTH is age-independent. The levels of serum phosphate in the same donors was significantly positively correlated ($r^2 = 0.35$, $p \leq 0.0001$) with serum MEPE values (Figure 2b, inset).
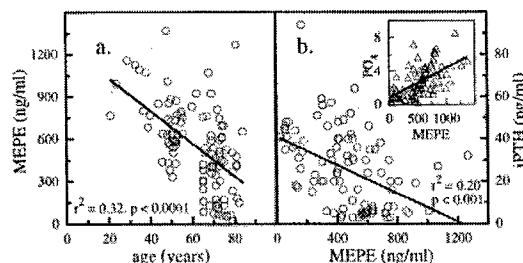

Figure 2. MEPE levels in serum correlate with age (a) and parathyroid hormone levels (b). Serum inorganic phosphorus levels were also determined (inset).
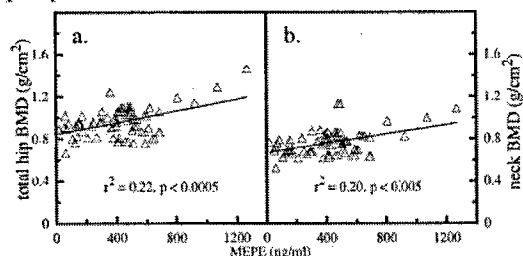

Figure 3. MEPE serum levels correlate with BMD values for total hip (a) and femur neck (b).

In addition to serum and urine markers of bone metabolism, BMD measurements were obtained on a subset of normal subjects (n = 60). The BMD values (g/cm^2) determined were analyzed for correlation with MEPE levels in the corresponding subject's serum (Fig. 3). MEPE levels were significantly positively correlated with bone mineral density values for total hip and femur neck. MEPE levels were also correlated with femur trochanter BMD ($r^2 = 0.13$, $p \leq 0.01$), while the correlation with total spine BMD did not reach statistical significance (data not shown). The correlation of serum MEPE

levels with BMD was still significant when adjusted for subject age using multiple regression analysis and StatView software (SAS Institute, Inc.)

Discussion

MEPE and its rodent homologue, OF45, have been implicated in bone and mineral metabolism (3, 4, 13). The increase in bone density found in the OF45 knockout mouse in the presence of normal serum phosphorus and calcium without evidence of a mineralization defect, suggests that it may have a direct effect on bone formation (6). In that report, the MEPE knockout animal had, what is for a gene knockout model, a relatively subtle increase in the amount of bone. While histomorphometric analysis was performed, there were no data on the parameters of mineralization (osteoid thickness, etc.), only formation and resorption. Elevated levels of MEPE mRNA expression by tumors from patients with hypophosphatemia and osteomalacia suggested that it may be involved in mineral homeostasis. The control of systemic phosphate homeostasis is incompletely understood. Key modulators include PTH, calcium, phosphorus, vitamin D, as well as novel phosphatonin(s), and the bone and kidney organs. Candidate phosphaturic factors include MEPE; PHEX, a putative endopeptidase believed to process factors regulating bone mineralization and renal phosphate reabsorption (5); FGF23, a phosphaturic factor in fibrous dysplasia (14), tumor-induced osteomalacia and autosomal-dominant hypophosphatemic rickets (15, 16) and secreted frizzled-related protein 4, an antagonist of renal Wnt-signaling (17). These phosphate regulators remain to be fully characterized both individually, and in their interactions which will lead to the description of a new hormonal pathway.

Demonstration of significant levels of MEPE in the serum of normal humans, as well as a clear age-related decrease suggest that MEPE may be an interesting marker of normal human bone and mineral metabolism. While the positive correlation between MEPE and phosphorus might suggest an anti-phosphaturic effect, it may represent a secondary response to higher serum phosphorus levels. This idea is supported by the significant correlation of serum MEPE levels with the important constituents of mineral metabolism serum, PTH and phosphorus. The relationships between serum MEPE and PTH, MEPE and phosphorus, and phosphorus and PTH are all internally consistent, and the relationship between phosphorus and PTH is consistent with established

physiology. The correlation of MEPE levels with BMD suggests that it may be involved in mineralization in the human. The finding that MEPE is low in aged patients, when BMD is lower, and that MEPE levels are higher when BMD is high is corroborative, and suggests that these findings in humans are of physiologic significance. Two recent studies have provided contrasting data on the biological activity of MEPE. Recombinant MEPE promoted renal phosphate excretion in mice and inhibited BMP2-mediated mineralization in a mouse osteoblasts cell line (18). The inhibitory action was mapped to the carboxy terminal region of the molecule. In a second study, a peptide fragment corresponding to the RGD-containing mid region stimulated new bone formation in neonatal mouse calvarial organ culture and increased osteoblast proliferation and alkaline phosphatase activity (19). Our current study demonstrates the association of serum MEPE levels with serum phosphate, PTH and bone mineral density but does not address causality.

Acknowledgements

References

1. **Fisher LW, Torchia DA, Fohr B, Young MF, Fedarko NS** 2001 The solution structures of two SIBLING proteins, bone sialoprotein and osteopontin, by NMR. Biochem Bophys Res Comm 280:460-465

2. **Fisher LW, Fedarko NS** 2003 Six genes expressed in bones and teeth constitute the current members of the SIBLING family of proteins. Connective Tissue Res. 44:1-8

3. **Rowe PS, de Zoysa PA, Dong R, Wang HR, White KE, Econs MJ, Oudet CL** 2000 MEPE, a new gene expressed in bone marrow and tumors causing osteomalacia. Genomics 67:54-68

4. **Argiro L, Desbarats M, Glorieux FH, Ecarot B** 2001 Mepe, the gene encoding a tumor-secreted protein in oncogenic hypophosphatemic osteomalacia, is expressed in bone. Genomics 74:342-51

5. **Quarles LD** 2003 FGF23, PHEX, and MEPE regulation of phosphate homeostasis and skeletal mineralization. Am J Physiol Endocrinol Metab 285:E1-9

6. **Gowen LC, Petersen DN, Mansolf AL, Qi H, Stock JL, Tkalcevic GT, Simmons HA, Crawford DT, Chidsey-Frink KL, Ke HZ, McNeish JD, Brown TA** 2003 Targeted disruption of the osteoblast/osteocyte factor 45 gene (OF45) results in increased bone formation and bone mass. J Biol Chem 278:1998-2007

7. **Fedarko NS, Fohr B, Gehron Robey P, Young MF, Fisher LW** 2000 Factor H binding to bone sialoprotein and osteopontin enables molecular

8. **Jain A, Karadag A, Fohr B, Fisher LW, Fedarko NS** 2002 Three Small Integrin Binding LIgands N-linked Glycoproteins (SIBLINGs) enhance Factor H's cofactor activity enabling MCP-like cellular evasion of complement-mediated attack. J Biol Chem 277:13700-13708

9. **Fedarko NS, Jain A, Karadag A, Van Eman MR, Fisher LW** 2001 Elevated serum bone sialoprotein and osteopontin in colon, breast, prostate, and lung cancer. Clin Cancer Res 7:4060-6

10. **Towbin H, Staehelin T, Gordon J** 1979 Electrophoretic transfer of proteins from polyacrylamide gels to nitrocellulose sheets: procedure and some applications. Proc Natl Acad Sci U S A 76:4350-4

11. **Mazzachi BC, Peake MJ, Ehrhardt V** 2000 Reference range and method comparison studies for enzymatic and Jaffe creatinine assays in plasma and serum and early morning urine. Clin Lab 46:53-55

12. **Daly JA, Ertingshausen G** 1972 Direct method for determining inorganic phosphate in serum with the "CentrifiChem". Clin Chem 18:263-5

13. **Petersen DN, Tkalcevic GT, Mansolf AL, Rivera-Gonzalez R, Brown TA** 2000 Identification of osteoblast/osteocyte factor 45 (OF45), a bone- specific cDNA encoding an RGD-containing protein that is highly expressed in osteoblasts and osteocytes. J Biol Chem 275:36172-80

14. **Riminucci M, Collins MT, Fedarko NS, Cherman N, Corsi A, White KE, Waguespack S, Gupta A, Hannon T, Econs MJ, Bianco P, Gehron Robey P** 2003 FGF-23 in fibrous dysplasia of bone and its relationship to renal phosphate wasting. J Clin Invest 112:683-92

15. **Shimada T, Mizutani S, Muto T, Yoneya T, Hino R, Takeda S, Takeuchi Y, Fujita T, Fukumoto S, Yamashita T** 2001 Cloning and characterization of FGF23 as a causative factor of tumor-induced osteomalacia. Proc Natl Acad Sci U S A 98:6500-5

16. **White KE, Carn G, Lorenz-Depiereux B, Benet-Pages A, Strom TM, Econs MJ** 2001 Autosomal-dominant hypophosphatemic rickets (ADHR) mutations stabilize FGF-23. Kidney Int 60:2079-86

17. **Berndt T, Craig TA, Bowe AE, Vassiliadis J, Reczek D, Finnegan R, Jan De Beur SM, Schiavi SC, Kumar R** 2003 Secreted frizzled-related protein 4 is a potent tumor-derived phosphaturic agent. J Clin Invest 112:785-94

18. **Rowe PS, Kumagai Y, Gutierrez G, Garrett IR, Blacher R, Rosen D, Cundy J, Navvab S, Chen D, Drezner MK, Quarles LD, Mundy GR** 2004 MEPE has the properties of an osteoblastic phosphatonin and minhibin. Bone 34:303-19

19. **Hayashibara T, Hiraga T, Yi B, Nomizu M, Kumagai Y, Nishimura R, Yoneda T** 2004 A synthetic peptide fragment of human MEPE stimulates new bone formation in vitro and in vivo. J Bone Miner Res 19:455-62

APPENDIX II

Bone Sialoprotein, Matrix Metalloproteinase 2, and $\alpha_v\beta_3$ Integrin in Osteotropic Cancer Cell Invasion

Abdullah Karadag, Kalu U. E. Ogbureke, Neal S. Fedarko, Larry W. Fisher

Background: Bone sialoprotein (BSP) interacts separately with both matrix metalloproteinase 2 (MMP-2) and integrin $\alpha_v\beta_3$ and is overexpressed in many metastatic tumors. Its role in tumor biology, however, remains unclear. We investigated whether BSP enhances cancer cell invasiveness by forming a trimolecular complex with MMP-2 and cell-surface integrin $\alpha_v\beta_3$. *Methods:* Invasiveness of breast, prostate, lung, and thyroid tumor cell lines was measured with a modified Boyden chamber assay. Binding and co-localization of BSP, MMP-2, and integrin $\alpha_v\beta_3$ were investigated with immunoprecipitation and *in situ* hybridization. All statistical tests were two-sided. *Results:* Treatment with BSP increased invasiveness of many breast, prostate, lung, and thyroid cancer cells through Matrigel in a dose-dependent manner. BSP at 50 n*M* increased the invasiveness of SW-579 thyroid cancer cells (95.2 units, 95% confidence interval [CI] = 90.4 to 100 units) by approximately 10-fold compared with that of untreated control SW-579 cells (9.1 units, 95% CI = 5.7 to 12.5 units) (*P*<.001). Addition of an inactive mutated BSP, in which BSP's integrin-binding RGD tripeptide was altered, or addition of integrin $\alpha_v\beta_3$-blocking antibodies resulted in invasiveness equivalent to that of untreated cells. Inhibiting cellular MMP-2 activity with chemical inhibitors or a specific antibody also blocked BSP-enhanced invasiveness. Osteopontin and dentin matrix protein 1, proteins related to BSP that also bind integrin $\alpha_v\beta_3$ and form complexes with other MMPs (but not MMP-2), did not enhance invasiveness. Immunoprecipitation showed that a complex containing BSP, integrin $\alpha_v\beta_3$, and MMP-2 formed *in vitro*. Addition of BSP increased the amount of MMP-2 bound by cells in an integrin-dependent fashion. Co-expression of BSP, integrin $\alpha_v\beta_3$, and MMP-2 in papillary thyroid carcinoma cells was shown by *in situ* hybridization. *Conclusion:* Cancer cells appear to become more invasive when BSP forms a cell-surface trimolecular complex by linking MMP-2 to integrin $\alpha_v\beta_3$. [J Natl Cancer Inst 2004;96:956–65]

The members of the SIBLING (small integrin-binding ligand N-linked glycoprotein) family of secreted proteins contain an integrin-binding tripeptide (arginine-glycine-aspartate, or RGD) and several conserved serine/threonine (Ser/Thr) phosphorylation and N-glycosylation sites. SIBLINGs include bone sialoprotein (BSP), osteopontin, dentin matrix protein 1 (DMP1), dentin sialophosphoprotein, and matrix extracellular phosphoglycoprotein *(1)*. Genes for all of these SIBLINGs are clustered within a 375 000 base-pair (bp) region of human chromosome 4 (chromosome 5 in the mouse) *(2)*. SIBLING expression is normally restricted to skeletal tissues in adults but also includes trophoblasts during embryonic development *(3–5)*. Osteopontin is an exception, being expressed in normal kidney *(6)*, lactating breast *(7)*, and immune cells *(8)*. BSP normally interacts only with cell-surface integrins, such as integrin $\alpha_v\beta_3$ (also known as the vitronectin receptor), whereas osteopontin and DMP1 bind to both integrins and CD44 *(9–13)*.

BSP is overexpressed by many malignant tissues, including breast *(14)*, prostate *(15)*, lung *(16)*, and thyroid *(17)* cancers and

melanoma *(18)*. BSP expression has been associated with clinical severity and poor survival among patients with breast cancer *(19)* or with prostate cancer *(15)*. Recently developed serum immunoassays for BSP and osteopontin show that serum from patients with breast, lung, colon, or prostate cancer had statistically significantly elevated levels of BSP and/or osteopontin *(20)*. However, the role of BSP in these cancers is unclear.

Matrix metalloproteinases (MMPs), a class of zinc-dependent endopeptidases, are collectively capable of digesting all extracellular matrix components. In addition to their role in normal tissue development and remodeling, MMPs appear to play major roles in tumor cell invasion and metastasis *(21)*. Although the mechanism by which tumors invade surrounding tissues is not completely understood, MMPs may play an important role by removing physical barriers to invasion. In particular, MMP-2 (gelatinase A) and MMP-9 (gelatinase B) degrade extracellular matrix macromolecules in basement membranes and other interstitial connective tissues *(22)*. Active MMP-2 can localize to the cell surface by binding directly to integrin $\alpha_v\beta_3$ *(23)*, and proteolytically active MMP-9 can associate with CD44 *(24)*, thereby focusing proteolytic activity on the cell membrane at the leading edge of the invasive cell.

The integrins are a family of transmembrane receptor proteins composed of heterodimeric complexes of α and β chains *(25)*. There are 18 α and eight β chains, and these chains can dimerize to form at least 25 different complexes, each binding to a specific set of ligands. For example, integrin $\alpha_v\beta_3$ binds to BSP, osteopontin, and DMP1. In addition to regulating cell adhesion to the extracellular matrix, integrins modulate many cellular processes including proliferation, apoptosis, migration, and invasiveness by activating various signaling pathways *(26)*. Some integrins are overexpressed in malignant tumors. For example, integrin $\alpha_v\beta_3$ is expressed at the invasive front of malignant melanoma cells and on angiogenic blood vessels *(27)*. The level of integrin $\alpha_v\beta_3$ expression in breast cancers is associated with the aggressiveness of the disease *(28)*.

It is generally accepted that latent pro-MMPs are enzymatically activated by removal of their inhibitory propeptide. BSP, osteopontin, and DMP1 bind with nanomolar affinity to the latent and active forms of MMP-2, MMP-3, and MMP-9, respectively. When purified SIBLINGs are incubated with their pro-MMP partners, increased proteolytic activity is detected *(29)*. Therefore, we hypothesize that one or more SIBLINGs increase the invasiveness of cancer cells by interacting with their specific MMP and integrin partners. To test this hypothesis, we used a modified Boyden chamber cell invasion assay, as described previously *(30)*, to measure the invasiveness of various cancer cell lines through a layer of Matrigel (a mixture of basement membrane components), and we determined whether BSP increases the invasiveness of cancer cells by forming a trimolecular complex in which BSP acts as a bridge to link MMP-2 to integrin $\alpha_v\beta_3$.

MATERIALS AND METHODS

Materials

Human breast cancer cell lines MDA-MB-231 (HTB-26), MDA-MB-435S (HTB-29), BT-474 (HTB-20), and MCF-7 (HTB-22); human prostate cancer cell lines PC-3 (CRL-1435), LNCaP (CRL-1740), and DU-145 (HTB-81); human thyroid cancer cell line SW-579 (HTB-107); human lung cancer cell line NCI-H520 (HTB-182); and human osteosarcoma cell lines SK-ES-1 (HTB-86), SaOS-2 (HTB-85), and MG-63 (CRL-1427) were obtained from the American Type Culture Collection (Manassas, VA). The mouse fibroblastic cell line NIH 3T3 was provided by Dr. Hynda Kleinman (National Institute of Dental and Craniofacial Research, National Institutes of Health, Bethesda, MD). Fetal bovine serum was purchased from Equitech-Bio (Kerrville, TX). RPMI-1640 medium, L-glutamine, 2-mercaptoethanol, sodium pyruvate, modified Eagle medium (MEM) nonessential amino acids, Hanks' balanced salt solution (HBSS), phosphate-buffered saline (PBS), Versene (0.53 mM EDTA in PBS), and 10% zymogram gelatin gels were from Invitrogen (Carlsbad, CA). Matrigel was from Collaborative Research (Bedford, MA; provided by Dr. Hynda Kleinman). Transwell inserts and companion plates were purchased from BD Biosciences Discovery Labware (Bedford, MA). Calcein acetoxymethyl ester dye and the Alexa Fluor 488 protein labeling kit were purchased from Molecular Probes (Eugene, OR). Mouse anti-human vitronectin receptor monoclonal antibody immobilized on immunoaffinity gel matrix (GEM1976), vitronectin receptor complex in Triton X-100 (CC1018), and mouse anti-MMP-2 monoclonal antibody (MAB 13435) were obtained from CHEMICON International (Temecula, CA). Pro-MMP-2 and active MMP-2 were from Oncogene Research Products (Boston, MA). pBluescript II KS vector was purchased from Stratagene (La Jolla, CA). Digoxigenin labeling mixture was obtained from Roche Biochemicals (Indianapolis, IN). The *in situ* hybridization kit, which included 5-bromo-4-chloro-3-indolyl phosphate/nitroblue tetrazolium (BCIP/NBT; product SH-3018-01), was from InnoGenex (San Ramon, CA). 1,10-Phenanthroline was from Sigma Chemical Co. (St. Louis, MO). MMP-2 inhibitor I, *cis*-9-octadecenoyl-*N*-hydroxylamideleoyl-*N*-hydroxylamide, and anti-integrin $\alpha_v\beta_3$ monoclonal antibody (LM609, MAB 1976Z) were obtained from Calbiochem (San Diego, CA). Rhodamine Red–conjugated AffiniPure goat anti-rabbit immunoglobulin G (IgG; heavy- and light-chain) and Cy2-conjugated AffiniPure goat anti-mouse IgG (heavy- and light-chain) were purchased from Jackson ImmunoResearch Laboratories (West Grove, PA). Vectashield mounting medium for fluorescence microscopy with 4′,6-diamidino-2-phenylindole (DAPI; product H-1200) was obtained from Vector Laboratories (Burlingame, CA). The Probe-Quant G-50 microcolumn was from Amersham Pharmacia Biotech (Piscataway, NJ). The Microcon YM-30 centrifugal filter device was from Millipore (Bedford, MA). *In situ*-ready human thyroid papillary adenocarcinoma serial paraffin sections (product 70452-3) were purchased from Novagen, (Madison, WI).

Cell Culture

The human cancer cell lines used, as described above, were first grown in RPMI-1640 medium supplemented with 10% fetal bovine serum, 2 mM L-glutamine, 5 mM 2-mercaptoethanol, 2 mM sodium pyruvate, and 0.1 mM MEM nonessential amino acids in a humidified atmosphere of 5% CO_2/95% air at 37 °C. When the cells were approximately 80% confluent, they were used in the experiments described below or subcultured for up to 20 passages at a split ratio of 1:10.

SIBLING Production and Purification

Recombinant BSP, BSP-KAE (BSP in which the RGD sequence was replaced with the sequence KAE), osteopontin, and DMP1 with posttranslational modifications, including glycosylation, sulfation, and possibly phosphorylation, were made as described previously *(9,11)*. Briefly, adenoviral constructs containing full-length human BSP *(31)*, BSP-KAE *(9)*, osteopontin *(32)*, or bovine DMP1 *(33)* were subcloned into high-expression, replication-deficient adenovirus type 5 under the control of the elongation factor 1 (EF-1) promoter for BSP or the cytomegalovirus (CMV) promoter for BSP-KAE, osteopontin, and DMP1. The BSP-KAE constructs were made by *in situ* mutagenesis in pBluescript; the entire insert was checked for fidelity and then shuttled to the adenovirus plasmid *(34)*. The adenoviruses were selected, purified, and expressed as previously described *(9)*. Recombinant SIBLINGs were generated by infecting mid-passage subconfluent normal human bone marrow stromal fibroblasts (gift from Dr. P. Gehron Robey, National Institute of Dental and Craniofacial Research, National Institutes of Health, Bethesda, MD). Harvested serum-free medium was subjected to anion-exchange chromatography, as described *(9,11)*, to isolate SIBLINGs. The purity of each SIBLING was greater than 95%, as measured after sodium dodecyl sulfate (SDS)–polyacrylamide gel electrophoresis.

Modified Boyden Chamber Cell Invasion Assay

Invasiveness of each cancer cell line was measured by using a UV-opaque transwell polycarbonate membrane insert with a diameter of 6.4 mm and pore size of 8 μm in a modified Boyden chamber cell invasion assay. Transwell inserts were placed in a 24-well plate, precoated with Matrigel (5–10 μg in 50 μL per well), and dried overnight in a laminar airflow hood. Preconfluent cells were removed from culture dishes with 0.53 m*M* EDTA in PBS, washed twice in HBSS, and resuspended in serum-free RPMI-1640 culture medium at a final density of 4×10^5 cells per milliliter. Quadruplicate cultures of cells were briefly pretreated in a final volume of 250 μL of serum-free medium (containing 0.1% bovine serum albumin) with either buffer or SIBLINGs in 1.5-mL Eppendorf microcentrifuge tubes for 10 minutes and then placed in the upper compartment of a Boyden chamber. In some cases, cells were first treated for 20 minutes with inhibitors, blocking antibodies, or isotype control IgGs in the tube and then placed in the upper chamber. In the latter cases, buffer or recombinant SIBLING was then added directly to the chamber. To induce migration through the Matrigel layer, the lower chambers were filled with 750 μL of serum-free medium conditioned by mouse NIH 3T3 fibroblastic cells and containing 0.1% bovine serum albumin. Cells were then incubated in a humidified incubator at 37 °C for 6–24 hours, depending on the cell line. Cells that had not migrated through the barrier were removed from the top compartment, and inserts were moved to another 24-well plate in which each well contained 0.5 mL of the fluorescent dye calcein acetoxymethyl ester at 4 μg/mL. The plate was incubated at 37 °C for 45 minutes to allow the living cells to take up and activate the dye, and then the fluorescent intensity was read from the bottom of the insert with a fluorescence plate reader (Wallac 1420 VICTOR^2 Multilabel Reader; PerkinElmer Life Sciences, Boston, MA). Fluorescence intensity was proportional to the number of cells migrating to the bottom of the UV-opaque membrane.

Immunoprecipitation Experiments

Commercial mouse anti-human vitronectin receptor (integrin $\alpha_v\beta_3$) monoclonal antibody immobilized on immunoaffinity gel matrix (i.e., beads) was washed three times in ice-cold Triton buffer (TB; 20 m*M* Tris–HCl [pH 7.4], 150 m*M* NaCl, 0.2% Triton X-100, 2 m*M* MgCl$_2$, and 0.1 m*M* CaCl$_2$) and incubated in 1 mL of TB containing 1% bovine serum albumin at 4 °C for 30 minutes with gentle shaking. After washing three times with 1 mL of ice-cold TB, the beads were gently shaken with or without 10 μg of integrin $\alpha_v\beta_3$ in 50 μL of TB at 4 °C for 10 minutes. The beads were then pelleted, the liquid was carefully removed, and the beads were washed in 1 mL of TB. The beads were then resuspended in 1 mL of buffer and separated into aliquots. An aliquot was gently shaken with buffer alone or buffer containing 500 n*M* BSP or 500 n*M* BSP-KAE (in a final volume of 50 μL) at 4 °C for 10 minutes. The beads were then pelleted, washed in 1 mL of TB, and incubated in 50 μL of TB containing 1 μg of pro-MMP-2 or 1 μg of active MMP-2 at 4 °C for 10 minutes. The beads were pelleted and washed with 1 mL of TB. The MMPs were eluted from the beads with 80 μL of 1× SDS sample buffer (2.5 mL of 0.5 *M* Tris–HCl [pH 6.8], 2 mL of glycerol, 4 mL of 10% (wt/vol) SDS, and 0.5 mL of 0.1% bromophenol blue, adjusted to 20 mL with distilled water) and resolved by electrophoresis on a 10% gelatin zymogram gel.

SDS–Polyacrylamide Gel Electrophoresis and Zymography

Samples in zymogram gel sample buffer were loaded on a 10% gelatin zymogram gel, subjected to electrophoresis, and processed as recommended by the manufacturer. Resulting Coomassie-stained gels were visualized with an EagleEye II imaging system (Stratagene, La Jolla, CA) by dynamic integrated exposure with an initial integration time of 3 seconds and an increment of 3 seconds (the camera sums frames of 1/30 second for a 3-second period, sends the image to the computer, collects light for 6 seconds, sends the image to the computer, and continues in this progression until integration is stopped).

Labeling of Purified Human Active MMP-2 and Pro-MMP-2 With Alexa 488 Dye

Latent (pro-MMP-2) or active MMP-2 was fluorescently labeled with the Alexa Fluor 488 protein labeling kit according to the manufacturer's protocol but was adjusted to the smaller amounts of protein being labeled. Briefly, shipping buffer from 50 μg of pro-MMP-2 or 50 μg of active MMP-2 was exchanged for the reaction buffer (PBS) on ProbeQuant G-50 microcolumns, and the resulting mixture was concentrated to approximately 50 μL with a prewashed Microcon YM-30 centrifugal filter device. Sodium bicarbonate (0.1 *M*, 5 μL) was added to raise the pH to 7.5–8.5 for efficient labeling. All steps were performed at 4 °C. The reactive dye was dissolved in 0.5 mL of PBS containing 0.1 *M* sodium bicarbonate, 50 μL of Alexa Fluor 488 dye was added to the MMP-2 solution, and the reaction mixture was stirred at 4 °C for 2 hours. The labeled MMP-2 protein was then separated from the unreacted dye on ProbeQuant G-50 microcolumns (in PBS) and stored as aliquots at −80 °C until use.

Flow Cytometry

Cells were detached from culture dishes with PBS containing 0.53 m*M* EDTA, washed twice in HBSS, and then incubated at

2×10^6 cells per milliliter with buffer alone or buffer containing 500 nM BSP or 500 nM BSP-KAE at room temperature for 10 minutes. For the studies involving the blocking anti-integrin $\alpha_v\beta_3$ antibody, cells were incubated with buffer alone or buffer containing anti-integrin $\alpha_v\beta_3$ antibody (LM609, 4 μg/mL) or isotype control IgG_1 (4 μg/mL) at room temperature for 10 minutes, and then the mixture was incubated with 500 nM BSP for 10 minutes. In the final step for all samples, cells were pelleted at 225g for 10 minutes at room temperature, washed once in HBSS, and then incubated at room temperature with Alexa Fluor 488–labeled purified human pro-MMP-2 at 1 μg/mL or active MMP-2 at 1 μg/mL for 10 minutes. The cells were pelleted, washed once, resuspended in HBSS, and analyzed immediately with a FACSCalibur cell sorter equipped with a 488-nm argon laser and Cellquest software (BD Pharmingen, Bedford, MA).

Fluorescent Immunocytochemistry

To localize BSP, MMP-2, and integrin $\alpha_v\beta_3$ on individual cells, 1 mL containing 1×10^3 SW-579 cells was placed in each well of a two-well chamber slide and incubated at 37 °C for 24 hours. The cells were then washed with serum-free RPMI-1640 medium and incubated in this medium at 37 °C with no additions, with 100 nM BSP-KAE, or with 100 nM BSP for 24 hours. The cells were then washed and incubated at 37 °C with recombinant pro-MMP-2 (1 μg/mL per well) for 20 minutes. After three washes in PBS, the cells were fixed in absolute ethanol at 4 °C for 30 minutes, washed three times in PBS, and incubated in PBS with affinity-purified human anti-BSP polyclonal antibody (LF-84) and mouse anti-MMP-2 monoclonal antibody at the same time at 4 °C for 24 hours. The cells then were washed and incubated with Rhodamine Red–coupled AffiniPure goat anti-rabbit IgG and Cy2-coupled AffiniPure goat anti-mouse IgG secondary antibodies at room temperature for 30 minutes. The slides were detached from the chamber, washed three times with PBS, and immediately mounted in Vectashield mounting medium for fluorescence with DAPI for nuclear staining under a coverslip. The samples were analyzed with a fluorescence microscope that could simultaneously visualize both dye signals.

In Situ Hybridization

To generate strand-specific probes for *in situ* hybridization, a polymerase chain reaction–amplified human MMP-2 cDNA fragment (317 bp) was subcloned into the *Bam*HI site of pBluescript II KS vector. The oligonucleotides for amplification of the MMP-2–specific probes were 5'-ATTAGGATCCGGTCACAG CTACTTCTTCAAG-3' (forward) and 5'-ATATGGATCCG CCTGGGAGGAGTACAG-3' (reverse). The BSP template was the full-length human BSP cDNA B6-5g *(31)*. The human integrin α_v cDNA (1200 bp) insert originally cloned into the pUC12 vector was released with *Eco*RI and *Hin*dIII *(35)*, and human integrin β_3 cDNA (2275 bp) originally cloned into the pUC12 vector *(36)* was released with *Eco*RI. Both cDNA inserts were then subcloned in pBluescript II KS, a vector that contains the T3 and T7 RNA polymerase promoters for RNA probe synthesis. After the plasmids were linearized with the appropriate restriction enzymes, the probes were labeled with a digoxigenin-labeling mixture (1 mM ATP, 1 mM CTP, 1 mM GTP, 0.65 mM UTP, and 0.35 mM DIG-11-UTP [digoxigenin coupled to UTP at position 11], pH 7.5) to produce the specific digoxigenin-labeled single-stranded antisense and sense RNA fragments. *In situ* hybridization for thyroid papillary carcinoma serial sections was carried out with the InnoGenex *in situ* hybridization BCIP/ NBT kit according to the manufacturer's instructions with minor modifications. Slides were deparaffinized in xylene and rehydrated through a graded ethanol series. After a 10-minute incubation in the kit's proteinase K solution, the slides were fixed in 1% formaldehyde for 10 minutes. Approximately 50 μL of hybridization buffer containing pre-titrated digoxigenin-labeled RNA probes (antisense or sense) were applied to each slide. The hybridization reaction included a 3-minute denaturation at 80 °C followed by overnight incubation at 37 °C. After hybridization, washes at room temperature consisted of rinsing with 2× PBS to remove the coverslip, followed by one 10-minute wash and two 5-minute washes in PBS. The sections were then treated with antibody-blocking solution (InnoGenex, product BS-1310-06) for 5 minutes at room temperature, and the blocking agent was gently removed. Biotinylated mouse anti-digoxigenin monoclonal antibody (InnoGenex, product AS-3000-06) was then applied to the sections for 5 minutes at 37 °C, washed for two 5-minute periods in PBS, and then incubated at 37 °C with alkaline phosphatase streptavidine conjugate (provided by the manufacturer) for 5 minutes. After washing twice with PBS, activation buffer was then applied to each section for 1 minute before incubating in BCIP/NBT substrate chromogen solution until satisfactory color reaction was observed (approximately 15 minutes). Sections were then counterstained with nuclear fast red, dehydrated through a graded series of alcohol and xylene, and mounted under a coverslip. Sections were photographed with an AxioCam MR-MRGrab camera imaging system (Carl Zeiss Vision, Munchen, Germany), which included an Axioplan2 microscope, an AxioCam MRm camera, and AxioVision 3.1 software.

Statistical Analysis

Data are the mean of quadruplicate determinations and its 95% confidence interval (CI). Each experiment was repeated at least two times. In each case, data from a single representative experiment are shown. Multiple comparisons were performed with a one-way analysis of variance followed by Dunnett's test for treatment versus control comparisons. Pairwise comparisons were carried out by performing a nonparametric Mann–Whitney U test. In each analysis, differences were considered statistically significant for P values less than .05. All statistical tests were two-sided.

RESULTS

BSP and Invasiveness of Cancer Cells *In Vitro*

Recent reports *(14–20)* that BSP is elevated in tumors and serum from patients with breast, prostate, lung, or thyroid cancers prompted us to investigate whether BSP has a role in the invasion of cancer cells. Invasiveness was measured with a modified Boyden chamber cell invasion assay. Treatment with BSP caused dose-dependent increases in the invasiveness of the breast cancer cell lines MDA-MB-231, MDA-MB-435S, and MCF-7; prostate cancer cell lines PC-3 and DU-145; lung cancer cell line NCI-H520; and thyroid cancer cell line SW-579. Results from a representative cell line for each cancer type are shown in Fig. 1. MDA-MB-231 cells showed a clear dose-
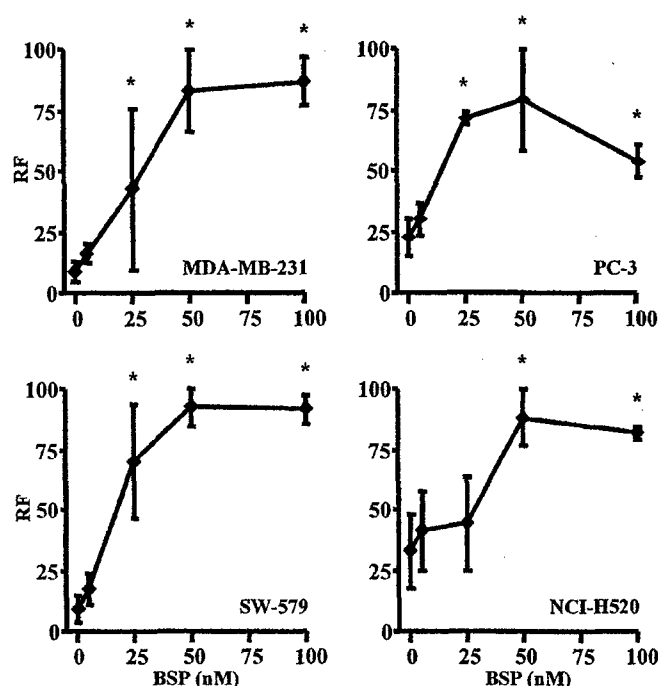
Fig. 1. Bone sialoprotein (BSP) and the invasion of selected cancer cell lines *in vitro*. BSP-treated breast (MDA-MB-231), prostate (PC-3), thyroid (SW-579), and lung (NCI-H520) cancer cells were placed in the Matrigel-coated upper chamber of a Boyden chamber with a UV-opaque transwell insert. The lower chambers contained serum-free conditioned medium as a chemoattractant. The cells were incubated at 37 °C for 6–24 hours. Invasive cells that penetrated the Matrigel artificial basement membrane into the lower chamber were detected by calcein acetoxymethyl ester (AM) fluorescent dye, which is activated by living cells. The relative fluorescence (RF) in the lower chamber corresponds directly to the number of cells that have migrated through the Matrigel. Data are the means of quadruplicate samples, and **error bars** are the 95% confidence intervals. A P value of $<.001$ was obtained for multiple comparisons within each panel, by use of one-way analysis of variance. Each treatment group was also individually compared with the control untreated group by use of Dunnett's test. *$P<.001$ compared with untreated cells by Dunnett's test. All statistical tests were two-sided.

response increase in their invasiveness through a Matrigel barrier, with a maximum increase of approximately 10-fold at 100 n*M* BSP (93.1 units [U; 1 U represents 1% of the maximum number of cells invaded], 95% CI = 86.6 to 99.6 U) compared with that of untreated cells (9.5 U, 95% CI = 6.8 to 12.2 U) ($P<.001$) (Fig. 1). MDA-MB-435S cells showed an approximately twofold increase at 100 n*M* BSP (84.7 U, 95% CI = 69.4 to 100.0 U) compared with that of untreated cells (43.7 U, 95% CI = 36.8 to 50.6 U) ($P<.001$). In addition, MCF-7 cells, which are usually not aggressive in Boyden chamber cell invasion assays, showed a statistically significant approximately ninefold increased invasiveness after treatment with 100 n*M* BSP (79.5 U, 95% CI = 59.0 to 100.0 U) compared with untreated cells (8.5 U, 95% CI = 3.0 to 14.0 U) ($P<.001$).

Addition of recombinant human BSP to cultured prostate cancer cell lines PC-3 and DU-145 increased their invasiveness. The invasiveness of PC-3 cells increased more than threefold after the addition of 50 n*M* BSP (86.2 U, 95% CI = 72.4 to 100.0 U) compared with untreated cells (25.0 U, 95% CI = 19.7 to 30.3 U) ($P<.001$) (Fig. 1). Treatment with 100 n*M* BSP caused an approximately 17-fold increase in the invasiveness of DU-145 cells (84.6 U, 95% CI = 69.3 to 99.9 U) compared with

untreated cells (5.0 U, 95% CI = 4.7 to 5.3 U) ($P<.001$) but caused no change in the invasiveness of another prostate cancer cell line, LNCaP (data not shown). BSP at 50 n*M* enhanced the invasiveness of the less aggressive lung squamous cell carcinoma NCI-H520 cells by approximately 2.7-fold (92.5 U, 95% CI = 85.0 to 100.0 U) compared with untreated control NCI-H520 cells (34.2 U, 95% CI = 24.4 to 44.0 U) ($P<.001$) (Fig. 1). The thyroid squamous cell carcinoma SW-579 cells responded maximally to the addition of 50 n*M* BSP with an approximately 10-fold increase in invasiveness (95.2 U, 95% CI = 90.4 to 100.0 U) compared with untreated cells (9.1 U, 95% CI = 5.7 to 12.5 U) ($P<.001$) (Fig. 1). BSP did not increase the invasiveness of the osteosarcoma cell lines SK-ES-1, SaOS-2, and MG-63 (data not shown). None of the cell lines used in these experiments expressed an appreciable level of BSP, as measured by northern blot hybridization (data not shown).

The increase in the invasiveness of these cancer cell lines was specific to BSP, because the same dose range of osteopontin and DMP1, the two other members of the SIBLING family that can support cell attachment but cannot bind to MMP-2, did not increase the invasiveness of any of the cell lines tested (data not shown).

BSP-Enhanced Invasion, Integrin $\alpha_v\beta_3$, and MMP-2

The same invasiveness studies were performed with BSP-KAE, a recombinant BSP protein whose integrin-binding RGD sequence was replaced with the chemically similar but inactive tripeptide KAE. Treatment with BSP-KAE did not increase the invasiveness of any cell line that had previously responded to BSP compared with the invasiveness of untreated cells. Results from representative breast, prostate, thyroid, and lung cancer cell lines are shown in Fig. 2.

BSP binds to the vitronectin receptor, which is also known as $\alpha_v\beta_3$ integrin *(37)*. As shown in Fig. 3, when SW-579 thyroid cancer cells were pretreated with isotype control IgG$_1$ and then treated with BSP, their invasiveness increased about fivefold (90.3 U, 95% CI = 80.6 to 100.0 U) compared with untreated cells (19.4 U, 95% CI = 16.0 to 22.8 U). However, when cells were first incubated with the same amount of the integrin $\alpha_v\beta_3$ monoclonal antibody LM609, which blocks RGD binding, and then treated with BSP, invasiveness (21.7 U, 95% CI = 10.9 to 32.5 U) was similar to that of untreated cells (19.4 U, 95% CI = 16.0 to 22.8 U). Thus, the BSP-mediated increased invasiveness of cancer cells apparently requires BSP to have an active RGD sequence to bind to integrin $\alpha_v\beta_3$.

Integrins, particularly integrin $\alpha_v\beta_3$, modulate cancer cell invasiveness by directly interacting with MMP-2 *(23)*, and BSP specifically binds to both active and pro-MMP-2 with nanomolar affinity *(29)*. Because two other integrin $\alpha_v\beta_3$-binding SIBLINGs, osteopontin and DMP1, did not stimulate the invasion of cancer cells, we hypothesized that BSP increases invasiveness by interacting with both MMP-2 and integrin $\alpha_v\beta_3$. BSP-enhanced SW-579 cell invasion was completely inhibited by the addition of 10 μ*M* 1,10-phenanthroline, a general MMP inhibitor ($P<.001$; Fig. 3). The role of MMP-2 in the BSP-enhanced cancer cell invasion was further investigated by use of a specific MMP-2 inhibitor (MMP-2 inhibitor I) and a monoclonal antibody against MMP-2. Both the specific MMP-2 inhibitor and the blocking antibody reduced the BSP-enhanced invasiveness of SW-579 cells to that of untreated control cells ($P<.001$; Fig. 3).
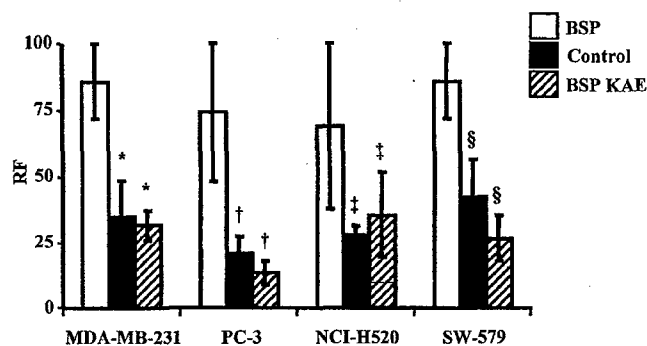
Fig. 2. Bone sialoprotein (BSP)-enhanced invasion and the RGD domain of BSP. MDA-MB-231, PC-3, NCI-H520, and SW-579 cells treated with 100 nM BSP or with 100 nM BSP-KAE (an inactive version of BSP in which the RGD domain was replaced with the chemically similar but inactive KAE tripeptide) were placed in the Matrigel-coated upper chamber of a Boyden chamber with a UV-opaque transwell insert. The lower chambers contained serum-free conditioned medium as a chemoattractant. The cells were incubated at 37 °C for 6–24 hours. Invasive cells that penetrated the Matrigel artificial basement membrane into the lower chamber were detected by calcein acetoxymethyl ester fluorescent dye, which is activated by living cells. The relative fluorescence (RF) in the lower chamber corresponds directly to the number of cells that have migrated through the Matrigel. The controls were untreated cells under the same culture conditions. The invasive activity of cells treated with BSP-KAE was similar to that of untreated cells. Relative fluorescence, which corresponds directly to the number of cells that migrated through the Matrigel, is as described in Fig. 1. Data are the means of quadruplicate samples, and **error bars** are 95% confidence intervals. A Mann–Whitney U test was used for the comparison of BSP-treated cells with either untreated control cells or BSP-KAE-treated cells. A P value of $<.01$ was obtained for MDA-MB-231 cells (*), PC-3 cells (†), NCI-H520 cells (‡), and SW-579 cells (§). All statistical tests were two-sided.

In Vitro Interaction of BSP, MMP-2, and Integrin $\alpha_v\beta_3$

Because the BSP-enhanced invasion can be blocked by interfering with the activity of either integrin $\alpha_v\beta_3$ or MMP-2 and because BSP can form a complex with integrin $\alpha_v\beta_3$ and a complex with MMP-2, we hypothesized that these three molecules form an RGD-dependent complex in which BSP acts as a bridge to link MMP-2 and integrin $\alpha_v\beta_3$. We tested this hypothesis with immunoprecipitation experiments using purified components. Integrin $\alpha_v\beta_3$ was incubated with immunoaffinity gel beads with covalently attached anti-integrin $\alpha_v\beta_3$ monoclonal antibodies to allow integrin binding. The beads were washed to remove unattached integrins, and the washed beads were then incubated with buffer alone or buffer containing recombinant BSP or recombinant BSP-KAE. After washing to remove unbound proteins, beads were incubated with soluble active MMP-2 or inactive pro-MMP-2. The beads were washed again, and then the amount of bound MMP-2 activity was measured by use of gelatin zymogram electrophoresis. No MMP activity was detected when integrin $\alpha_v\beta_3$-free beads were used, which showed that the immunoprecipitation assay had a very low background (data not shown). Beads with bound integrin $\alpha_v\beta_3$ but no BSP bound a small but reproducible amount of pro-MMP-2 and an even smaller amount of active MMP-2 (Fig. 4, lane 2). This result confirms that of Brooks et al. *(23)* and suggests that some MMP-2 can bind directly to integrin $\alpha_v\beta_3$. Addition of BSP-KAE, which lacks an active integrin-binding RGD sequence, did not increase the binding between integrin $\alpha_v\beta_3$ and either MMP-2 or pro-MMP-2 (Fig. 4, lane 4). However, addition of BSP and then of MMP-2 (active MMP-2 or
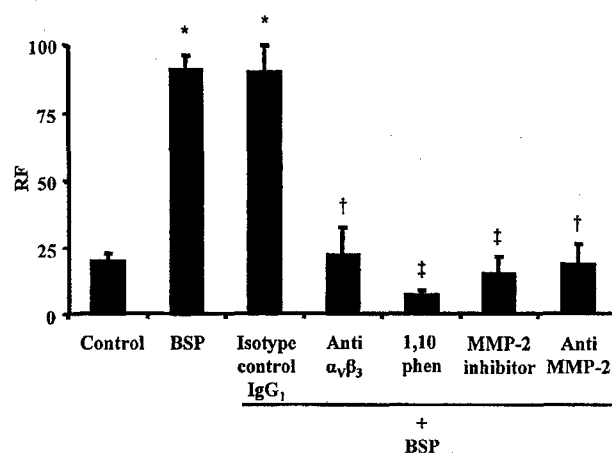

+
BSP

Fig. 3. Bone sialoprotein (BSP) activity and agents that block integrin $\alpha_v\beta_3$ or matrix metalloproteinase 2 (MMP-2) activities. SW-579 cells were placed in the Matrigel-coated upper chamber of a Boyden chamber with a UV-opaque transwell insert. The lower chambers contained serum-free conditioned medium as a chemoattractant. Invasive cells that penetrated the Matrigel artificial basement membrane into the lower chamber were detected by calcein acetoxymethyl ester fluorescent dye, which is activated by living cells. Cells were treated with isotype control immunoglobulin G_1 (IgG$_1$) (5 μg/mL), anti-integrin $\alpha_v\beta_3$ monoclonal antibody (5 μg/mL), anti-MMP-2 monoclonal antibody (5 μg/mL), the general MMP inhibitor 1,10-phenanthroline (1,10 phen) at 10 μM, or the specific MMP-2 inhibitor termed MMP-2 inhibitor 1 at 5 μM for 20 minutes, before 100 nM BSP was added to the inserts. The cells were incubated at 37 °C for 24 hours. Interfering with the functions of MMP or integrin negated BSP-enhanced Matrigel invasion. Relative fluorescence (RF) is as described in Fig. 1. Data are the means of quadruplicate samples from a representative experiment, and **error bars** are 95% confidence intervals. A P of less than .001 was obtained for multiple comparisons by use of one-way analysis of variance. Each group was also individually compared with untreated control group by use of the Dunnett test. *, $P<.001$ compared with untreated control cells; †, $P<.001$ compared with cells treated with isotype control IgG$_1$ and BSP; ‡, $P<.001$ compared with BSP-treated cells. All statistical tests were two-sided.

pro-MMP-2) to integrin $\alpha_v\beta_3$-coated beads increased MMP activity associated with the beads, indicating that BSP stimulated the formation of a complex between integrin $\alpha_v\beta_3$ and MMP-2, presumably by linking the two proteins (Fig. 4, lane 3).

To investigate whether the complex of BSP, integrin $\alpha_v\beta_3$, and MMP-2 also occurs on living cells, we used flow cytometry, SW-579 cells, and purified active MMP-2 and pro-MMP-2 that had been covalently labeled with AlexaFluor-488. SW-579 cells were treated with anti-integrin $\alpha_v\beta_3$ monoclonal antibody or with an isotype control IgG$_1$ and then washed. These cells were incubated with buffer alone, buffer containing BSP, or buffer containing BSP-KAE, washed again, and then incubated with labeled pro-MMP-2. Flow cytometry was used to determine the amount of labeled pro-MMP-2 bound to these cells relative to that bound to untreated cells. Addition of BSP produced a 43% increase in the signal of labeled pro-MMP-2 bound to SW-579 cells compared with that of untreated cells (Fig. 5, A), whereas addition of BSP-KAE produced no change in this signal (Fig. 5, B). Addition of anti-integrin $\alpha_v\beta_3$ monoclonal antibodies almost completely blocked the binding of the labeled pro-MMPs to SW-579 cells compared with that of untreated control cells (Fig. 5, C) or cells treated with isotype control IgG$_1$ (Fig. 5, D). When labeled active MMP-2 was used for the binding analysis, BSP produced a 23% and 22% increase in signal of labeled MMP-2 bound to SW-579 cells compared with untreated control or BSP-KAE-treated cells, respectively (data not shown). Essen-
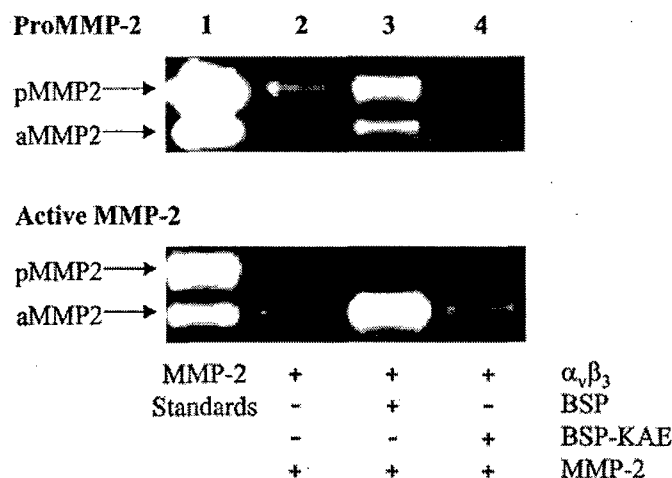
ProMMP-2   1   2   3   4

pMMP2⟶
aMMP2⟶

Active MMP-2

pMMP2⟶
aMMP2⟶

MMP-2	+	+	+	$\alpha_v\beta_3$
Standards	-	+	-	BSP
	-	-	+	BSP-KAE
	+	+	+	MMP-2

Fig. 4. Immunoprecipitation experiments and complexes of integrin $\alpha_v\beta_3$, bone sialoprotein (BSP), and matrix metalloproteinase 2 (MMP-2). Integrin $\alpha_v\beta_3$ was first bound to an anti-integrin monoclonal antibody covalently attached to immunoaffinity gel beads. After washing, the beads were incubated with buffer alone or buffer containing 500 nM BSP or 500 nM BSP-KAE, washed, and subsequently treated with recombinant pro-MMP-2 or active MMP-2. The washed samples were then separated by electrophoresis on 10% gelatin gels and examined by gelatin zymography. Note that the addition of BSP (**lane 3**) but not BSP-KAE (**lane 4**) enabled both pro-MMP-2 (**upper panel**) and active MMP-2 (**lower panel**) to be immunoprecipitated with the integrin-bound beads. Trace amounts of both pro-MMP-2 and active MMP-2 were observed without addition of BSP (**lane 2**), as described by Brooks et al. *(23)*. **Arrows** = pro-MMP-2 (pMMP2) and active MMP-2 (aMMP2) and identify the migration positions of MMP standards in **lane 1**.

tially the same results for both active MMP-2 and pro-MMP-2 were obtained with PC-3 cells (data not shown).

Fluorescent immunocytochemistry experiments showed that BSP, MMP-2, and $\alpha_v\beta_3$ integrin co-localized in single cells. SW-579 cells were first treated with BSP overnight and then treated with MMP-2 for 20 minutes. BSP and MMP-2 were detected at the same locations in these cells (Fig. 6, A–C). Neither BSP nor MMP-2 was detected on untreated cells or cells treated with BSP-KAE (data not shown), suggesting that BSP rapidly localizes MMP-2 to the cell surface *in vitro* by binding to integrin $\alpha_v\beta_3$.

Finally, to verify that the complex of BSP, MMP-2, and integrin $\alpha_v\beta_3$ may occur naturally *in vivo*, *in situ* hybridization experiments were performed on serial paraffin sections of human papillary thyroid carcinomas. The purple-blue cytoplasmic staining with antisense probes verified that all four mRNAs are expressed in the same cells and/or areas of tissue (Fig. 7), showing that all the components of the complex are synthesized simultaneously by cells. Hybridization with similar amounts of the sense probes revealed no signal (data not shown).
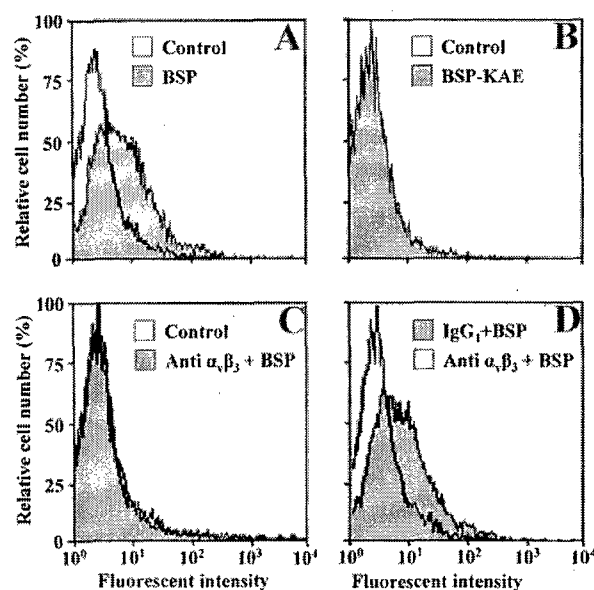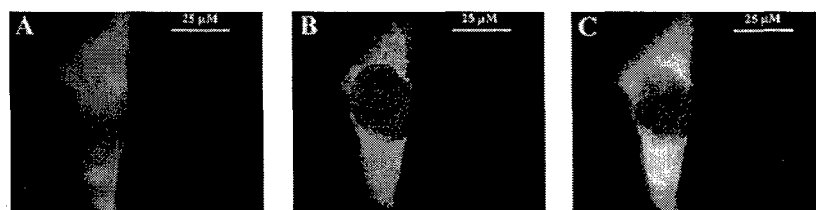

Fig. 5. Bone sialoprotein (BSP)-enhanced binding of fluorescently labeled pro-matrix metalloproteinase 2 (pro-MMP-2) to SW-579 cells. Pro-MMP-2 was labeled with Alexa Fluor-488 and incubated with cells treated as indicated or untreated cells (Control). **A**) Pretreating the cells with BSP (**shaded area**) increased the amount of labeled pro-MMP-2 bound to the living cells compared with untreated cells. **B**) Pretreating cells with BSP-KAE (**shaded area**) showed no increased binding of labeled pro-MMP-2 compared with that of untreated cells (**open area**). **C**) Blocking cell-surface integrin $\alpha_v\beta_3$ with an anti-integrin monoclonal antibody (**shaded area**) also completely blocked the BSP-enhanced binding of the labeled pro-MMP-2 (**open area**). **D**) Treating cells with a nonimmune isotype specific immunoglobulin G_1 (IgG_1) had no effect on the ability of BSP to enhance the binding of pro-MMP-2.

DISCUSSION

Cellular invasion requires dynamic coordination of many cellular components, including cell adhesion molecules and proteolytic agents. MMPs and integrins participate in degradation of the basement membrane and, consequently, in the invasion of cancer cells. Several studies have reported that increased activation of MMP-2, MMP-3, MMP-9, MMP-13, MMP-14, and/or MMP-15 is associated with tumor cell invasion *(23,38–44)*. Two studies have demonstrated that the progression of various cancers is also associated with the overexpression of integrins $\alpha_v\beta_3$, $\alpha_3\beta_1$, $\alpha_4\beta_1$, and/or $\alpha_2\beta_3$ *(23,45)*. Finally, several co-localization studies have reported that integrin $\alpha_v\beta_3$ may function not only as an adhesion and/or migration receptor but may also activate and properly distribute proteases that degrade the extracellular matrix during invasion *(23,46,47)*.

Because it is overexpressed in malignant tissues, BSP may play a role in the progression and invasion of a number of

Fig. 6. Localization of bone sialoprotein (BSP) and matrix metalloproteinase 2 (MMP-2) on SW-579 thyroid cancer cells. Cells were treated first with BSP and then with pro-MMP-2. The cells were incubated with a polyclonal antibody against BSP and a monoclonal antibody against MMP-2, and both proteins were detected by indirect immunofluorescence with Rhodamine Red–conjugated AffiniPure goat anti-rabbit immunoglobulin G (IgG) for BSP and Cy2-conjugated AffiniPure goat anti-mouse IgG for MMP-2. The red color in **panel A** shows the location of BSP, the green color in **panel B** shows the location of MMP-2, and the yellow color in **panel C** shows that the two proteins co-localize. 4′,6-Diamidino-2-phenylindole (DAPI) was used as a nuclear counterstain (blue color). **Scale bar** = 25 µm.
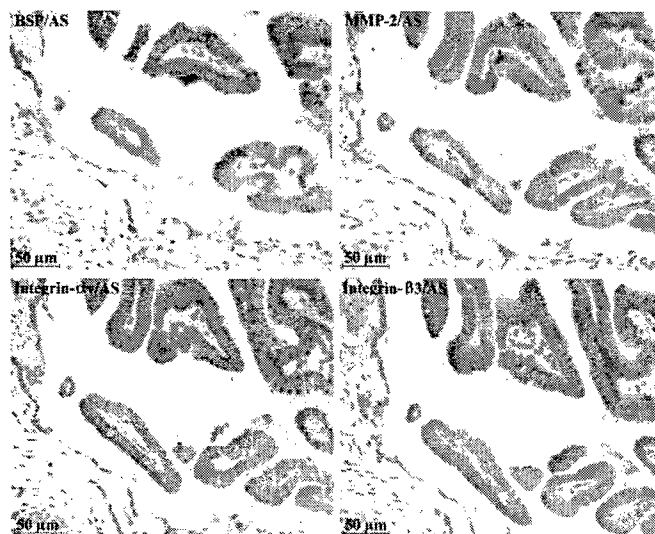
Fig. 7. mRNA for bone sialoprotein (BSP), matrix metalloproteinase 2 (MMP-2), and both chains of integrin $\alpha_v\beta_3$ in sections of an invasive thyroid papillary carcinoma. Deparaffinized sections of an invasive thyroid papillary carcinoma were incubated with digoxigenin-labeled antisense probes specific for BSP, MMP-2, the α_v chain, and the β_3 chain. Indirect localization of the probes was determined with anti-digoxigenin antibodies and colorimetric staining. Cytoplasmic purple-blue color indicates that mRNAs for BSP (**upper left**), MMP-2 (**upper right**), α_v chain (**lower left**), and β_3 chain (**lower right**) are in the same cells, suggesting that all proteins required for formation of complexes of integrin $\alpha_v\beta_3$, BSP, and MMP-2 are likely to be expressed in the same cells. Fast red was used as a nuclear counterstain (nuclear red color). **Scale bar** = 50 μm.

Fig. 8. Proposed trimolecular complex of bone sialoprotein (BSP), matrix metalloproteinase 2 (MMP-2), and integrin $\alpha_v\beta_3$. (**Left**) BSP with an intact RGD domain acts as a bridge between MMP-2 and integrin $\alpha_v\beta_3$. (**Middle**) BSP-KAE, mutant BSP in which the RGD is replaced with KAE, can bind to MMP-2, but the complex does not interact with the integrin $\alpha_v\beta_3$ heterodimer. (**Right**) As shown in Fig. 4 and by others (23), some MMP-2 may also interact with integrin $\alpha_v\beta_3$ even in the absence of BSP. **Double line** = cell membrane; **scissors** = active site of MMP-2.

osteotropic cancers, including breast, prostate, lung, and thyroid cancers (14–17,20). Addition of BSP stimulates the in vitro migration of breast cancer cells via a mechanism involving integrin $\alpha_v\beta_3$ (48,49). Strong and specific in vitro interactions (with nanomolar affinity) have been described (29) between three members of the SIBLING family (BSP, osteopontin, and DMP1) and specific MMPs (MMP-2, MMP-3, and MMP-9, respectively). Thus, the combination of BSP, MMP-2, and integrin $\alpha_v\beta_3$ appears to play an important role in cancer cell invasion. This study demonstrated that BSP, but not osteopontin or DMP1, increased the Matrigel invasiveness of a large subset of breast, prostate, lung, and thyroid cancer cell lines. Addition of BSP-KAE, a recombinant form of BSP in which the RGD sequence was replaced with KAE, or addition of an antibody that blocks BSP binding to integrin $\alpha_v\beta_3$ through RGD sequence blocked all BSP-enhanced invasive activity, suggesting that BSP acts through this integrin. The BSP-enhanced invasion by these cells was also inhibited by specific chemical inhibitors of MMP-2 and by an antibody for MMP-2. Formation of a complex containing BSP, integrin $\alpha_v\beta_3$, and MMP-2 was demonstrated by immunoprecipitation experiments, immunofluorescence experiments, and flow cytometry. These results suggest that cells use BSP as a bridge to link MMP-2 to its cell surface receptor, integrin $\alpha_v\beta_3$, which thereby increases their ability to invade basement membranes and other connective tissues. Fig. 8 shows BSP with an intact RGD bridging MMP-2 to its cell-surface receptor, integrin $\alpha_v\beta_3$. When the integrin-binding RGD sequence is replaced with the chemically similar but inactive KAE sequence, MMP-2 may still bind to the BSP-KAE protein, but the complex between MMP-2 and BSP-KAE does not interact with cell-surface integrin.
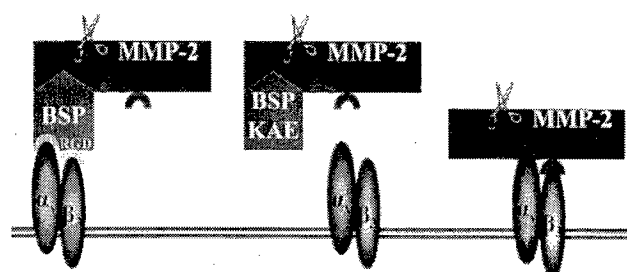
Because BSP enhances the attachment and migration of several cancer cell lines, we also tested the effect of two other members of the SIBLING family, osteopontin and DMP1, that support cell attachment. Osteopontin also supports migration (50). For all 16 cell lines tested, neither osteopontin nor DMP1 increased the invasiveness of these cells through Matrigel, even though the increased expression of these proteins in various cancers has been reported (20,51–53). We have recently shown in vitro that osteopontin and DMP1 bind specifically to MMP-3 and MMP-9, respectively, with nanomolar affinity but do not bind to MMP-2 (29). Because the Boyden chamber cell invasion assay can detect differences only in those functions that result in a net change in rate-limiting steps in the in vitro invasion process (54), it is reasonable to conclude that the binding and possible activation of MMP-2 by BSP overcomes such a rate-limiting step for the cell lines tested, whereas cell attachment alone or the binding and activation of MMP-3 by osteopontin or MMP-9 by DMP1 does not overcome such a step.

In conclusion, we have shown that recombinant BSP can enhance the invasiveness of some, but not all, breast, prostate, lung, and thyroid cancer cell lines in a modified Boyden chamber assay through formation of an RGD-dependent complex with MMP-2 and integrin $\alpha_v\beta_3$.

REFERENCES

(1) Fisher LW, Torchia DA, Fohr B, Young MF, Fedarko NS. Flexible structures of SIBLING proteins, bone sialoprotein, and osteopontin. Biochem Biophys Res Commun 2001;280:460–5.

(2) Fisher LW, Fedarko NS. Six genes expressed in bones and teeth encode the current members of the SIBLING family of proteins: special issue: 7th International Conference on the Chemistry and Biology of Mineralized Tissues. Connect Tissue Res 2003;44 Suppl 1:33–40.

(3) Bianco P, Fisher LW, Young MF, Termine JD, Robey PG. Expression of bone sialoprotein (BSP) in developing human tissues. Calcif Tissue Int 1991;49:421–6.

(4) MacDougall M. Refined mapping of the human dentin sialophosphoprotein (DSPP) gene within the critical dentinogenesis imperfecta type II and dentin dysplasia type II loci. Eur J Oral Sci 1998;106 Suppl 1:227–33.

(5) Omigbodun A, Daiter E, Walinsky D, Fisher L, Young M, Hoyer J, et al. Regulated expression of osteopontin in human trophoblasts. Ann N Y Acad Sci 1995;760:346–9.

(6) Hampel DJ, Sansome C, Romanov VI, Kowalski AJ, Denhardt DT, Goligorsky MS. Osteopontin traffic in hypoxic renal epithelial cells. Nephron Exp Nephrol 2003;94:e66–76.

(7) Dhanireddy R, Senger D, Mukherjee BB, Mukherjee AB. Osteopontin in human milk from mothers of premature infants. Acta Paediatr 1993;82: 821–2.

(8) Gravallese EM. Osteopontin: a bridge between bone and the immune system. J Clin Invest 2003;112:147–9.

(9) Fedarko NS, Fohr B, Robey PG, Young MF, Fisher LW. Factor H binding to bone sialoprotein and osteopontin enables tumor cell evasion of complement-mediated attack. J Biol Chem 2000;275:16666–72.

(10) Weber GF, Ashkar S, Glimcher MJ, Cantor H. Receptor-ligand interaction between CD44 and osteopontin (Eta-1). Science 1996;271:509–12.

(11) Jain A, Karadag A, Fohr B, Fisher LW, Fedarko NS. Three SIBLINGs (small integrin-binding ligand, N-linked glycoproteins) enhance factor H's cofactor activity enabling MCP-like cellular evasion of complement-mediated attack. J Biol Chem 2002;277:13700–8.

(12) Ue T, Yokozaki H, Kitadai Y, Yamamoto S, Yasui W, Ishikawa T, et al. Co-expression of osteopontin and CD44v9 in gastric cancer. Int J Cancer 1998;79:127–32.

(13) Zohar R, Suzuki N, Suzuki K, Arora P, Glogauer M, McCulloch CA, et al. Intracellular osteopontin is an integral component of the CD44-ERM complex involved in cell migration. J Cell Physiol 2000;184:118–30.

(14) Bellahcene A, Merville MP, Castronovo V. Expression of bone sialoprotein, a bone matrix protein, in human breast cancer. Cancer Res 1994;54: 2823–6.

(15) Waltregny D, Bellahcene A, Van Riet I, Fisher LW, Young M, Fernandez P, et al. Prognostic value of bone sialoprotein expression in clinically localized human prostate cancer. J Natl Cancer Inst 1998;90: 1000–8.

(16) Bellahcene A, Maloujahmoum N, Fisher LW, Pastorino H, Tagliabue E, Menard S, et al. Expression of bone sialoprotein in human lung cancer. Calcif Tissue Int 1997;61:183–8.

(17) Bellahcene A, Albert V, Pollina L, Basolo F, Fisher LW, Castronovo V. Ectopic expression of bone sialoprotein in human thyroid cancer. Thyroid 1998;8:637–41.

(18) Riminucci M, Corsi A, Peris K, Fisher LW, Chimenti S, Bianco P. Coexpression of bone sialoprotein (BSP) and the pivotal transcriptional regulator of osteogenesis, Cbfa1/Runx2, in malignant melanoma. Calcif Tissue Int 2003.

(19) Bellahcene A, Menard S, Bufalino R, Moreau L, Castronovo V. Expression of bone sialoprotein in primary human breast cancer is associated with poor survival. Int J Cancer 1996;69:350–3.

(20) Fedarko NS, Jain A, Karadag A, Van Eman MR, Fisher LW. Elevated serum bone sialoprotein and osteopontin in colon, breast, prostate, and lung cancer. Clin Cancer Res 2001;7:4060–6.

(21) Matrisian LM. Cancer biology: extracellular proteinases in malignancy. Curr Biol 1999;9:R776–8.

(22) Kleiner DE, Stetler-Stevenson WG. Matrix metalloproteinases and metastasis. Cancer Chemother Pharmacol 1999;43 Suppl:S42–51.

(23) Brooks PC, Stromblad S, Sanders LC, von Schalscha TL, Aimes RT, Stetler-Stevenson WG, et al. Localization of matrix metalloproteinase MMP-2 to the surface of invasive cells by interaction with integrin alpha v beta 3. Cell 1996;85:683–93.

(24) Yu Q, Stamenkovic I. Localization of matrix metalloproteinase 9 to the cell surface provides a mechanism for CD44-mediated tumor invasion. Genes Dev 1999;13:35–48.

(25) Hynes RO. Integrins: versatility, modulation, and signaling in cell adhesion. Cell 1992;69:11–25.

(26) Aplin AE, Howe AK, Juliano RL. Cell adhesion molecules, signal transduction and cell growth. Curr Opin Cell Biol 1999;11:737–44.

(27) Hood JD, Cheresh DA. Role of integrins in cell migration and invasion. Nature Rev Cancer 2002;2:91–100.

(28) Gasparini G, Brooks PC, Biganzoli E, Vermeulen PB, Bonoldi E, Dirix LY, et al. Vascular integrin alpha(v)beta3: a new prognostic indicator in breast cancer. Clin Cancer Res 1998;4:2625–34.

(29) Fedarko NS, Jain A, Karadag A, Fisher LW. Three small integrin binding ligand N-linked glycoproteins (SIBLINGs) bind and activate specific matrix metalloproteinases. FASEB J 2004;18:734–6.

(30) Albini A, Iwamoto Y, Kleinman HK, Martin GR, Aaronson SA, Kozlowski JM, et al. A rapid in vitro assay for quantitating the invasive potential of tumor cells. Cancer Res 1987;47:3239–45.

(31) Fisher LW, McBride OW, Termine JD, Young MF. Human bone sialoprotein. Deduced protein sequence and chromosomal localization. J Biol Chem 1990;265:2347–51.

(32) Kiefer MC, Bauer DM, Barr PJ. The cDNA and derived amino acid sequence for human osteopontin. Nucleic Acids Res 1989;17:3306.

(33) Hirst KL, Ibaraki-O'Connor K, Young MF, Dixon MJ. Cloning and expression analysis of the bovine dentin matrix acidic phosphoprotein gene. J Dent Res 1997;76:754–60.

(34) Becker TC, Noel RJ, Coats WS, Gomez-Foix AM, Alam T, Gerard RD, et al. Use of recombinant adenovirus for metabolic engineering of mammalian cells. Methods Cell Biol 1994;43:161–89.

(35) Fitzgerald LA, Poncz M, Steiner B, Rall SC Jr, Bennett JS, Phillips DR. Comparison of cDNA-derived protein sequences of the human fibronectin and vitronectin receptor alpha-subunits and platelet glycoprotein IIb. Biochemistry 1987;26:8158–65.

(36) Fitzgerald LA, Steiner B, Rall SC Jr, Lo SS, Phillips DR. Protein sequence of endothelial glycoprotein IIIa derived from a cDNA clone. Identity with platelet glycoprotein IIIa and similarity to "integrin". J Biol Chem 1987; 262:3936–9.

(37) Oldberg A, Franzen A, Heinegard D, Pierschbacher M, Ruoslahti E. Identification of a bone sialoprotein receptor in osteosarcoma cells. J Biol Chem 1988;263:19433–6.

(38) Collier IE, Wilhelm SM, Eisen AZ, Marmer BL, Grant GA, Seltzer JL, et al. H-ras oncogene-transformed human bronchial epithelial cells (TBE-1) secrete a single metalloprotease capable of degrading basement membrane collagen. J Biol Chem 1988;263:6579–87.

(39) Pyke C, Ralfkiaer E, Huhtala P, Hurskainen T, Dano K, Tryggvason K. Localization of messenger RNA for Mr 72,000 and 92,000 type IV collagenases in human skin cancers by in situ hybridization. Cancer Res 1992; 52:1336–41.

(40) Monteagudo C, Merino MJ, San-Juan J, Liotta LA, Stetler-Stevenson WG. Immunohistochemical distribution of type IV collagenase in normal, benign, and malignant breast tissue. Am J Pathol 1990;136:585–92.

(41) Lochter A, Galosy S, Muschler J, Freedman N, Werb Z, Bissell MJ. Matrix metalloproteinase stromelysin-1 triggers a cascade of molecular alterations that leads to stable epithelial-to-mesenchymal conversion and a premalignant phenotype in mammary epithelial cells. J Cell Biol 1997;139:1861–72.

(42) Belien AT, Paganetti PA, Schwab ME. Membrane-type 1 matrix metalloprotease (MT1-MMP) enables invasive migration of glioma cells in central nervous system white matter. J Cell Biol 1999;144:373–84.

(43) Ala-Aho R, Johansson N, Baker AH, Kahari VM. Expression of collagenase-3 (MMP-13) enhances invasion of human fibrosarcoma HT-1080 cells. Int J Cancer 2002;97:283–9.

(44) Hotary K, Allen E, Punturieri A, Yana I, Weiss SJ. Regulation of cell invasion and morphogenesis in a three-dimensional type I collagen matrix by membrane-type matrix metalloproteinases 1, 2, and 3. J Cell Biol 2000;149:1309–23.

(45) Klein CE, Steinmayer T, Kaufmann D, Weber L, Brocker EB. Identification of a melanoma progression antigen as integrin VLA-2. J Invest Dermatol 1991;96:281–4.

(46) Deryugina EI, Bourdon MA, Luo GX, Reisfeld RA, Strongin A. Matrix metalloproteinase-2 activation modulates glioma cell migration. J Cell Sci 1997;110:2473–82.

(47) Deryugina EI, Bourdon MA, Jungwirth K, Smith JW, Strongin AY. Functional activation of integrin alpha V beta 3 in tumor cells expressing membrane-type 1 matrix metalloproteinase. Int J Cancer 2000;86:15–23.

(48) Sung V, Stubbs JT 3rd, Fisher L, Aaron AD, Thompson EW. Bone sialoprotein supports breast cancer cell adhesion proliferation and migration through differential usage of the alpha(v)beta3 and alpha(v)beta5 integrins. J Cell Physiol 1998;176:482–94.

(49) Byzova TV, Kim W, Midura RJ, Plow EF. Activation of integrin alpha (V)beta(3) regulates cell adhesion and migration to bone sialoprotein. Exp Cell Res 2000;254:299–308.

(50) Xuan JW, Hota C, Shigeyama Y, D'Errico JA, Somerman MJ, Chambers AF. Site-directed mutagenesis of the arginine-glycine-aspartic acid sequence in osteopontin destroys cell adhesion and migration functions. J Cell Biochem 1995;57:680–90.

(51) Chambers AF, Wilson SM, Kerkvliet N, O'Malley FP, Harris JF, Casson AG. Osteopontin expression in lung cancer. Lung Cancer 1996; 15:311–23.

(52) Tuck AB, O'Malley FP, Singhal H, Harris JF, Tonkin KS, Kerkvliet N, et al. Osteopontin expression in a group of lymph node negative breast cancer patients. Int J Cancer 1998;79:502–8.

(53) Chaplet M, De Leval L, Waltregny D, Detry C, Fornaciari G, Bevilacqua G, et al. Dentin matrix protein 1 is expressed in human lung cancer. J Bone Miner Res 2003;18:1506–12.

(54) Albini A. Tumor and endothelial cell invasion of basement membranes. The matrigel chemoinvasion assay as a tool for dissecting molecular mechanisms. Pathol Oncol Res 1998;4:230–41.

NOTES

Small Integrin Binding Ligand *N*-Linked Glycoprotein Gene Family Expression in Different Cancers

Larry W. Fisher,[1] Alka Jain,[2] Matt Tayback,[2] and Neal S. Fedarko[2]

[1]Craniofacial and Skeletal Diseases Branch, National Institute of Dental and Craniofacial Research, National Institutes of Health, Department of Health and Human Services, Bethesda, Maryland; and [2]Division of Geriatric Medicine, Department of Medicine, Johns Hopkins University, Baltimore, Maryland

ABSTRACT

Purpose: Members of the small integrin binding ligand *N*-linked glycoprotein (SIBLING) gene family have the capacity to bind and modulate the activity of matrix metalloproteinases (MMPs). The expression levels of five SIBLING gene family members [bone sialoprotein (BSP), osteopontin (OPN), dentin matrix protein 1 (DMP1), matrix extracellular phosphoglycoprotein (MEPE), and dentin sialophosphoprotein (DSPP)] and certain MMPs were determined using a commercial cancer array.

Experimental Design: Cancer profiling arrays containing normalized cDNA from both tumor and corresponding normal tissues from 241 individual patients were used to screen for SIBLING and MMP expression in nine distinct cancer types.

Results: Significantly elevated expression levels were observed for BSP in cancer of the breast, colon, stomach, rectum, thyroid, and kidney; OPN in cancer of the breast, uterus, colon, ovary, lung, rectum, and thyroid; DMP1 in cancer of the breast, uterus, colon, and lung; and dentin sialophosphoprotein in breast and lung cancer. The degree of correlation between a SIBLING and its partner MMP was found to be significant within a given cancer type (*e.g.,* BSP and MMP-2 in colon cancer, OPN and MMP-3 in ovarian cancer; DMP1 and MMP-9 in lung cancer). The expression levels of SIBLINGs were distinct within subtypes of cancer (*e.g.,* breast ductal tumors compared with lobular tumors). In general, SIBLING expression increased with cancer stage for breast, colon, lung, and rectal cancer.

Conclusions: These results suggest SIBLINGs as potential markers of early disease progression in a number of different cancer types, some of which currently lack vigorous clinical markers.

INTRODUCTION

The small integrin-binding ligand *N*-linked glycoprotein (SIBLING) gene family is clustered on human chromosome 4, and its members include bone sialoprotein (BSP), osteopontin (OPN), dentin matrix protein 1 (DMP1), matrix extracellular phosphoglycoprotein (MEPE), and dentin sialophosphoprotein (DSPP; ref. 1). SIBLINGs are normally thought to be restricted in expression to mineralizing tissue such as bones and teeth (1). Retrospective studies using pathological specimens have shown that OPN expression occurs in cancer of the breast, colon, stomach, ovary, lung, thyroid, kidney, prostate, and pancreas (2, 3). The expression of other SIBLING members in cancer has not been extensively studied. BSP expression was been reported in breast (4, 5), prostate (6), lung (7), and thyroid cancer (8). DMP1 has been shown to be strongly up-regulated in lung cancer (9). Elevated levels of MEPE mRNA expression by tumors from patients with hypophosphatemia and osteomalacia have been reported (10). The neoplastic expression pattern of DSPP has not been defined.

Matrix metalloproteinases (MMPs) are critical for development, wound healing, and the progression of cancer. We have recently shown that BSP, OPN, and DMP1 specifically bind to pro–MMP-2, pro–MMP-3, and pro–MMP-9, respectively, thereby activating the latent proteolytic activity (11). Furthermore, it was shown that active MMPs inhibited by either tissue inhibitors of MMPs or low molecular weight synthetic inhibitors were reactivated by their corresponding SIBLING. The current study was undertaken to determine the mRNA expression patterns of SIBLINGs in nine different types of cancer. An additional goal was to determine whether SIBLINGs exhibited expression levels that correlated with their MMP partners as well as various measures of tumor progression.

MATERIALS AND METHODS

Cancer Array Analysis. A cancer profiling array (product 7841-1; Clontech, Palo Alto, CA) containing normalized cDNA from tumor and corresponding normal tissues from 241 individual patients was used to screen for SIBLING and MMP expression (12). Several cancer profiling arrays were hybridized in ExpressHyb hybridization solution (Clontech) with ^{32}P-labeled cDNA probes as per the manufacturer's instructions. Briefly, 1 to 2×10^7 cpm of random-prime labeled cDNA was made single stranded by heating to 95°C for 5 minutes and allowed to hybridize with the prepared membrane overnight at 65°C. Membranes were washed in a series of high stringency washes as recommended by the manufacturer. The washed membranes were quantified by exposure to PhosphorImager screens for 1 to 24 hours, and the exposed screen was analyzed on a PhosphorImager (Amersham Biosciences, Piscataway, NJ)

using the manufacturer's ImageQuant program. All polymerase chain reaction (PCR) products were subcloned into a shuttle plasmid, cloned, and sequenced, and the inserts were gel-purified before ^{32}P labeling by random priming. Unincorporated label was removed before hybridization.

SIBLING Probes. The labeled DNA used for probing was obtained as follows. Human BSP and OPN were cDNA inserts released from OP-10 and B6-5g plasmids, respectively (13, 14). Human DMP1 insert was the ~1.4-kb coding region of exon 6 (15) amplified from human genomic DNA subcloned into pBluescript at the *Eco*RI and *Bam*HI sites using oligonucleotides ATTATAGAATTCAAATGAAGACCCCAGTGAC-AG (forward) and TAATTAGGATCCAATAGCCGTCTTG-GCAGTC (reverse). The MEPE probe was a 1.45-kb, exon 5, cDNA insert corresponding to the last exon of human MEPE, which constitutes 95% of the mature protein as defined by Rowe *et al.* (10). The exon was amplified by PCR from human genomic DNA using a 5' oligonucleotide with a *Nde*I restriction site engineered in AGTACCCATATGAAAGACAATATTGG-TTTTCACCAT and a 3' oligonucleotide with a *Bam*HI site (CTGATGGGATCCCTAGTCACCATCGCTCTCAC). The PCR product was subcloned into pBluescript and sequenced, and the ~1.5-kb insert was released with *Nde*I plus *Bam*HI and labeled. The DSPP probe corresponding to the last exon was similarly amplified using a 5' oligonucleotide with a *Hind*III restriction site engineered in CTGTTGGTACCGATATC-GAAATCAAGGGTCCCAGCAG and a 3' oligonucleotide with a *Kpn*I restriction site (GTGCAAAGCTTCTAATCAT-CACTGGTTGAGTGG), subcloned, and sequenced, and the released ~2.6-kb insert was labeled.

Matrix Metalloproteinase Probes. Specific probes of ~300 bp each for human MMP-2, MMP-3, and MMP-9 were made by PCR using human genomic DNA as template and the following oligonucleotides: MMP-2, ATTAGGATCCGGTCA-CAGCTACTTCTTCAAG (forward with *Bam*HI site added for subcloning) and ATATGGATCCGCCTGGGAGGAGTACAG (reverse with *Bam*HI site); MMP-3, ATATGGATCCAGCTG-GCTTAATTGTTGAAAG (forward with *Bam*HI) and TAA-TGGATCCAACTGACAAATCGTCTTTATTA (reverse with *Bam*HI); and MMP-9, AATTGAATTCAGAGAAAGCCTA-TTTCTGCCAG (forward with *Eco*RI) and TAATGAATTCG-GTTAGAGAATCCAAGTTTATTAG (reverse with *Eco*RI). In each case, the PCR products were subcloned into pBluescript and verified by sequencing, and the ~0.3-kb inserts were released and labeled. Membranes were used up to three times, each time removing the previous probe according to the manufacturer's instructions. The stripped membranes were reimaged by PhosphorImager to verify the removal of the previous probe.

Statistical Analysis. Clinical data linked to samples spotted on the cancer profiling array were accessed through the manufacturer's World Wide Web-based database.[3] Comparisons between normal and tumor tissue (derived from the same subject) were performed using a paired *t* test. The coordinated expression of SIBLINGs with MMP binding partners in tumors was tested by regression analysis. Significant differences in

tumor subtype expression of SIBLINGs was tested by Student's *t* test. The association of SIBLING expression levels with tumor stage was investigated using a conservative statistical approach. The nonparametric Spearman rank order correlation was used to examine the correlation of tumor stage and SIBLING expression. The analysis was performed on untransformed data, and the adjusted Spearman correlation coefficient (r_S) is reported. All statistical calculations were carried out using StatView software (SAS Institute, Inc., Cary, NC).

RESULTS

SIBLINGs Are Elevated in Multiple Cancer Types. Because BSP and OPN protein expression have been found to be greatly increased in many separate, often immunohistochemistry-based studies of different neoplasms, the expression levels of five SIBLING gene family members were determined using a commercial cancer array. The array included normalized cDNA from tumor and corresponding normal tissues from 241 individual patients, as well as certain internal controls (Fig. 1). Because the sample sizes were too small for some tumor types on the array, the tissues reported for this study include only breast, uterus, colon, stomach, ovary, lung, kidney, rectum, and thyroid. In each array experiment, the patient's normal and tumor cDNA was separately hybridized with ^{32}P-labeled probes for BSP, OPN, DMP1, MEPE, and DSPP, and the array was digitized by PhosphorImager. Whereas BSP, DMP1, and DSPP exhibited minimal normal tissue expression, significant OPN expression by normal tissues was observed. In fact, the highest levels of expression of OPN were seen in normal kidney. Because MEPE expression was minimal in both normal and tumor tissue, its expression was not analyzed further (data not shown). The amount of hybridized probe was quantified, and the average expression values of BSP, OPN, DMP1, and DSPP in normal and tumor tissue were compared (Fig. 2). The expression levels of BSP were significantly elevated (from 2- to 6-fold) in cancer of the breast, colon, rectum, thyroid, and kidney. OPN expression was significantly elevated (2- to 4-fold) in cancer of the breast, uterus, colon, ovary, lung, rectum, and thyroid. DMP1 exhibited significant (1.7- to 3-fold) elevated expression in cancer of the breast, uterus, colon, and lung, whereas DSPP exhibited significant (2-fold) increase in cancer of the breast and lung. Elevated SIBLING family expression was greatest in breast cancer, in which expression of four different family members was increased. Colon, lung, and thyroid cancer had significantly elevated expression of three different SIBLING family members. Of the nine different types of tumors quantified, each one had a significantly high expression of at least one SIBLING.

Matrix Metalloproteinases Are Elevated in Multiple Cancer Types. We have recently shown that three members of the SIBLING family can specifically bind and modulate the activity of three different MMPs (11). The SIBLINGs BSP, OPN, and DMP1 were found to bind to and modulate the activity of MMP-2, MMP-3, and MMP-9, respectively. Corresponding MMP partners for DSPP and MEPE, if any, have yet to be identified. Because MMPs have been postulated to play major roles in tumor cell progression and metastasis (16), the expression levels of SIBLING-matched MMPs were screened in
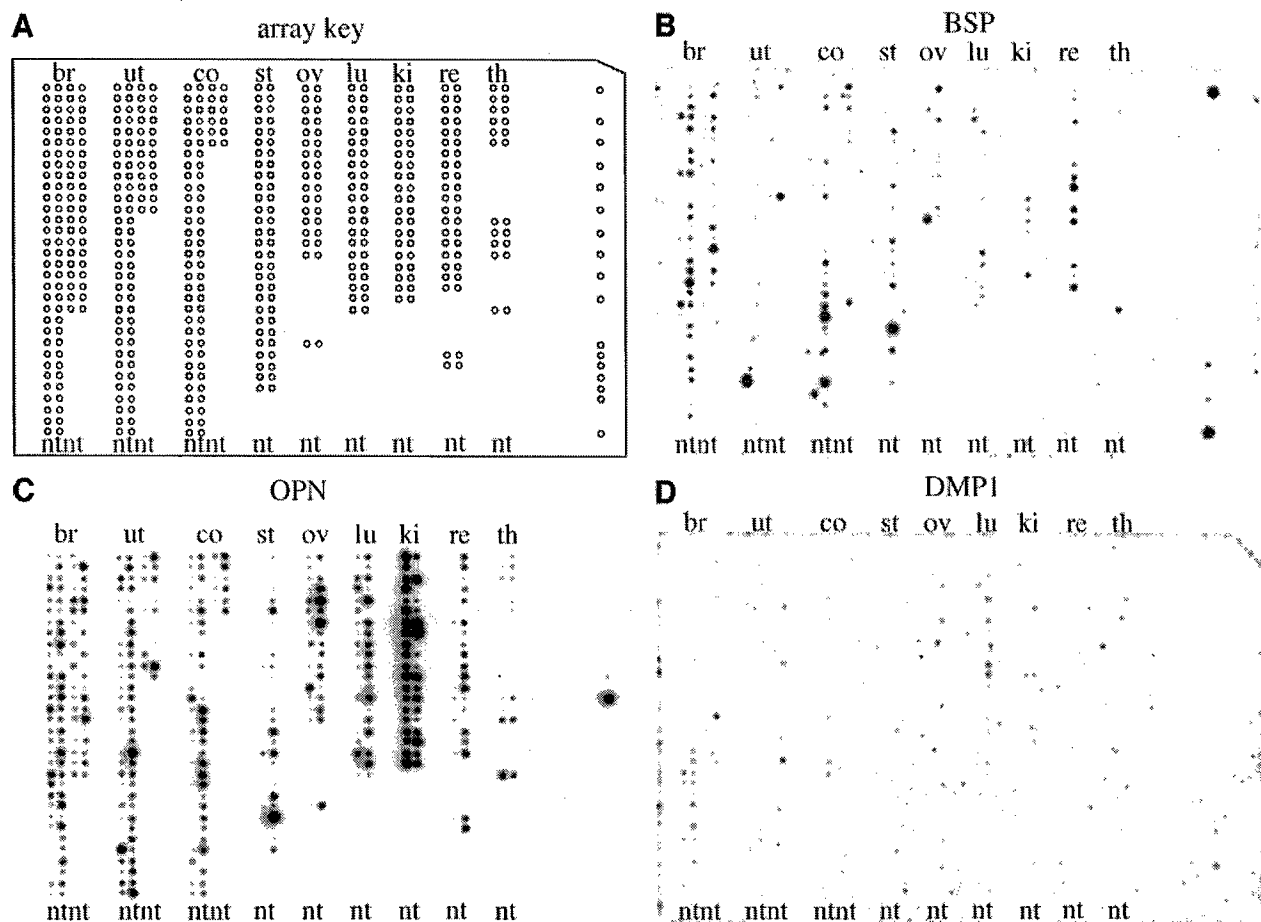
Fig. 1 SIBLING expression in different cancer types. A cancer profiling array was hybridized with cDNA probes for SIBLINGs. The arrays contained samples from 13 different types of cancer with paired normal and tumor tissue mRNA from individual subjects (*A*). The amount of hybridized probe for BSP (*B*), OPN (*C*), and DMP1 (*D*) was visualized by PhosphorImager. *br*, breast cancer; *ut*, uterine cancer; *co*, colon cancer; *st*, stomach cancer; *ov*, ovarian cancer; *lu*, lung cancer; *ki*, kidney cancer; *re*, rectal cancer; *th*, thyroid cancer; *n*, normal tissue; *t*, tumor tissue. Those hybridization spots that are not contiguous with the identified tumor types represent patient samples with tumor types too few in number to be statistically useful.

different cancer types. The cancer arrays were separately hybridized with probes for MMP-2, MMP-3, and MMP-9, and the expression values between normal tissue and the corresponding tumor sample for each patient were compared (Fig. 3). MMP-2 expression was significantly elevated in cancer of the colon, stomach, lung, and rectum. MMP-3 expression exhibited significant elevation in cancer of the breast, colon, stomach, and rectum. MMP-9 expression levels were significantly elevated in cancer of the breast, uterus, colon, stomach, ovary, lung, rectum, and kidney. The increases in expression ranged from 2- to 3-fold higher for MMP-2 and MMP-3, whereas expression levels were increased 2- to 7-fold for MMP-9.

Correlated Expression of SIBLINGs and Their Partner Matrix Metalloproteinases. Given the observed binding and activation specificity seen with SIBLINGs and their partner MMPs [BSP with MMP-2, OPN with MMP-3, and DMP1 with MMP-9 (11)], it was reasonable to postulate that SIBLINGs and their paired MMPs might exhibit correlated expression levels. When the levels of SIBLING and matched MMP expressed by

individual tumors were analyzed by regression analysis, significant correlation was seen within different cancer types (Fig. 4). The expression of BSP and MMP-2 was significantly correlated in breast and colon cancer [$r^2 = 0.40$ ($P \leq 0.0001$) and $r^2 = 0.36$ ($P \leq 0.0001$), respectively]. OPN pairing with MMP-3 showed a significant correlation in stomach and ovarian cancer [$r^2 = 0.52$ ($P \leq 0.0001$) and $r^2 = 0.45$ ($P \leq 0.005$), respectively]. DMP1 and MMP-9 expression was significantly correlated in lung and kidney cancer [$r^2 = 0.60$ ($P \leq 0.001$) and $r^2 = 0.39$ ($P \leq 0.05$), respectively]. Mismatched pairs of BSP with MMP-3, OPN with MMP-2, or DMP1 with MMP-2, for example, showed no significant correlation (data not shown).

SIBLING Expression Is Distinct in Different Cancer Subtypes. Within cancers arising from a given tissue/organ, there are histopathologically defined subtypes that are often used in assessing disease course and treatment. There were sufficient numbers of breast cancer array samples to permit segregation by clinically defined subtypes of ductal *versus* lobular tumors. The results of microarray screening of SIBLING
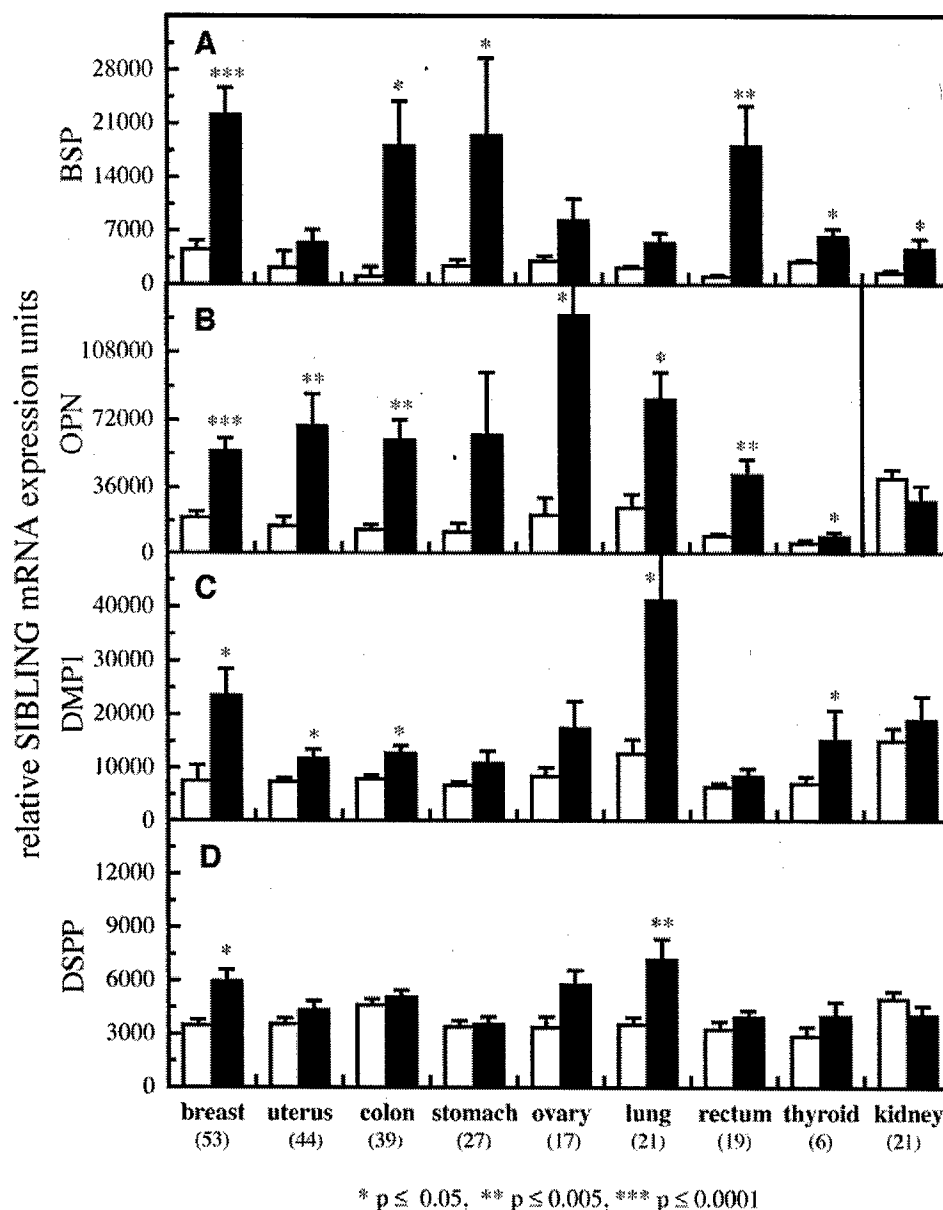
Fig. 2 SIBLING mRNAs are induced in multiple cancer types. Digitized exposures from Fig. 1 were quantified using ImageQuant software, and the mean values of relative expression of BSP (*A*), OPN (*B*), DMP1 (*C*), and DSPP (*D*) in normal tissue (□) and tumor tissue (■) were determined for each of nine different cancer types. *Asterisks* denote the statistical significance as determined by paired *t* tests. *, $P \le 0.05$; **, $P \le 0.005$; ***, $P \le 0.0001$. *Error bars* represent the SE, and *numbers in parentheses* represent the number of subjects. OPN expression in both normal and tumor tissue from kidney is shown at one-tenth the actual mean values.

* $p \le 0.05$, ** $p \le 0.005$, *** $p \le 0.0001$

expression in breast cancer tissue were segregated by the pathological classification, and the average values of each group were compared (Fig. 5*A*). SIBLING mRNA levels were significantly higher in the ductal cancer groups, whereas the levels in the lobular group were intermediate between normal and ductal levels.

A similar analysis was carried out on uterine cancer samples, where there were sufficient numbers to permit segregation into clinically defined subtypes of adenocarcinoma, squamous cell, and benign tumors (Fig. 5*B*). OPN expression was significantly different between the two subtypes of malignant uterine tumors ($P \le 0.005$) and between malignant and benign tumors ($P \le 0.05$). The adenocarcinoma subtype expressed higher levels than the squamous cell subtype.

SIBLING Expression and Tumor Stage. Defined cancer stages represent how large the tumor is and how far it may have spread. The association of SIBLING expression levels with tumor progression was investigated by identifying tumor types with sufficient clinical detail to stratify into different tumor stages. Tumors from colon, rectal, and lung cancer were grouped by stage, and the distribution of SIBLINGs was compared (Fig. 6). In general, cancer stages mark tumors that were either localized and had a relatively small size (stage I), localized and larger in size (stage II), metastasized to lymph nodes (stage III), or metastasized to distant sites (stage IV). Colon cancer tumors exhibited mean values of BSP, OPN, DMP1, and DSPP that increased between stage I and stage III. Colon tumors with distant metastases exhibited SIBLING values with a sim-

Fig. 3 MMP mRNAs are induced in multiple cancer types. Cancer profiling arrays were hybridized with cDNA probes for different MMPs, the amount of hybridized probe was quantified using ImageQuant software, and the mean values of expression of MMP-2 (*A*), MMP-3 (*B*), and MMP-9 (*C*) in normal tissue (□) and tumor tissue (■) were determined for each of nine different cancer types. *Asterisks* denote the statistical significance as determined by paired t tests. *, $P \leq 0.05$; **, $P \leq 0.005$; ***, $P \leq 0.0001$. *Error bars* represent the SE, and *numbers in parentheses* represent the number of subjects.

$* \ p \leq 0.05, \ ** \ p \leq 0.005, \ *** \ p \leq 0.0001$
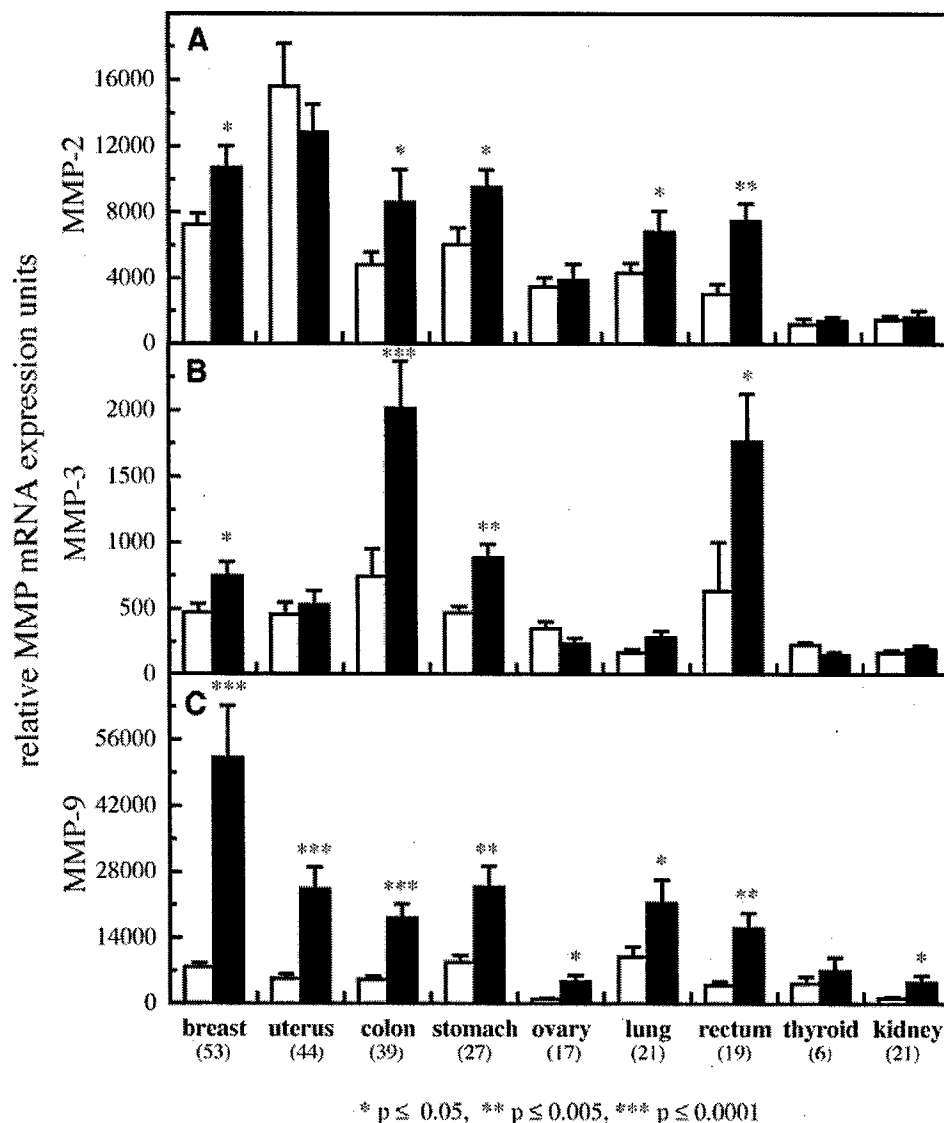
ilar or lower pattern of distribution than that of stage III tumors. Rectal cancer tumors showed increasing BSP, OPN, and DMP1 levels from stage I to stage IV, whereas DSPP values were unchanged across different stages. In lung cancer, BSP, OPN, and DSPP levels increased with increasing stage. When the association of SIBLING expression and tumor stage in colon cancer was analyzed by Spearman rank order correlation analysis, only BSP was significantly correlated (Table 1). In rectal tumors, BSP, OPN, and DMP1 levels correlated with stage, whereas for lung cancer, BSP, OPN, and DSPP levels correlated with stage.

Breast cancer tumors were stratified into tumor-node-metastasis (TNM) stages, which reflect tumor size (T), lymph node involvement (N), and metastatic state (M). Enough breast tumor samples were analyzed to enable the analysis of SIB-LING expression and tumor progression. Tumors were grouped by TNM stage, and the stages were ordered in sequence of

increasing progression. The sequence of tumors ranged from those with no nodal involvement or metastasis state (N_0M_0) that increased in size as well as N_1M_0 tumors that increased in size. For BSP, OPN, DMP1, and DSPP, significant differences were observed in the expression pattern as a function of tumor progression (Fig. 7; Table 1). Spearman rank order correlation analysis of SIBLING values and TNM stage yielded significant correlation for all four SIBLINGs.

DISCUSSION

Microarray technology has been typically used to screen the simultaneous expression of many genes using an array spotted with thousands of genes and measuring hybridization of target cDNA generated from a given tissue or cell type. In contrast, the cancer profiling array used in the current study was developed to enable the quantification of expression of a single
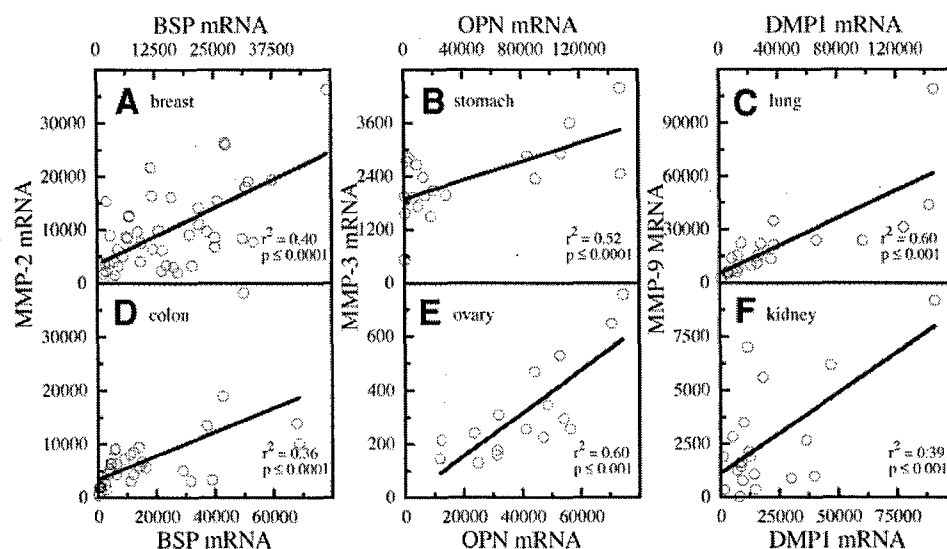
Fig. 4 Paired SIBLING and MMP expression is correlated in specific cancers. The expression levels of SIBLINGs and their respective binding partner MMPs were analyzed by regression analysis. BSP and MMP-2 levels in breast (*A*) and colon cancer (*D*), OPN and MMP-3 levels in stomach (*B*) and ovarian cancer (*E*), as well as DMP1 and MMP-9 levels in lung (*C*) and rectal cancer (*F*) were paired by subject and analyzed by regression analysis.

gene across multiple tissue types and tumor stages. The cancer profiling array contained multiple cDNA pairs from normal and tumor tissues including breast, uterus, colon, stomach, ovary, lung, kidney, rectum, thyroid, prostate, small intestine, pancreas, and cervix. Complementary DNA was generated by an efficient cDNA amplification technique that is based on the switching

mechanism at the 5′ end of mRNA templates (17). This methodology has been shown to yield a high representation of mRNA transcripts, avoidance of biased amplification, linearity of signal, and recapitulation of the complexity of the original mRNA (12). Because the expression of individual housekeeping genes varies between normal and tumor tissue (18–20), the
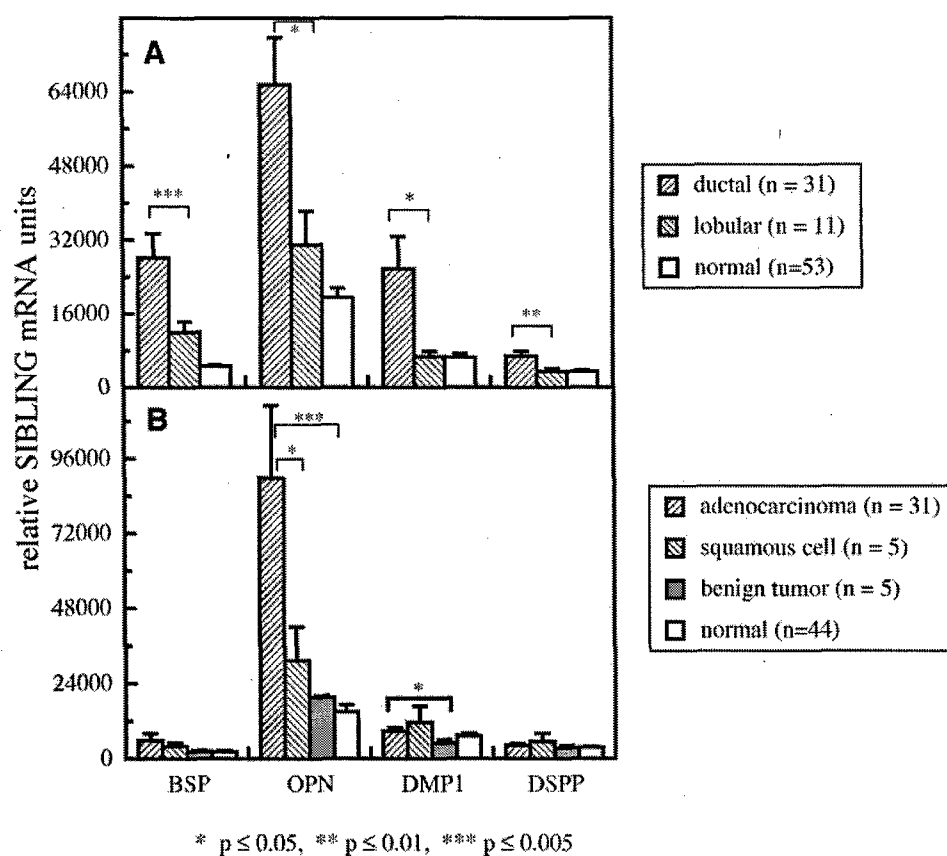

Fig. 5 SIBLING expression distinguishes cancer subtypes for breast and uterine tumors. The expression values of BSP, OPN, DMP1, and DSPP by breast cancer tumors were stratified by pathological classification (ductal *versus* lobular), and the average values were compared (*A*). Similarly, the expression of SIBLINGs by uterine tumors stratified into groups defined as adenocarcinoma, squamous cell, or benign tumor were averaged and compared (*B*). *Asterisks* denote the statistical significance as determined by *t* test. *, $P \leq 0.05$; **, $P \leq 0.01$; ***, $P \leq 0.005$. *Error bars* represent the SE.

* $p \leq 0.05$, ** $p \leq 0.01$, *** $p \leq 0.005$

Fig. 6 Comparison of SIB-LING mRNA levels with tumor stage in colon, rectal, and lung cancer. The expression values of BSP (*A—C*), OPN (*D—F*), DMP1 (*G—I*), and DSPP (*J—L*) by colon cancer tumors (*A, D, G,* and *J*), rectal cancer tumors (*B, E, H,* and *K*), and lung cancer tumors (*C, F, I,* and *L*) were stratified by pathological classification (stage), and the average values were compared. *Top line, bottom line,* and *line through the middle* correspond to 75th percentile, 25th percentile, and 50th percentile (median), respectively. *Error bar whiskers* represent the 10th and 90th percentile, whereas ■ indicates the arithmetic mean. Rectal and colon cancer stages were as follows: I, tumor invaded submucosa; II, tumor invaded through muscularis propia; III, invasive tumor with metastasis in one to three pericolic or perirectal lymph nodes; and IV, invasive tumor with metastasis in pericolic or perirectal lymph nodes and distant metastasis. Lung cancer stages were as follows: I, tumor < 3 cm in greatest dimension; IB, tumor > 3 cm in greatest dimension, involved main bronchus, associated with atelectasis or obstructive pneumonitis; II, metastasis to ipsilateral peribronchial and/or ipsolateral lymph nodes; and III, metastasis to ipsilateral mediastinal, and/or subcarinal lymph nodes. The number of subjects (*n*) for each group is shown at the bottom.
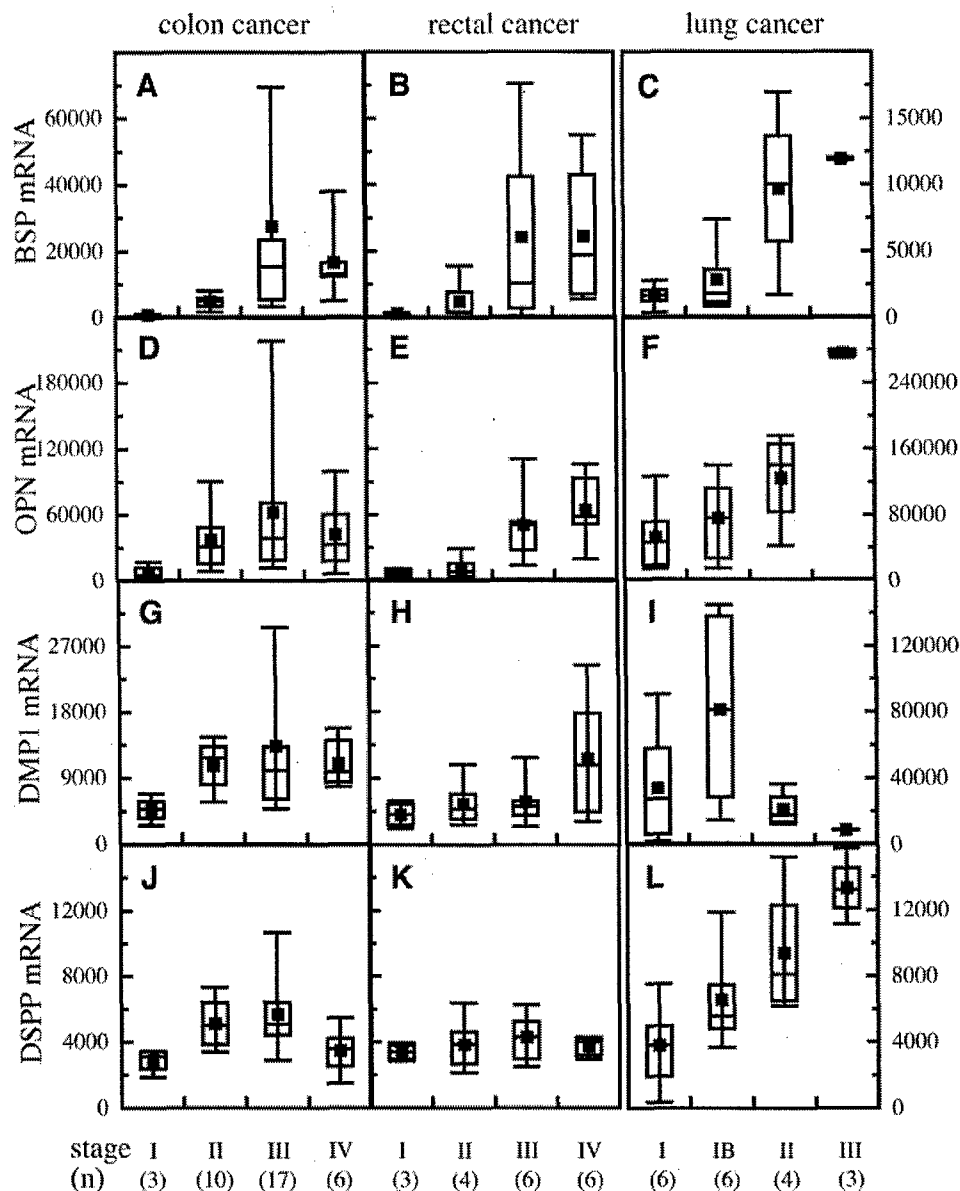
equal loading of cDNA onto the array membrane was carried out by normalizing to the average expression of three housekeeping genes: ubiquitin, β-actin, and M_r 23,000 highly basic protein (12, 21). The array has recently been used to profile a number of genes that exhibited either up- or down-regulation in cancer including gelsolin and glutathione peroxidase (12), netrin 1 (22), thiamin transporter THTR2 (23), PAGE 4 (24), and XAGE-1 (25). Strong correlation between tumor tissue expression by the current cDNA microarray and by *in situ* hybridization (24, 25) as well as reverse transcription-PCR and immunohistochemical staining (26, 27) has been observed.

The microarray design pairing normalized cDNA from an individual subject's tumor and normal tissue enabled differences in expression to be analyzed by paired *t* test, which provided a greater power to detect significant differences. Another method

of evaluating the significance of biomarker elevation is to compare target tissue measures to a cut point of the mean of normal levels plus twice the SD (m + 2 SD). A value of >m + 2 SD translates to a <5% probability that the elevation is due to chance (95% of normal values will lie within the m + 2 SD range). The overall significance of the microarray results was assessed by comparing concordance between these two methods of analysis, as well as comparison with the published results of other studies (Table 2). Elevated BSP expression was identified in two tissues (breast and thyroid), in agreement with previous studies. The current results for BSP did not replicate previous reports on elevated expression in cancer of the uterus or lung. Novel expression was identified in four different cancer types (colon, stomach, rectum, and kidney). Elevated OPN expression was observed in the current study in four different cancer types

Table 1 SIBLING expression and tumor staging

Spearman rank order correlation	BSP	OPN	DMP1	DSPP
Colon cancer*				
Spearman coefficient (r_S)	0.61	0.29	0.26	0.20
P	<0.001	>0.05	>0.05	>0.05
Rectal cancer*				
Spearman coefficient (r_S)	0.61	0.72	0.49	0.28
P	<0.005	<0.001	<0.05	>0.05
Lung cancer*				
Spearman coefficient (r_S)	0.70	0.70	−0.18	0.77
P	<0.001	<0.001	>0.05	<0.0005
Breast cancer†				
Spearman coefficient (r_S)	0.62	0.38	0.37	0.47
P	<0.0005	<0.05	<0.05	<0.005

* Spearman rank order correlation between mean SIBLING values and tumor stage. The Spearman coefficient value (r_S) is an adjusted value (corrected for ties). Tumor stages for colon, rectal, and lung cancer were defined as stated in the Fig. 5 legend.

† Correlation between mean SIBLING values and breast tumor progression. Spearman rank order correlation was performed on breast tumor SIBLING expression levels grouped by TNM stage and ordered across increasing progression ($T_1N_0M_0$, $T_2N_0M_0$, $T_3N_0M_0$, $T_1N_1M_0$, $T_2N_1M_0$, $T_3N_1M_0$). Breast tumor T stages were defined as stated in the Fig. 6 legend.

(breast, colon, ovary, and lung) in agreement with other published studies. For cancer of the stomach, thyroid, and kidney, the OPN expression levels and published literature were not in concordance. Novel expression of OPN in cancer of the uterus

and rectum was identified. Elevated DMP1 expression was confirmed in lung cancer and newly identified in breast cancer. DMP1 levels in cancer of the uterus and colon, although significantly elevated by paired *t* test, did not satisfy the $>m + 2$
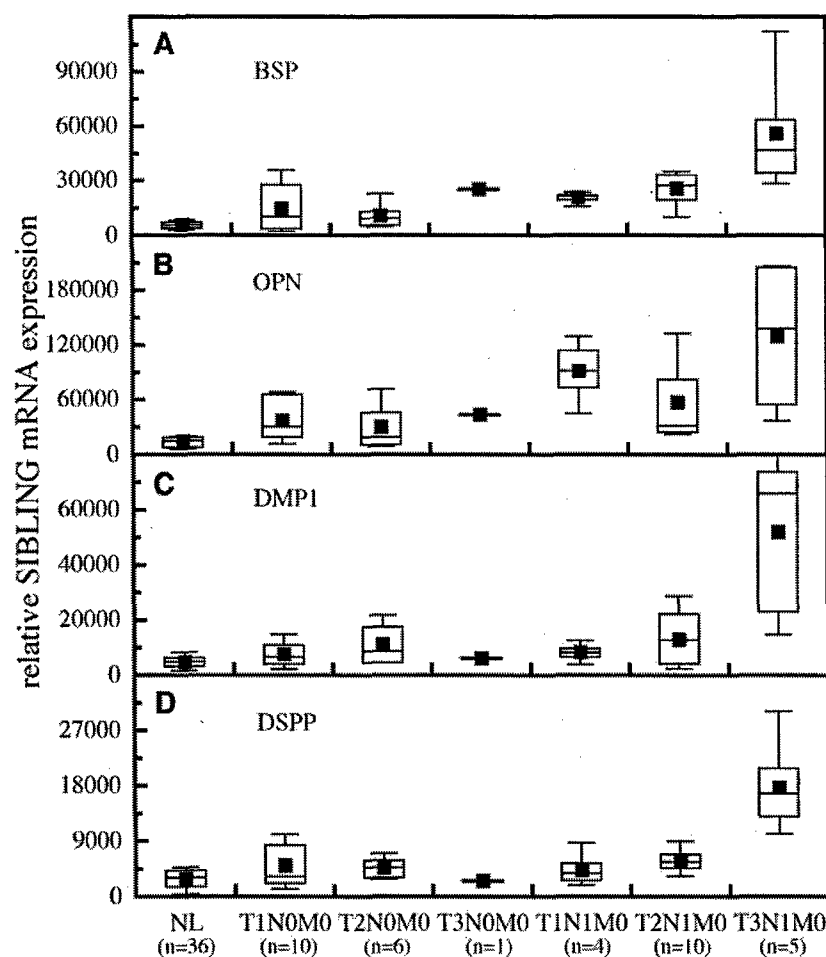

Fig. 7 Comparison of SIBLING mRNA levels and tumor stage in breast cancer. The expression values of BSP (*A*), OPN (*B*), DMP1 (*C*), and DSPP (*D*) by breast cancer tumors were stratified by increasing TNM stage, and the values were compared. *Top line, bottom line,* and *line through the middle* correspond to 75th percentile, 25th percentile, and 50th percentile (median), respectively. *Error bar whiskers* represent the 10th and 90th percentile, whereas ■ indicates the arithmetic mean. Breast cancer TNM staging was as follows: T_1, tumor ≤ 2 cm in greatest dimension; T_2, 2 cm < tumor < 5 cm; T_3, tumor > 5 cm; N_0, no regional lymph node metastasis; N_1, metastasis to movable ipsilateral axillary lymph node(s); N_2, metastasis to movable ipsilateral axillary lymph node(s) fixed to one another or to other structure; M_0, no distant metastasis; and M_1, distant metastasis. The number of subjects (*n*) for each group is shown at the *bottom*. The normal group consisted of the 36 normal breast tissue samples corresponding to the 36 paired tumor tissues with well-defined TNM stage.

Table 2 SIBLING expression in different cancer types

	Breast cancer	Uterine cancer	Colon cancer	Stomach cancer	Ovarian cancer	Lung cancer	Rectal cancer	Thyroid cancer	Kidney cancer
BSP									
t test*	Yes	No	Yes	Yes	No	No	Yes	Yes	Yes
>m + 2 SD†	Yes	No	Yes	Yes	Yes	Yes	Yes	Yes	Yes
Other studies (ref. no.)‡	4 and 28	29				7		8	
OPN									
t test*	Yes	Yes	Yes	No	Yes	Yes	Yes	Yes	No
>m + 2 SD†	Yes	Yes	Yes	Yes	Yes	Yes	Yes	No	No
Other studies (ref. no.)‡	30 and 31		32 and 33	34 and 35	36 and 37	38 and 39		40	2
DMP1									
t test*	Yes	Yes	Yes	No	No	Yes	No	No	No
>m + 2 SD†	Yes	No	No	No	No	Yes	No	No	No
Other studies (ref. no.)‡						9			
DSPP									
t test*	Yes	No	No	No	No	Yes	No	No	No
>m + 2 SD†	No	No	No	No	No	Yes	No	No	No
Other studies (ref. no.)‡									

* Significant elevation defined by a paired t test pairing individual subject's normal and tumor tissue expression levels.
† Significant elevation defined by a mean cancer tissue level of expression >m + 2SD.
‡ Published studies finding increased expression of SIBLINGs in a given tumor type.

SD criteria. DSPP expression was elevated significantly by both criteria in lung cancer, but only by paired t test in breast cancer. Cancers for which the two analysis methods were not in accordance are obvious targets for further, more extensive studies.

The observed increase in MMP-2 expression observed in tumor samples is consistent with previous studies of breast (41, 42), colon (43–47), stomach (48, 49), lung (50–53), rectal (43, 54), and kidney cancer (55–57). Whereas a strong association of increased MMP-3 has been found in breast cancer (41, 58–61), the increased expression levels observed in other tumor types are not as well supported by published literature. Altered MMP-3 levels have been observed in colon (62–64), stomach (65–67), and rectal (68) cancer, although in some cases, the increases were relatively small. In addition, studies have indicated that the MMP-3 source was not necessarily tumor cell but stromal cell or another infiltrating cell type, distinct from the tumor. The observed increases in MMP-9 expression are consistent with published studies of breast (41, 69), uterine (70, 71), colon (46, 53, 72), stomach (73–75), ovarian (76, 77), lung (50, 78), rectal (43, 79), and kidney cancer (56, 80).

A correlation of SIBLING message expression levels with MMP message levels of their partners (BSP with MMP-2, OPN with MMP-3, and DMP1 with MMP-9) was observed. That, in association with the recently described ability of these SIBLINGs to bind to and modulate the activity of specific MMPs, suggests that the same factors that activate SIBLING genes in tumor progression may be the same ones that can activate the corresponding MMP genes. It is also possible that the expression of one SIBLING member in a tumor may induce the production of its corresponding MMP partner, or *vice versa*. Interestingly, SIBLING production by tumors could facilitate angiogenesis because both BSP and OPN have been shown to possess angiogenesis activity *in vivo* (81, 82).

SIBLING expression was different between different subtypes of cancer. Whereas the historical basis for the distinction between the main two types of breast cancer (the belief that ductal carcinomas arose from ducts and lobular carcinomas arose from lobules) is subject to debate (both can arise from the terminal duct lobular unit), there is evidence that the two classes as used clinically refer to disease entities that differ in tumor size, shape, dissemination, and proliferation rates (83). The most common hallmark associated with the lobular classification is multifocality. Lobular tumors tend to be more slowly proliferating than ductal tumors. They also tend to frequently exhibit hormone receptor positivity and show distinct chromosomal changes (84, 85). The more rapidly progressing ductal tumors had an associated higher level of SIBLING expression. OPN was recently identified by microarray analysis as a discriminating marker between ductal and lobular cancer (86). In our current study, OPN, as well as BSP, DMP1, and DSPP were significantly different between lobular and ductal tumors. Similarly, the association of higher OPN expression with adenocarcinomas as opposed to squamous cell carcinomas in uterine cancer may be associated with different size, shape, and progression rates.

SIBLING expression correlated with tumor stages associated with changing size and lymph node involvement. These observations are consistent with SIBLING expression coupled with MMP activity modulation having an effect on early tumor progression. These results suggest SIBLINGs as potential markers of early disease progression in a number of different cancers. Future studies of SIBLING expression and serum levels will address the degree to which these tumor biomarkers can be correlated with disease progression.

REFERENCES

1. Fisher LW, Fedarko NS. Six genes expressed in bones and teeth encode the current members of the SIBLING family of proteins. Connect Tissue Res 2003;44(Suppl 1):33–40.

2. Brown LF, Papadopoulos-Sergiou A, Berse B, et al. Osteopontin expression and distribution in human carcinomas. Am J Pathol 1994; 145:610–23.

3. Coppola D, Szabo M, Boulware D, et al. Correlation of osteopontin protein expression and pathological stage across a wide variety of tumor histologies. Clin Cancer Res 2004;10:184–90.

4. Bellahcene A, Merville MP, Castronovo V. Expression of bone sialoprotein, a bone matrix protein, in human breast cancer. Cancer Res 1994;54:2823–6.

5. Waltregny D, Bellahcene A, de Leval X, et al. Increased expression of bone sialoprotein in bone metastases compared with visceral metastases in human breast and prostate cancers. J Bone Miner Res 2000;15: 834–43.

6. Waltregny D, Bellahcene A, Van Riet I, et al. Prognostic value of bone sialoprotein expression in clinically localized human prostate cancer. J Natl Cancer Inst (Bethesda) 1998;90:1000–8.

7. Bellahcene A, Maloujahmoum N, Fisher LW, et al. Expression of bone sialoprotein in human lung cancer. Calcif Tissue Int 1997;61: 183–8.

8. Bellahcene A, Albert V, Pollina L, et al. Ectopic expression of bone sialoprotein in human thyroid cancer. Thyroid 1998;8:637–41.

9. Chaplet M, De Leval L, Waltregny D, et al. Dentin matrix protein 1 is expressed in human lung cancer. J Bone Miner Res 2003;18:1506–12.

10. Rowe PS, de Zoysa PA, Dong R, et al. MEPE, a new gene expressed in bone marrow and tumors causing osteomalacia. Genomics 2000;67:54–68.

11. Fedarko NS, Jain A, Karadag A, Fisher LW. Three small integrin binding ligand N-linked glycoproteins (SIBLINGs) bind and activate specific matrix metalloproteinases. FASEB J 2004;18:734–6.

12. Zhumabayeva B, Diatchenko L, Chenchik A, Siebert PD. Use of SMART-generated cDNA for gene expression studies in multiple human tumors. Biotechniques 2001;30:158–63.

13. Fisher LW, McBride OW, Termine JD, Young MF. Human bone sialoprotein. Deduced protein sequence and chromosomal localization. J Biol Chem 1990;265:2347–51.

14. Oldberg A, Franzen A, Heinegard D. Cloning and sequence analysis of rat bone sialoprotein (osteopontin) cDNA reveals an Arg-Gly-Asp cell-binding sequence. Proc Natl Acad Sci USA 1986;83:8819–23.

15. Hirst KL, Simmons D, Feng J, et al. Elucidation of the sequence and the genomic organization of the human dentin matrix acidic phosphoprotein 1 (DMP1) gene: exclusion of the locus from a causative role in the pathogenesis of dentinogenesis imperfecta type II. Genomics 1997; 42:38–45.

16. Freije JM, Balbin M, Pendas AM, et al. Matrix metalloproteinases and tumor progression. Adv Exp Med Biol 2003;532:91–107.

17. Chenchik A, Zhu YY, Diatchenko L, Li R, Hill J, Siebert PD. Generation and use of high-quality cDNA from small amounts of total RNA by SMART PCR. In: Siebert P, Larrick J, editors. Gene Cloning and Analysis by RT-PCR. Natick, MA: Eaton Publishing; 1998. p. 305–19.

18. Blanquicett C, Johnson MR, Heslin M, Diasio RB. Housekeeping gene variability in normal and carcinomatous colorectal and liver tissues: applications in pharmacogenomic gene expression studies. Anal Biochem 2002;303:209–14.

19. Rondinelli RH, Epner DE, Tricoli JV. Increased glyceraldehyde-3-phosphate dehydrogenase gene expression in late pathological stage human prostate cancer. Prostate Cancer Prostatic Dis 1997;1:66–72.

20. Aerts JL, Gonzales MI, Topalian SL. Selection of appropriate control genes to assess expression of tumor antigens using real-time RT-PCR. Biotechniques 2004;36:84–6, 88, 90–1.

21. Zhumabayeva B, Chenchik A, Siebert PD, Herrler M. Disease profiling arrays: reverse format cDNA arrays complimentary to microarrays. Adv Biochem Eng Biotechnol 2004;86:191–213.

22. Thiebault K, Mazelin L, Pays L, et al. The netrin-1 receptors UNC5H are putative tumor suppressors controlling cell death commitment. Proc Natl Acad Sci USA 2003;100:4173–8.

23. Liu S, Huang H, Lu X, et al. Down-regulation of thiamine transporter THTR2 gene expression in breast cancer and its association with resistance to apoptosis. Mol Cancer Res 2003;1:665–73.

24. Iavarone C, Wolfgang C, Kumar V, et al. PAGE4 is a cytoplasmic protein that is expressed in normal prostate and in prostate cancers. Mol Cancer Ther 2002;1:329–35.

25. Egland KA, Kumar V, Duray P, Pastan I. Characterization of overlapping XAGE-1 transcripts encoding a cancer testis antigen expressed in lung, breast, and other types of cancers. Mol Cancer Ther 2002;1:441–50.

26. Sers C, Husmann K, Nazarenko I, et al. The class II tumour suppressor gene H-REV107-1 is a target of interferon-regulatory factor-1 and is involved in IFNgamma-induced cell death in human ovarian carcinoma cells. Oncogene 2002;21:2829–39.

27. Wiechen K, Diatchenko L, Agoulnik A, et al. Caveolin-1 is down-regulated in human ovarian carcinoma and acts as a candidate tumor suppressor gene. Am J Pathol 2001;159:1635–43.

28. Bellahcene A, Menard S, Bufalino R, Moreau L, Castronovo V. Expression of bone sialoprotein in primary human breast cancer is associated with poor survival. Int J Cancer 1996;69:350–3.

29. Detry C, Waltregny D, Quatresooz P, et al. Detection of bone sialoprotein in human (pre)neoplastic lesions of the uterine cervix. Calcif Tissue Int 2003;73:9–14.

30. Gillespie MT, Thomas RJ, Pu ZY, et al. Calcitonin receptors, bone sialoprotein and osteopontin are expressed in primary breast cancers. Int J Cancer 1997;73:812–5.

31. Tuck AB, O'Malley FP, Singhal H, et al. Osteopontin expression in a group of lymph node negative breast cancer patients. Int J Cancer 1998;79:502–8.

32. Yeatman TJ, Chambers AF. Osteopontin and colon cancer progression. Clin Exp Metastasis 2003;20:85–90.

33. Agrawal D, Chen T, Irby R, et al. Osteopontin identified as lead marker of colon cancer progression, using pooled sample expression profiling. J Natl Cancer Inst (Bethesda) 2002;94:513–21.

34. Maeng HY, Choi DK, Takeuchi M, et al. Appearance of osteonectin-expressing fibroblastic cells in early rat stomach carcinogenesis and stomach tumors induced with N-methyl-N'-nitro-N-nitrosoguanidine. Jpn J Cancer Res 2002;93:960–7.

35. Ue T, Yokozaki H, Kitadai Y, et al. Co-expression of osteopontin and CD44v9 in gastric cancer. Int J Cancer 1998;79:127–32.

36. Kim JH, Skates SJ, Uede T, et al. Osteopontin as a potential diagnostic biomarker for ovarian cancer. JAMA 2002;287:1671–9.

37. Tiniakos DG, Yu H, Liapis H. Osteopontin expression in ovarian carcinomas and tumors of low malignant potential (LMP). Hum Pathol 1998;29:1250–4.

38. Zhang J, Takahashi K, Takahashi F, et al. Differential osteopontin expression in lung cancer. Cancer Lett 2001;171:215–22.

39. Chambers AF, Wilson SM, Kerkvliet N, et al. Osteopontin expression in lung cancer. Lung Cancer 1996;15:311–23.

40. Tunio GM, Hirota S, Nomura S, Kitamura Y. Possible relation of osteopontin to development of psammoma bodies in human papillary thyroid cancer. Arch Pathol Lab Med 1998;122:1087–90.

41. Lebeau A, Nerlich AG, Sauer U, Lichtinghagen R, Lohrs U. Tissue distribution of major matrix metalloproteinases and their transcripts in human breast carcinomas. Anticancer Res 1999;19:4257–64.

42. Onisto M, Riccio MP, Scannapieco P, et al. Gelatinase A/TIMP-2 imbalance in lymph-node-positive breast carcinomas, as measured by RT-PCR. Int J Cancer 1995;63:621–6.

43. Liabakk NB, Talbot I, Smith RA, Wilkinson K, Balkwill F. Matrix metalloprotease 2 (MMP-2) and matrix metalloprotease 9 (MMP-9) type IV collagenases in colorectal cancer. Cancer Res 1996;56:190–6.

44. Ornstein DL, MacNab J, Cohn KH. Evidence for tumor-host cooperation in regulating MMP-2 expression in human colon cancer. Clin Exp Metastasis 1999;17:205–12.

45. Karakiulakis G, Papanikolaou C, Jankovic SM, et al. Increased type IV collagen-degrading activity in metastases originating from primary tumors of the human colon. Invasion Metastasis 1997;17:158–68.

46. Collins HM, Morris TM, Watson SA. Spectrum of matrix metalloproteinase expression in primary and metastatic colon cancer: relationship to the tissue inhibitors of metalloproteinases and membrane type-1-matrix metalloproteinase. Br J Cancer 2001;84:1664–70.

47. Papadopoulou S, Scorilas A, Arnogianaki N, et al. Expression of gelatinase-A (MMP-2) in human colon cancer and normal colon mucosa. Tumour Biol 2001;22:383–9.

48. Mori M, Mimori K, Shiraishi T, et al. Analysis of MT1-MMP and MMP2 expression in human gastric cancers. Int J Cancer 1997;74: 316–21.

49. Ohtani H, Nagai T, Nagura H. Similarities of in situ mRNA expression between gelatinase A (MMP-2) and type I procollagen in human gastrointestinal carcinoma: comparison with granulation tissue reaction. Jpn J Cancer Res 1995;86:833–9.

50. Nakagawa H, Yagihashi S. Expression of type IV collagen and its degrading enzymes in squamous cell carcinoma of lung. Jpn J Cancer Res .1994;85:934–8.

51. Yamamoto M, Mohanam S, Sawaya R, et al. Differential expression of membrane-type matrix metalloproteinase and its correlation with gelatinase A activation in human malignant brain tumors in vivo and in vitro. Cancer Res 1996;56:384–92.

52. Suzuki M, Iizasa T, Fujisawa T, et al. Expression of matrix metalloproteinases and tissue inhibitor of matrix metalloproteinases in non-small-cell lung cancer. Invasion Metastasis 1998;18:134–41.

53. Creighton C, Hanash S. Expression of matrix metalloproteinase 9 (MMP-9/gelatinase B) in adenocarcinomas strongly correlated with expression of immune response genes. In Silico Biol 2003;3:301–11.

54. Chan CC, Menges M, Orzechowski HD, et al. Increased matrix metalloproteinase 2 concentration and transcript expression in advanced colorectal carcinomas. Int J Colorectal Dis 2001;16:133–40.

55. Kitagawa Y, Kunimi K, Uchibayashi T, Sato H, Namiki M. Expression of messenger RNAs for membrane-type 1, 2, and 3 matrix metalloproteinases in human renal cell carcinomas. J Urol 1999;162: 905–9.

56. Hagemann T, Gunawan B, Schulz M, Fuzesi L, Binder C. mRNA expression of matrix metalloproteases and their inhibitors differs in subtypes of renal cell carcinomas. Eur J Cancer 2001;37:1839–46.

57. Slaton JW, Inoue K, Perrotte P, et al. Expression levels of genes that regulate metastasis and angiogenesis correlate with advanced pathological stage of renal cell carcinoma. Am J Pathol 2001;158:735–43.

58. Freije JM, Diez-Itza I, Balbin M, et al. Molecular cloning and expression of collagenase-3, a novel human matrix metalloproteinase produced by breast carcinomas. J Biol Chem 1994;269:16766–73.

59. Basset P, Bellocq JP, Anglard P, et al. Stromelysin-3 and other stromelysins in breast cancer: importance of epithelialstromal interactions during tumor progression. Cancer Treat Res 1996;83:353–67.

60. Iwata H, Kobayashi S, Iwase H, et al. Production of matrix metalloproteinases and tissue inhibitors of metalloproteinases in human breast carcinomas. Jpn J Cancer Res 1996;87:602–11.

61. Chenard MP, O'Siorain L, Shering S, et al. High levels of stromelysin-3 correlate with poor prognosis in patients with breast carcinoma. Int J Cancer 1996;69:448–51.

62. Baker EA, Bergin FG, Leaper DJ. Matrix metalloproteinases, their tissue inhibitors and colorectal cancer staging. Br J Surg 2000;87: 1215–21.

63. Gallegos NC, Smales C, Savage FJ, Hembry RM, Boulos PB. The distribution of matrix metalloproteinases and tissue inhibitor of metalloproteinases in colorectal cancer. Surg Oncol 1995;4:21–9.

64. Matrisian LM, Wright J, Newell K, Witty JP. Matrix-degrading metalloproteinases in tumor progression. Princess Takamatsu Symp 1994;24:152–61.

65. Murray GI, Duncan ME, Arbuckle E, Melvin WT, Fothergill JE. Matrix metalloproteinases and their inhibitors in gastric cancer. Gut 1998;43:791–7.

66. Nomura H, Fujimoto N, Seiki M, Mai M, Okada Y. Enhanced production of matrix metalloproteinases and activation of matrix metalloproteinase 2 (gelatinase A) in human gastric carcinomas. Int J Cancer 1996;69:9–16.

67. Saarialho-Kere UK, Vaalamo M, Puolakkainen P, et al. Enhanced expression of matrilysin, collagenase, and stromelysin-1 in gastrointestinal ulcers. Am J Pathol 1996;148:519–26.

68. Imai K, Yokohama Y, Nakanishi I, et al. Matrix metalloproteinase 7 (matrilysin) from human rectal carcinoma cells. Activation of the precursor, interaction with other matrix metalloproteinases and enzymic properties. J Biol Chem 1995;270:6691–7.

69. Pacheco MM, Mourao M, Mantovani EB, Nishimoto IN, Brentani MM. Expression of gelatinases A and B, stromelysin-3 and matrilysin genes in breast carcinomas: clinico-pathological correlations. Clin Exp Metastasis 1998;16:577–85.

70. Davidson B, Goldberg I, Liokumovich P, et al. Expression of metalloproteinases and their inhibitors in adenocarcinoma of the uterine cervix. Int J Gynecol Pathol 1998;17:295–301.

71. Davidson B, Goldberg I, Kopolovic J, et al. Expression of matrix metalloproteinase-9 in squamous cell carcinoma of the uterine cervix-clinicopathologic study using immunohistochemistry and mRNA in situ hybridization. Gynecol Oncol 1999;72:380–6.

72. Takeha S, Fujiyama Y, Bamba T, et al. Stromal expression of MMP-9 and urokinase receptor is inversely associated with liver metastasis and with infiltrating growth in human colorectal cancer: a novel approach from immune/inflammatory aspect. Jpn J Cancer Res 1997; 88:72–81.

73. Parsons SL, Watson SA, Collins HM, et al. Gelatinase (MMP-2 and -9) expression in gastrointestinal malignancy. Br J Cancer 1998;78: 1495–502.

74. Torii A, Kodera Y, Ito M, et al. Matrix metalloproteinase 9 in mucosally invasive gastric cancer. Gastric Cancer 1998;1:142–5.

75. Wang L, Zhang LH, Li YL, Liu Z. Expression of MMP-9 and MMP-9 mRNA in gastric carcinoma and its correlation with angiogenesis [in Chinese]. Zhonghua Yi Xue Za Zhi 2003;83:782–6.

76. Sakata K, Shigemasa K, Nagai N, Ohama K. Expression of matrix metalloproteinases (MMP-2, MMP-9, MT1-MMP) and their inhibitors (TIMP-1, TIMP-2) in common epithelial tumors of the ovary. Int J Oncol 2000;17:673–81.

77. Davidson B, Goldberg I, Gotlieb WH, et al. High levels of MMP-2, MMP-9, MT1-MMP and TIMP-2 mRNA correlate with poor survival in ovarian carcinoma. Clin Exp Metastasis 1999;17:799–808.

78. Kremer EA, Chen Y, Suzuki K, Nagase H, Gorski JP. Hydroxyapatite induces autolytic degradation and inactivation of matrix metalloproteinase-1 and -3. J Bone Miner Res 1998;13:1890–902.

79. Roeb E, Dietrich CG, Winograd R, et al. Activity and cellular origin of gelatinases in patients with colon and rectal carcinoma differential activity of matrix metalloproteinase-9. Cancer (Phila) 2001;92: 2680–91.

80. Inoue K, Kamada M, Slaton JW, et al. The prognostic value of angiogenesis and metastasis-related genes for progression of transitional cell carcinoma of the renal pelvis and ureter. Clin Cancer Res 2002;8: 1863–70.

81. Hirama M, Takahashi F, Takahashi K, et al. Osteopontin overproduced by tumor cells acts as a potent angiogenic factor contributing to tumor growth. Cancer Lett 2003;198:107–17.

82. Bellahcene A, Bonjean K, Fohr B, et al. Bone sialoprotein mediates human endothelial cell attachment and migration and promotes angiogenesis. Circ Res 2000;86:885–91.

83. Sainsbury JRC, Anderson TJ, Morgan DAL. Breast cancer. Br Med J 2000;321:745–50.

84. Coradini D, Pellizzaro C, Veneroni S, Ventura L, Daidone MG. Infiltrating ductal and lobular breast carcinomas are characterized by different interrelationships among markers related to angiogenesis and hormone dependence. Br J Cancer 2002;87:1105–11.

85. Gunther K, Merkelbach-Bruse S, Amo-Takyi BK, et al. Differences in genetic alterations between primary lobular and ductal breast cancers detected by comparative genomic hybridization. J Pathol 2001;193: 40–7.

86. Korkola JE, DeVries S, Fridlyand J, et al. Differentiation of lobular versus ductal breast carcinomas by expression microarray analysis. Cancer Res 2003;63:7167–75.

BONE SIALOPROTEIN BINDING TO MATRIX METALLOPROTEINASE-2 ALTERS ENZYME INHIBITION KINETICS.

Alka Jain[*], Larry W. Fisher[#], and Neal S. Fedarko[*]

From the [*]Department of Medicine, Johns Hopkins University, Baltimore, MD 21224 and [#]Craniofacial and Skeletal Diseases Branch, NIDCR, NIH, DHHS, Bethesda, MD. 20892.

Bone sialoprotein (BSP) is induced by multiple neoplasms *in vivo,* its expression levels correlate with tumor stage and it can modulate the activity of matrix metalloproteinase-2 (MMP-2). In this study, the hypothesis that BSP acts biologically to lessen the effectiveness of MMP inhibitors was investigated. Solution and solid phase binding assays were carried out demonstrating that binding between recombinant BSP and latent as well as active MMP-2 does not require the hemopexin domain. BSP binding restored activity to hemopexin-deleted MMP-2 inhibited by tissue inhibitor of matrix metalloproteinase-2 (TIMP2) when activity was measured using both natural, large macromolecular substrates and synthetic, small molecular weight, freely diffusable substrates. BSP effects on TIMP2 inhibition of wild type active MMP-2 were quantified by varying small molecular weight substrate concentrations at different fixed inhibitor concentrations, and solving a general linear mixed inhibition rate equation with a global curve fitting program. The results indicate an ~ 20-fold increase in the competitive inhibition constant and an ~ 10-fold increase in uncompetitive inhibition constant for the MMP-2+BSP complex. To address whether the failure of clinical trials of MMP inhibitors may be explained at least in part by the activity of BSP, the effect of BSP binding to MMP-2 on inhibition by a small molecular weight drug (illomastat) was similarly determined. An over 10-fold increase in K_I was observed. The ability of BSP to modulate MMP inhibitor action in an *in vitro* angiogenesis model system was tested. When human umbilical vein endothelial cells co-cultured with dermal fibroblasts in defined medium were treated with either nM TIMP2 or illomastat, the degree of tubule formation was reduced while the addition of equimolar BSP restored vessel formation.

The Small Integrin Binding LIgand N-linked Glycoprotein (SIBLING) gene family is clustered on human chromosome 4 and its members include bone sialoprotein (BSP), osteopontin, dentin matrix protein 1, matrix extracellular phosphoglycoprotein, and dentin sialophosphoprotein (1). BSP was once thought to be restricted in expression to mineralizing tissue such as bones and teeth (2) but has recently been shown to be expressed in ductal elements of salivary gland (3) and kidney (4). SIBLINGs, including BSP, are also induced in certain neoplasms (5-15). SIBLINGs can be co-localized to the cell surface through binding of $\alpha_v\beta_3$ and/or CD44 (16-18); exhibit correlation between expression levels and tumor stage (19); and bind and modulate the activity of different but specific matrix metalloproteinases (MMP)s (20). Indeed, BSP has been shown to enhance the invasion potential of many human cancer cell lines in vitro by bridging MMP-2 to the cell surface of the cells through the a_vb_3 integrin (18).

MMPs are a family of structurally and functionally related endoproteinases that are involved in development and wound healing as well as cancer angiogenesis and metastasis. We have recently shown that active MMPs inhibited by either tissue inhibitors of MMPs (TIMPs) or low molecular weight synthetic inhibitors can be reactivated by equimolar amounts of the appropriate SIBLING partner (20). The current study was undertaken to determine whether BSP action on MMP-2 inhibition involves the hemopexin domain, and to see if the SIBLING alters MMP affinity for substrates, TIMP2 or small molecular weight inhibitors. The biological consequences of these interactions were tested in an *in vitro* model system of angiogenesis.

Materials and Methods

Reagents. Pro- and active human MMP-2 was obtained from Oncogene Research Products (Boston, MA) and Research Diagnostic Systems, Inc. (Minneapolis, MN). Recombinant human MMP-2 lacking the hemopexin domain was

purchased from Biomol Research Laboratories, Inc. (Plymouth Meeting, PA). The inhibitor illomastat (GM6001, or N-[(2R)-2-(hydroxamido-carbonylmethyl)-4-methylpentanoyl]-L-tryptophan methylamide), substrate Ac-PLG-[2-mercapto-4-methyl-pentanoyl]-LG-OC$_2$H$_5$, and 5,5'-dithio-bis-2-nitrobenzoic acid (DTNB) were obtained from Calbiochem (La Jolla, CA). TIMP2 was a generous gift of Dr. H. Birkedal-Hansen, NIDCR, NIH. Human serum adsorbed goat anti-rabbit IgG conjugated to horseradish peroxidase (HRP) was obtained from Kirkegaard & Perry (Gaithersburg, MD). Recombinant human BSP that included post translational modifications was made using an adenovirus construct and eukaryotic cells and purified (> 95% purity as defined by acrylamide gel electrophoresis) as previously described (16).

Fluorescent binding studies. Intrinsic tryptophan fluorescence binding studies of BSP and mutant hemopexin-deleted MMP-2 were carried out as previously described (20). BSP contains no tryptophan groups while the hemopexin-deleted MMP-2, contains 8 so the intrinsic fluorescence changes are a result of the change in conformation of the MMP alone. Briefly, the relative change in fluorescence in the area under the emission curve (300 to 500 nm at 295 nm excitation) was used to determine binding curves. Fractional acceptor saturation (f_a) as a function of nM BSP added was determined by calculating $f_a = (y - y_f)/(y_b - y_f)$, where y_f and y_b are the area under the curve of the fluorescent emission profile of free and fully bound MMP-2. Scatchard plots were made by fitting the transformed data to the function $r/[BSP] = n/K_d - r/K_d$, where r represents the binding function, [BSP], BSP concentration, n the number of binding sites and K_d the dissociation constant.

Solid phase binding assays. The binding of BSP to purified and immobilized MMP-2 was measured by an indirect sandwich assay. Plates were coated with the different forms of MMP-2 by adding 0.1 ml of 3.5 nM recombinant purified MMP-2 in 50 mM NaHCO$_3$, pH 9.0 to each well of a Greiner high-binding 96-well microtiter plates (stock # 655061, Greiner Bio-One, Longwood, FL) incubated overnight at 4°C. The plates were blocked with 5 % (w/v) nonfat dry milk in TBS for 60 min and then rinsed three times with TBS

containing 0.05 % Tween 20. BSP was added in nM equivalents in TBS-Tween and incubated for 120 min at room temperature. After a second round of three washes, bound ligand was quantified by the addition of a 1:50,000 dilution of specific rabbit anti-BSP antibody, LF100 (21), followed by a 60 min incubation. After three washes, second antibody (1:2000 goat anti-rabbit horseradish peroxidase conjugated antibody) was added and incubated for a further 60 min and color was developed using diaminobenzamidine substrate, and the absorbance at 405 nm was measured. Non-specific binding was measured by determining the ligand binding to wells coated with BSA alone, and these values were subtracted from the corresponding values for MMP-coated wells.

High molecular weight substrate studies. Fluorescein-conjugated gelatin (Molecular Probes, Inc., Eugene, OR) substrate was used to follow proteolytic activity as previously described (20). This substrate is highly substituted with fluorescein moieties so that the fluorescent signal is self-quenched until proteolytic cleavage liberates fragments and a robust fluorescent emission is measured. The reaction mixture consisted of the fluorescein-substrate conjugate with 1.4 nM mutant hemopexin-free MMP -2 reacted with either 10 nM TIMP2, 10 nM TIMP2 + 10 nM BSP, 10 nM BSP, or buffer alone (50 mM Tris, pH 7.6, 150 mM NaCl, 5 mM CaCl$_2$). Relative velocity plots were determined by varying the substrate concentration between 0.025 and 15 µg/ml and determining the change in fluorescence over the first hour of reaction. Inhibitor titrations were carried out by varying TIMP2 concentration from 1.6 to 1600 nM. Fluorescent data was acquired with excitation at 485 nm and emission at 535 nm. Conditions were run in duplicate.

Low molecular weight substrates. The activities of mutant and wild type MMP-2 in the presence and absence of TIMP2 and BSP were measured using a small molecular weight thiopeptide substrate (Ac-PLG-[2-mercapto-4-methyl-pentanoyl]-LG-OC$_2$H$_5$). Substrate was incubated in assay buffer (50 mM HEPES, 10 mM CaCl$_2$, 0.05% Brij-35, 1 mM DTNB, pH 7.5) with 10 nM MMP-2 + different concentrations of

2

TIMP2, a 10 nM [MMP-2+BSP] preformed complex or MMP2 + TIMP2 + BSP added simultaneously. Data from the first six minutes were used to calculate velocity (pmols/sec) values. Substrate cleavage was monitored using a Perkin Elmer Victor 2 multilabel plate reader and absorbance was measured at 412 nM. Preformed complexes of [MMP-2+BSP] were formed by incubation at 37 C for 30 minutes prior to addition to the reaction mixture.

SDS PAGE, zymography. 10% zymogram gelatin gels were obtained from Invitrogen, Inc., (Carlsbad, CA). Samples in zymogram gel sample buffer were electrophoresed at a constant 125 V for 90 min. Gels were processed for zymography according to the manufacture's instructions, stained with 0.5% Coomassie Blue R250, and bands were visualized by dynamic integrated exposure using an AlphaInotech imaging system (Alpha Inotech Corp., San Leandro, CA).

In vitro angiogenesis. Human umbilical vein endothelial cell (HUVEC) and human dermal fibroblast co-cultures and EGM-2 defined medium were obtained from TCS Cell Works (Botolph Claydon, UK). The functional readout from this *in vitro* assay was tubule formation. Tubule formation was defined by the total number of tubules, total tubule length, mean tubule length, and number of branches. Test conditions were run in triplicate wells with 8 conditions per 24 well plate. The cells were treated starting on day six of culture with 5 nM BSP, 5 nM TIMP2, 5nM BSP + TIMP2, 5 nM GM6001, 5 nM GM6001 + BSP, or buffer alone. Medium was changed every other day with fresh medium containing experimental conditions. Cells were fixed in 70 % ethanol on day 12 and tubule formation was quantified following immunostaining with a mouse anti-human PECAM-1 monoclonal antibody (TCS Cell Works), and the secondary antibody being goat anti-mouse IgG alkaline phosphatase coupled antibody, with 5-bromo-4-chloro-3-indolyl phosphate/ nitro blue tetrazolium (BCIP/NBT; Sigma) as substrate. Images were visualized on a Nikon Diaphot inverted microscope and digitized with a Polaroid CCD digital camera and software. Two images per well were captured, digitized and the number of tubules, the number of branch points (junctions) between tubules, as well as the total tubule length (in pixels) determined using

AngioSys Version 1.0 software. (TCS Cell Works, Botolph Claydon, UK).

For zymographic analyses of MMP-2, a membrane-associated fraction was prepared from the HUVEC cocultures essentially as described by Ward et al (22). Briefly, HUVEC cells were scraped from culture wells in cold 5 mM Tris HCl (pH 7.8), homogenized, and crude membranes were prepared by centrifugation of the cell lysate at 10 000 x g for 15 minutes at 4°C. The supernatant was centrifuged at 105 000 x g for 1 hour at 4°C; then, the supernatant was removed and saved, and the membrane fraction was resuspended in 20 mM Tris HCl (pH 7.8), 10 mM $CaCl_2$, and 0.05% Brij 35.

RESULTS

Bone sialoprotein binding does not require the hemopexin domain. MMPs consist of a catalytic domain and a hemopexin-like domain thought to be essential for the binding of many natural substrates. TIMPs have binding sites in both the hemopexin and catalytic domains (23). We have shown previously that BSP can bind to both pro- and active MMP-2 (20). Whether BSP interacts with the hemopexin domain or, at least in part, with the catalytic region was investigated by studying the binding characteristic of BSP to recombinant human MMP-2 that lacks the hemopexin domain. When the intrinsic tryptophan fluorescence of the mutant MMP-2 was followed during titration with BSP, quenching of the signal similar to that previously seen for the intact MMP-2 was observed (Fig. 1). The area under the emission peaks was quantified and used to determine the change in fluorescence and calculate both the fractional acceptor saturation as a function of nM BSP added and a corresponding Scatchard plot. BSP binding was saturable and its affinity for the mutant protein was actually higher than that for intact MMP-2 (K_d = 0.07 ± 0.03 nM for mutant MMP-2 versus 0.32 ± 0.02 nM for active MMP-2, and 2.9 ± 0.9 nM for pro-MMP-2).

An alternative method to confirm BSP and MMP-2 binding was employed. Solid phase binding assays were developed to measure BSP binding to immobilized forms of MMP-2. Microtiter plates coated with either proMMP-2, active MMP-2 or hemopexin-deleted MMP-2 were

reacted with increasing concentrations of BSP and the amount bound quantified by specific antibodies (Fig. 1D). The binding of BSP to MMP variants was saturable. Scatchard plot analysis revealed BSP binding with a $K_d = 0.39 \pm 0.04$ nM for mutant MMP-2 versus 0.36 ± 0.04 nM for active MMP-2 and 2.1 ± 0.1 nM for pro- MMP-2 (Fig. 1E). While the pro- and active forms of MMP-2 exhibited essentially similar binding constants by the two different binding methods, the mutant form of MMP-2 exhibited a distinct K_d value which may be reflecting differences in solid phase binding orientation in the absence of the hemopexin domain.

Bone sialoprotein modulation of MMP-2 activity does not require the hemopexin domain. We recently reported that BSP can restore enzymatic activity to MMP-2 incubated with TIMP2 when activity was followed using a natural, large molecular weight substrate (gelatin) (20). The effect of BSP on the activity of the mutant MMP-2 was therefore investigated using the gelatin-fluorescein large molecular weight substrate assay (Fig. 2 A-C). The change in substrate fluorescence caused by mutant MMP-2 alone compared to a complex of equimolar mutant MMP-2 + BSP was not significantly different. As expected, the addition of equimolar TIMP2 to mutant MMP-2 caused a significant decrease in the rate of fluorescence change. However, inclusion of equimolar BSP to mutant MMP-2 + TIMP2 complexes restored the rate of fluorescence change to that of mutant MMP-2 alone showing that the TIMP2 became ineffective in the presence of bound BSP. Substrate velocity plots as a function of substrate concentration yielded no significant difference for mutant MMP-2 in the presence or absence of BSP. Titration of the large molecular weight substrate given to mutant MMP-2 + TIMP2 complexes revealed that over a 100-fold excess of TIMP2 was required to inhibit activity to 20 %. For complexes of equimolar mutant MMP-2 + TIMP2, the rate of the reaction was decreased to 67 %, while the presence of equimolar BSP restored activity to 97 %.

A low molecular weight peptide substrate assay, which provides a better measure of the catalytic site only, was next used and enabled kinetic parameters to be evaluated (Fig. 2 D-E).

Similar to results with the large molecular weight substrate, the addition of BSP alone did not significantly alter mutant MMP-2 enzyme product evolution. Furthermore, the TIMP2 inhibited product evolution as expected and the addition of BSP to the preformed mutant MMP-2/TIMP2 complex returned the digestion to uninhibited levels. Substrate velocity plots of mutant MMP-2 ± BSP yielded no statistically significant difference in fitted K_m or v_{max} values (Table I) verifying the observations with the larger substrate that the conformational changes induced by BSP did not significantly affect the actions of the active site itself. Titration of the small molecular weight substrate and mutant MMP-2 with varying concentrations of TIMP2 indicated that at 10-fold excess, TIMP2 inhibited mutant MMP-2 activity to 20 %, while equimolar TIMP2 inhibited mutant MMP-2 and to 34 %. The addition of equimolar BSP was able to restore the activity of mutant MMP-2 treated with TIMP2 to 85 %. These data suggest that BSP reactivation of TIMP2-inhibited MMP-2 does not require the hemopexin domain of MMP-2.

TIMP Inhibition kinetics. To determine the effect of BSP on active wild type MMP-2 and TIMP2 reaction kinetics, the small molecular weight substrate was employed to follow product evolution over time. MMP-2 incubated with increasing concentrations of TIMP2 exhibited the expected dose-dependent inhibition (Fig. 3A). The inhibition by TIMP2 was significantly decreased by the presence of either a performed complex of [MMP-2+BSP] or by the simultaneous addition of BSP and TIMP2 to MMP-2 (Fig. 3B, C). To investigate whether decreased inhibition of MMP-2 by TIMP2 in the presence of BSP was associated with an altered affinity, substrate-velocity plots were obtained by varying substrate concentrations of each at different but fixed inhibitor concentrations. Reaction conditions included either TIMP2 + 10 nM MMP-2, TIMP2 + preformed equimolar complexes of 10 nM [MMP-2+BSP], or simultaneous mixes of TIMP2 + 10 nM MMP-2 + 10 nM BSP (Fig. 3D - E).

Because there are two distinct binding sites for TIMP2 on MMP-2, TIMP2 does not act purely as a competitive inhibitor (24). The common types of inhibition (competitive,

uncompetitive, noncompetitive) are all special cases of linear mixed inhibition (25). The generalized linear mixed inhibition equation $v = V_{max}[S]/\{K_m(1+ [I]/K_{ic}) + [S](1+[I]/K_{iu})\}$, was employed to determine the reaction rate. V_{max} is the limiting rate, K_m is the Michaelis constant, K_{ic} is the competitive inhibition constant and K_{iu} is the uncompetitive inhibition constant. For competitive inhibition, $[I]/K_{iu}$ is negligible while for uncompetitive inhibition $[I]/K_{ic}$ is negligible. In pure noncompetitive inhibition the inhibition constants are equal.

The family of substrate-velocity curves (Fig. 3D-F) were solved for linear mixed inhibition using a global curve-fitting program (Prism 4, GraphPad Software, Inc.,) with V_{max}, K_m, K_{ic} and K_{iu} set as shared parameters. The results indicate a significant increase in K_{ic} and K_{iu} values for the [MMP-2+BSP] complex as well as the simultaneously added MMP-2 + BSP (Table I). This indicates a relatively poor affinity of the inhibitor for MMP-2 in the presence of BSP. The order of magnitude change in apparent inhibitor affinity for MMP-2 in the presence of BSP indicates that SIBLING modulation of MMPs can be physiologically significant.

Illomastat inhibitor kinetics. The MMP inhibitor illomastat was utilized to test whether small molecular weight drug inhibition of MMP-2 activity could be modulated by BSP. Illomastat at a 1 nM concentration inhibited the initial velocity of MMP-2 activity to 39 % of control activity, while the same concentration of inhibitor reduced the activity of the [MMP2+BSP] complex to only 70 % of control suggesting that the inhibitor is much less effective against MMP-2 in the conformation resulting from the binding of BSP (Figure 4A). To quantify the effects of BSP on MMP-2 inhibitor kinetics, substrate-velocity plots were obtained by varying substrate concentrations of each at different but fixed illomastat concentrations. Reaction conditions were either 10 nM MMP-2 alone, or with preformed 10 nM equimolar [MMP-2+BSP] complexes (Fig. 4B, C).

Because Illomastat is a competitive inhibitor, kinetic parameters in the presence and absence of BSP can be determined by fitting the substrate-velocity curves to the equation for competitive inhibition: $v = v_{max}[S]/K_m(1+[I]/K_{ic})+[S]$; where V_{max} is the limiting rate, K_m is the Michaelis constant, K_{ic} is the competitive inhibition constant, [S] is substrate concentration and [I] is illomastat concentration. The family of substrate-velocity curves were solved for competitive inhibition using a global curve-fitting program (Prism 4, GraphPad Software, Inc.,) with V_{max}, K_m, and K_{ic} set as shared parameters. The results indicated a significant increase (~ 100-fold) in K_{ic} value for the [MMP-2+BSP] complex (Table I). Thus illomastat exhibited a reduced affinity for MMP-2 in the presence of BSP.

BSP restores activity to inhibited MMPs in vitro. The ability of BSP to restore enzymatic activity to TIMP2- and illomastat-inhibited MMP-2 in a purified component assay led to a screen of the effects of BSP on MMP inhibitors in an *in vitro* angiogenesis system. 5 nM BSP alone stimulated tubule formation by HUVEC cells while separately illomastat (GM6001) and TIMP2 inhibited tubule formation below control levels (Figure 5). The inclusion of BSP with MMP-specific inhibitors restored tubule formation. Quantification of tubule formation using AngioSys Ver. 1.0 software revealed that the addition of BSP to TIMP2 or illomastat-treated cells restored not only the number of tubules but also the number of branch points and total tubule length (in pixels) to values not significantly different from BSP enhancement alone (Figure 6). The effect of BSP on MMP-2 levels and activity in the *in vitro* angiogenesis system was also studied by two other, complementary systems. MMP activity measured by the fluorescein-gelatin substrate assay and a rate of digestion of gelatin by zymography. Both assays exhibited a consistent pattern of increased enzymatic activity in BSP-treated conditions.

DISCUSSION

BSP is a member of the SIBLING gene family (2). It is extended and flexible in solution and such lack of ordered structure is shared by a number proteins that have multiple binding partners (1). BSP can bind the $\alpha_v\beta_3$ integrin (via its RGD sequence) (26,27) and to complement Factor H (16). BSP can also bind to and modulate

the activity of MMP-2 (20). BSP binding to latent MMP-2 was associated with increased proteolytic activity and BSP binding to TIMP2-inhibited MMP-2 restored activity (20). Binding of BSP to MMP-2 caused conformational changes as observed by fluorescent quenching of MMP-2's tryptophan residues during BSP binding titration (indicating a change in the microenvironment of the MMP's tryptophans). A trimolecular complex of BSP, $\alpha_v\beta_3$ and MMP-2 has been demonstrated by immunoprecipitation, flow cytometry, and *in situ* hybridization in cancer cells grown *in vitro* (18). BSP message was induced in multiple cancers and its expression correlated with paired MMP-2 expression as well as tumor stage (19).

MMP-2, a gelatinase that can degrade components of the extracellular matrix at physiological pH, is regulated *in vivo* by the naturally occurring TIMPs. TIMP2 binding to MMP-2 involves distinct domains on both the inhibitor and the enzyme (28-30). The binding and kinetics of MMP-2 and TIMP2 are more complex than simple competitive inhibition. In our analyses we have used a mixed linear model of mixed inhibition (25) and observed inhibition constants in the ≤ nM range. K_I values in sub-nanamolar range for TIMP2 and MMP-2 using the same substrate have been reported in the literature (31-33), though a more recent analysis has yielded 3- to 4-fold higher estimation (23). The different reported values are most likely due to differences in sources and concentrations of substrate, enzyme and inhibitor.

SIBLING binding to active MMPs inhibited by TIMP or small molecular weight MMP-specific inhibitors could restore activity through multiple mechanisms. Possible mechanisms include blocking inhibitor access (steric blocking), binding to the inhibitor (stripping), or by altering inhibitor affinity. The analysis of inhibitor kinetic parameters as well as binding order effects can be used to distinguish between steric blocking or affinity changes. Based on the current studies with BSP, MMP-2 and TIMP2, SIBLING binding to MMP did not significantly alter K_m values but did alter MMP affinity for inhibitor. SIBLING binding to inhibitor (stripping) was not observed.

BSP was found to significantly reduce the affinity of a small molecular weight synthetic inhibitor (illomastat) for MMP-2. Illomastat as a hydroxamate class inhibitor blocks the activity of multiple MMPs and has been used to disrupt angiogenesis and metastasis (34-36), TNFα processing (37), and experimental autoimmune encephalitis (38). The magnitude of change in apparent inhibitor affinity for MMP-2 in the presence of BSP indicates that SIBLING modulation of MMP inhibition by small molecular weight drugs can be physiologically significant.

Finally, a cell culture model system was used to test whether BSP modulation of MMP-2 inhibition occurs *in vitro*. The *in vitro* model of angiogenesis utilized human umbilical vein endothelial cells (HUVECs) co-cultured with normal adult human diploid dermal fibroblasts. The endothelial cells form small islands amongst the fibroblasts, proliferate, and migrate through the co-culture matrix to form thread-like tubule structures. These cord-like structures join up to form a network of anastomosing tubules. These linked tubules produce endothelial cell-specific components such as von Willebrand Factor and PECAM-1 (CD31) that can be stained immunohistochemically and quantified. The observed effects of BSP (stimulating basal tubule formation and restoring formation to TIMP2- or illomastat-inhibited cultures) was consistent with BSP modulating MMP-2 activity. Profiling MMP-2 levels and activity in the *in vitro* system (by zymography and fluorescent substrate assays) demonstrated changes with BSP treatment. BSP has been shown to promote angiogenesis in the chick chorioallantoic membrane system (40). Thus, BSP has biochemical and biological plausibility to be playing an active role in tumor progression *in vivo*. BSP is induced by multiple neoplasms *in vivo* and its modulation of MMP inhibition might contribute to the relative lack of efficacy seen in the recent clinical trials of MMP inhibitors in numerous cancers (39).

APPENDIX IV

Literature Cited

1. Fisher, L. W., Torchia, D. A., Fohr, B., Young, M. F., and Fedarko, N. S. (2001) *Biochem. Bophys. Res. Comm.* **280**, 460-465

2. Fisher, L. W., and Fedarko, N. S. (2003) *Connect Tissue Res* **44 Suppl 1**, 33-40

3. Ogbureke, K. U., and Fisher, L. W. (2004) *J Dent Res* **83**, 664-670

4. Ogbureke, K. U., and Fisher, L. W. (2005) *Kidney Int* **68**, 155-166

5. Craig, A. M., Bowden, G. T., Chambers, A. F., Spearman, M. A., Greenberg, A. H., Wright, J. A., McLeod, M., and Denhardt, D. T. (1990) *Int J Cancer* **46**, 133-137

6. Gillespie, M. T., Thomas, R. J., Pu, Z. Y., Zhou, H., Martin, T. J., and Findlay, D. M. (1997) *Int J Cancer* **73**, 812-815

7. Hirota, S., Nakajima, Y., Yoshimine, T., Kohri, K., Nomura, S., Taneda, M., Hayakawa, T., and Kitamura, Y. (1995) *J Neuropathol Exp Neurol* **54**, 698-703

8. Senger, D. R., Perruzzi, C. A., and Papadopoulos, A. (1989) *Anticancer Res* **9**, 1291-1299

9. Sung, V., Stubbs, J. T., 3rd, Fisher, L., Aaron, A. D., and Thompson, E. W. (1998) *J Cell Physiol* **176**, 482-494

10. Bellahcene, A., Kroll, M., Liebens, F., and Castronovo, V. (1996) *J Bone Miner Res* **11**, 665-670

11. Bellahcene, A., Albert, V., Pollina, L., Basolo, F., Fisher, L. W., and Castronovo, V. (1998) *Thyroid* **8**, 637-641

12. Bellahcene, A., Merville, M. P., and Castronovo, V. (1994) *Cancer Res* **54**, 2823-2826

13. Bellahcene, A., Maloujahmoum, N., Fisher, L. W., Pastorino, H., Tagliabue, E., Menard, S., and Castronovo, V. (1997) *Calcif Tissue Int* **61**, 183-188

14. Chaplet, M., De Leval, L., Waltregny, D., Detry, C., Fornaciari, G., Bevilacqua, G., Fisher, L. W., Castronovo, V., and Bellahcene, A. (2003) *J Bone Miner Res* **18**, 1506-1512

15. Rowe, P. S., de Zoysa, P. A., Dong, R., Wang, H. R., White, K. E., Econs, M. J., and Oudet, C. L. (2000) *Genomics* **67**, 54-68

16. Fedarko, N. S., Fohr, B., Gehron Robey, P., Young, M. F., and Fisher, L. W. (2000) *J. Biol. Chem.* **275**, 16666-16672

17. Jain, A., Karadag, A., Fohr, B., Fisher, L. W., and Fedarko, N. S. (2002) *J Biol Chem* **277**, 13700-13708

18. Karadag, A., Ogburke, K. U. E., Fedarko, N. S., and Fisher, L. W. (2004) *J. Natl. Cancer Inst.* **96**, In press.

19. Fisher, L. W., Jain, A., Tayback, M., and Fedarko, N. S. (2004) *Clin. Can. Res* **10**, 8501-8511

20. Fedarko, N. S., Jain, A., Karadag, A., and Fisher, L. W. (2004) *Faseb J* **18**, 734-736

21. Mintz, K. P., Grzesik, W. J., Midura, R. J., Robey, P. G., Termine, J. D., and Fisher, L. W. (1993) *J Bone Miner Res* **8**, 985-995

22. Ward, R. V., Atkinson, S. J., Slocombe, P. M., Docherty, A. J. P., Reynolds, J. J., and Murphy, G. (1991) *Biochim Biophys Acta.* **1079**, 242-246.

23. Olson, M. W., Gervasi, D. C., Mobashery, S., and Fridman, R. (1997) *Journal of Biological Chemistry* **272**, 29975-29983.

24. Kleiner, D. E., Jr., Unsworth, E. J., Krutzsch, H. C., and Stetler-Stevenson, W. G. (1992) *Biochemistry* **31**, 1665-1672

25. Cortes, A., Cascante, M., Cardenas, M. L., and Cornish-Bowden, A. (2001) *Biochem J* **357**, 263-268

26. Oldberg, A., Franzen, A., and Heinegard, D. (1986) *Proc Natl Acad Sci U S A* **83**, 8819-8823

27. Fisher, L. W., McBride, O. W., Termine, J. D., and Young, M. F. (1990) *J Biol Chem* **265**, 2347-2351

28. Willenbrock, F., Crabbe, T., Slocombe, P. M., Sutton, C. W., Docherty, A. J., Cockett, M. I., O'Shea, M., Brocklehurst, K., Phillips, I. R., and Murphy, G. (1993) *Biochemistry* **32**, 4330-4337

29. Nguyen, Q., Willenbrock, F., Cockett, M. I., O'Shea, M., Docherty, A. J., and Murphy, G. (1994) *Biochemistry* **33**, 2089-2095

30. Hutton, M., Willenbrock, F., Brocklehurst, K., and Murphy, G. (1998) *Biochemistry* **37**, 10094-10098

31. O'Shea, M., Willenbrock, F., Williamson, R. A., Cockett, M. I., Freedman, R. B., Reynolds, J. J., Docherty, A. J., and Murphy, G. (1992) *Biochemistry* **31**, 10146-10152

32. Murphy, G., and Docherty, A. J. (1992) *Am J Respir Cell Mol Biol* **7**, 120-125

33. O'Connell, J. P., Willenbrock, F., Docherty, A. J., Eaton, D., and Murphy, G. (1994) *J Biol Chem* **269**, 14967-14973

34. Boghaert, E. R., Chan, S. K., Zimmer, C., Grobelny, D., Galardy, R. E., Vanaman, T. C., and Zimmer, S. G. (1994) *J Neurooncol* **21**, 141-150

35. Galardy, R. E., Grobelny, D., Foellmer, H. G., and Fernandez, L. A. (1994) *Cancer Res* **54**, 4715-4718

36. Winding, B., NicAmhlaoibh, R., Misander, H., Hoegh-Andersen, P., Andersen, T. L., Holst-Hansen, C., Heegaard, A. M., Foged, N. T., Brunner, N., and Delaisse, J. M. (2002) *Clin Cancer Res* **8**, 1932-1939

37. Solorzano, C. C., Ksontini, R., Pruitt, J. H., Auffenberg, T., Tannahill, C., Galardy, R. E., Schultz, G. P., MacKay, S. L., Copeland, E. M., 3rd, and Moldawer, L. L. (1997) *Shock* **7**, 427-431

38. Gijbels, K., Galardy, R. E., and Steinman, L. (1994) *J Clin Invest* **94**, 2177-2182

39. Mandal, M., Mandal, A., Das, S., Chakraborti, T., and Sajal, C. (2003) *Mol Cell Biochem* **252**, 305-329

40. Bellahcene, A., Bonjean, K., Fohr, B., Fedarko, N. S., Robey, F. A., Young, M. F., Fisher, L. W., and Castronovo, V. (2000) *Circ Res* **86**, 885-891

FIGURE LEGENDS

Figure 1. BSP binding to MMP-2 does not require the hemopexin domain. Binding interactions between mutant MMP-2 lacking the hemopexin domain and BSP were followed by intrinsic tryptophan fluorescence of the MMP-2 protein (BSP has no tryptophans). 1 nM mutant MMP-2 was reacted with increasing concentration of BSP. Intrinsic tryptophan fluorescence was monitored by excitation at 295 nm and recording emission from 300 to 500 nm using a Photon Technology International Series M fluorimeter (A). Binding saturation was followed by monitoring the change in the area under the emission peak curve (inset). The area under the emission peak curve was used to determine a binding curve by calculating fractional acceptor saturation versus nM BSP added (B) and the corresponding Scatchard plot (C). The binding interaction between BSP and latent MMP-2 ($\diamond$), active MMP-2 (O) and mutant hemopexin-free MMP-2 ($\square$) were investigated by solid phase binding assays (D). Scatchard plots derived from solid phase binding assays of BSP and latent MMP-2, active MMP-2 and hemopexin-deleted MMP-2 were determined (E.).

Figure 2. BSP binding to hemopexin-deleted MMP-2 keeps TIMP2 from inhibiting the protease activity. The effect of BSP on the activity of the mutant MMP-2 was profiled using the fluorescein-labeled large molecular weight (gelatin) substrate assay (A). Reaction conditions included mutant MMP2 ($\square$), mutant MMP2 + BSP (O), mutant MMP2 + TIMP2 ($\triangle$), and mutant MMP2 + TIMP2 +BSP ($\blacktriangle$). The effect of a varying substrate concentration on the relative velocity of the mutant enzyme in the presence (O) or absence ($\square$) of BSP was analyzed by linear regression analysis over the first hour and the slope determined at each substrate concentration (B). Similarly, the relative rates of 12.5 µg/ml substrate cleavage by 1.4 nM mutant MMP-2 in the presence of increasing concentrations of TIMP2 were compared by plotting the fluorescent change/min at each dose (C). Conditions included mutant MMP2 alone ($\square$), mutant MMP2 + TIMP2 ($\triangle$), and mutant MMP2 + TIMP2 + BSP ($\blacktriangle$). The action of BSP on mutant MMP2 activity using a small molecular weight substrate was determined by following pmol product evolution over time (D), velocity plots (E) and TIMP2 inhibition curves (F). Reaction conditions included mutant MMP2 ($\square$), mutant MMP2 + BSP (O), mutant MMP2 + TIMP2 ($\triangle$), and mutant MMP2 + TIMP2 +BSP ($\blacktriangle$). For substrate titrations and TIMP2 dose response, three separate experiments were combined and values plotted present the mean with error bars representing the standard deviation.

Figure 3. BSP effects on TIMP2 inhibition of MMP-2. Small molecular weight substrate was incubated in assay buffer at a final concentration of 100 µM with (A) 10 nM MMP-2 and different concentrations of TIMP2 or (B) 10 nM preformed complex of [MMP-2+BSP] incubated with increasing concentrations of TIMP2, or (C) simultaneously added 10 nM MMP-2 + BSP and different concentrations of TIMP2. TIMP2 concentrations ranged from 0 ($\square$), 1 (O), 5 ($\triangle$), 10 ($\diamond$), and 20 (∇) nM TIMP2. MMP-2 and BSP concentration was 10 nM. Reaction rates were profiled by increasing substrate concentration from 10 to 200 µM. Data from the first six minutes of each reaction condition were used to calculate V_0 (pmols/sec) values. Substrate-velocity plots of MMP-2 incubated with different concentrations of TIMP2 (D), of [MMP-2+BSP] complexes incubated with varying concentrations of TIMP2 (E), or of MMP-2 incubated simultaneously with TIMP2 and BSP (F) were determined. Preformed complexes of [MMP-2+BSP] were formed by incubation at 37 C for 30 minutes prior to addition to the reaction mixture. Six separate experiments were combined for each condition and values shown represent the mean ± the standard deviation.

Figure 4. BSP effects on illomastat (GM6001) inhibition of MMP-2. 100 µM peptide substrate was incubated with 10 nM MMP-2 ($\square$), 10 nM MMP2 + 1 nM illomastat ($\triangle$), or [10 nM MMP2+10 nM BSP] + 1 nM illomastat ($\blacktriangle$) and the evolution of product followed by absorbance at 405 nm (A). Substrate-velocity plots were generated by increasing substrate concentration at different fixed inhibitor concentrations with the slope over the first six minutes being used to calculate V_0 values (B, C). Active MMP-2 was incubated with illomastat whose concentration varied from 0 ($\square$), 0.1 (O), 0.5 ($\triangle$), 1 ($\diamond$), 5

APPENDIX IV

(∇), and 10 ($\oplus$) nM. The inhibitor was added to either directly to MMP-2 (B) or to a preformed complex of [MMP-2+BSP] (C).

Figure 5. BSP stimulates angiogenesis and overcomes MMP-2 inhibitors *in vitro*. HUVEC cells were treated starting on day 6 of culture with vehicle alone (A), 5 nM GM6001 (B), 5 nM TIMP2 (C), 5 nM BSP (D), as well as combinations of 5 nM BSP + 5 nM GM6001 (E) or 5 nM BSP + 5 nM TIMP2 (F). The cells were fixed on day 12 and probed with a PECAM1 antibody (blue) to visualize tubule formation. Note that BSP stimulated tubule formation and in equimolar amounts overcame the inhibitory effects of both natural (TIMP) and synthetic (GM6001) MMP-2 inhibitors.

Figure 6. Quantification of the effects of recombinant BSP on tubule formation and in overcoming the effects of MMP-2 inhibitors. Two distinct fields from each triplicate well of the experimental conditions described were digitized as TIFF files and analyzed using AngioSys Ver. 1.0 software (TCS Cell Works, Buckingham UK). The image analysis package determined the number of tubules (A), the number of branch points or junctions (B) between tubules, as well as the total tubule length in pixels (C). In each case BSP stimulated the angiogenesis parameters even in the presence of the normally inhibitory effect of both natural (TIMP) and synthetic (GM6001) MMP-2 protease inhibitors. In addition a cell surface-associated pool from day 10 cohort cultures was assayed for MMP activity by the large fluorescein-gelatin substrate assay (D) and by zymography (E). Note that BSP caused increased cell surface accumulation of MMP-2 activity in the presence and absence of inhibitors. C, control, B, BSP; T, TIMP2; T+B, TIMP2 + BSP: G, GM6001; G+B, GM6001 + BSP. The region of the zymogram corresponding to active MMP-2 is shown.

TABLES

Table I. BSP & MMP-2 kinetic values.

	K_m	V_{max}	K_{ic}	K_{iu}	
mMMP2	96 ± 13	0.20 ± 0.01			
mMMP2+BSP	59 ± 14	0.18 ± 0.02			
MMP2	103 ± 14	$1.9 \quad 0.1$			
MMP2+BSP	90 ± 10	2.1 ± 2			
MMP2+TIMP2	103 ± 9	1.9 ± 0.8	0.67 ± 0.06 (0.45 ± 0.03)	1.4 ± 0.2 (0.19 ± 0.02)	
[MMP2+BSP]+TIMP2	127 ± 18	2.1 ± 0.2	24 ± 12 (20 ± 9)	7 ± 1 (9 ± 4)	
MMP2+TIMP2+BSP	98 ± 14	1.8 ± 0.1	10 ± 3 (13 ± 3)	9 ± 2 (10 ± 3)	
MMP2+GM6001	100 ± 23	1.8 ± 0.2	0.13 ± 0.03		
MMP2+BSP+GM6001	85 ± 10	1.5 ± 0.1	14 ± 4		

For the small molecular weight substrate peptide substrate, K_m values are µM and for TIMP2 and illomastat the K_I values are nM. Abreviations: mMMP2, mutant hemopexin-deleted MMP-2; BSP, bone sialoprotein; TIMP2, tissue inhibitor of matrix metalloproteinase-2; GM6001, illomastat. K_{ic} and K_{iu} values were determined by fitting the generalized linear mixed inhibition equation and K_I values determined using the equation for competitive inhibition.

FOOTNOTES

[1] The abbreviations used are: SIBLING, Small, Integrin-Binding LIgand, N-linked Glycoprotein; BSP, bone sialoprotein; MMP, matrix metalloproteinase; proMMP, pro-matrix metalloproteinase; TIMP, tissue inhibitor of matrix metalloproteinase; TBS, Tris buffered saline; HRP, horse radish peroxidase; r, binding function; C_S, total ligand concentration; C_A total acceptor concentration; f_a, fractional acceptor saturation.

Figure 1

A. control   B. +GM6001   C. +TIMP2

D. +BSP   E. +GM6001+BSP   F. +TIMP2+BSP

A.

tubules

400

300

200

100

0

C B T T+B G G+B

B.

branches

200

150

100

50

0

C B T T+B G G+B

C.

total tubule length

8000

6000

4000

2000

0

C B T T+B G G+B

D.

fluorescein-gelatin digestion/min

440

330

220

110

0

C B T T+B G G+B

E.

zymogram band intensity

160

120

80

40

0

C B T T+B G G+B
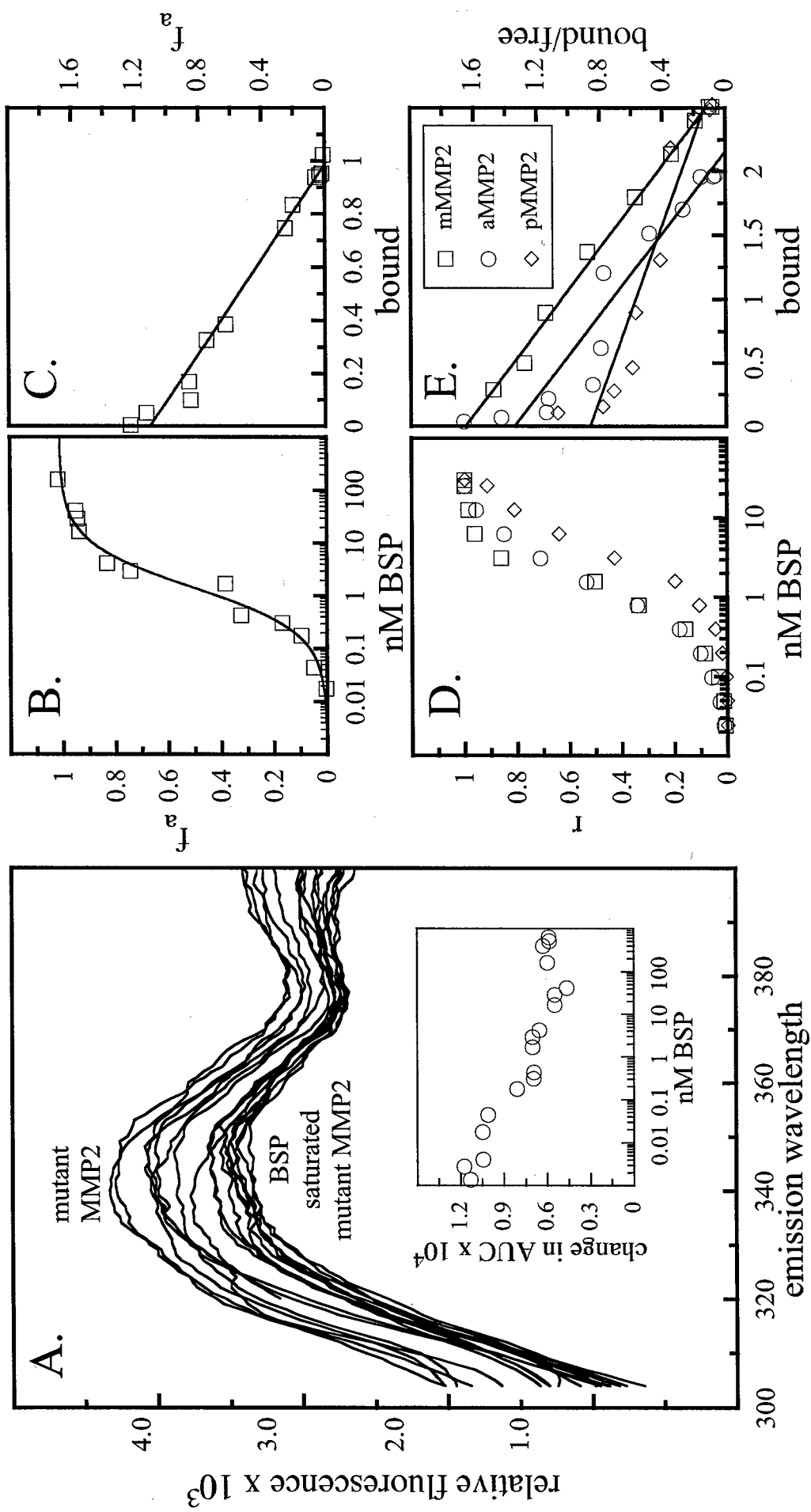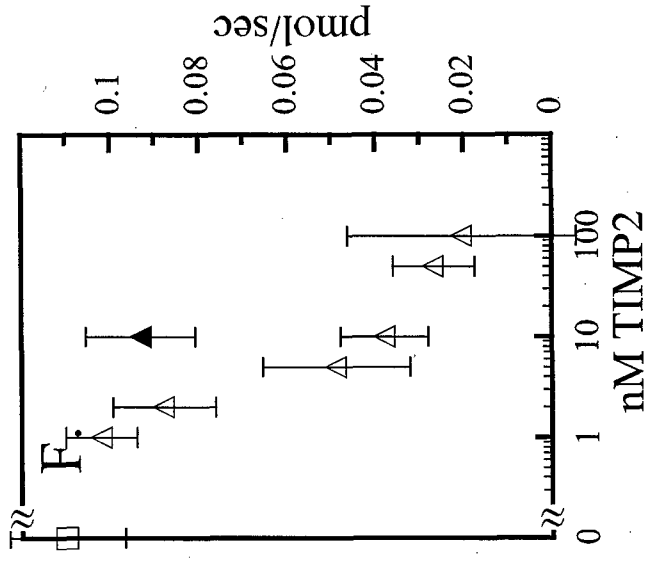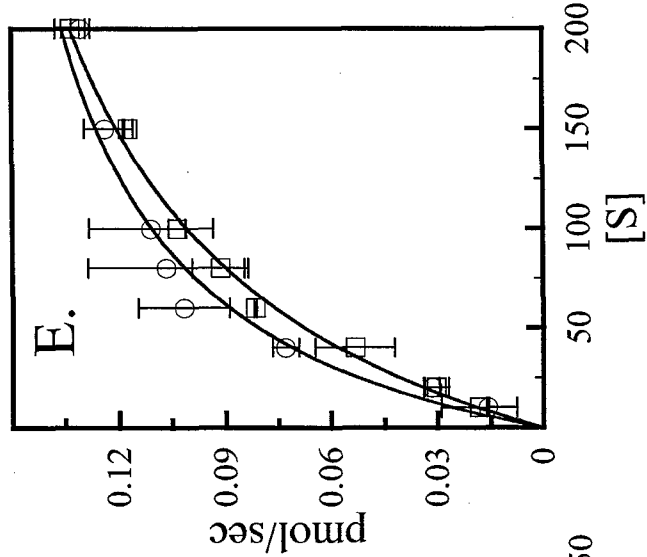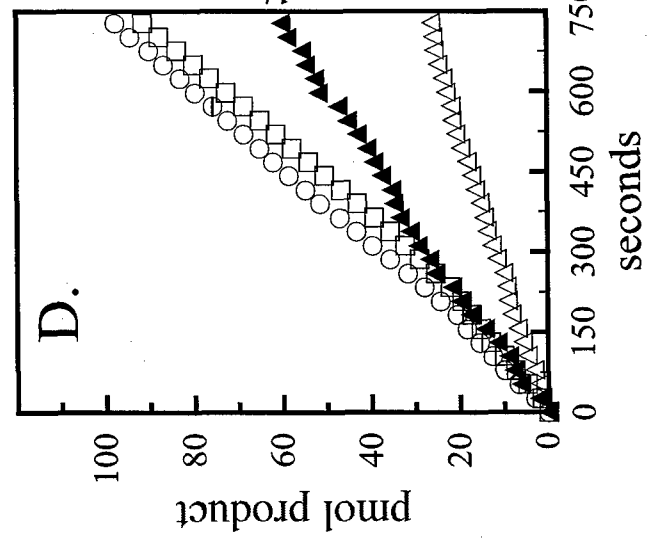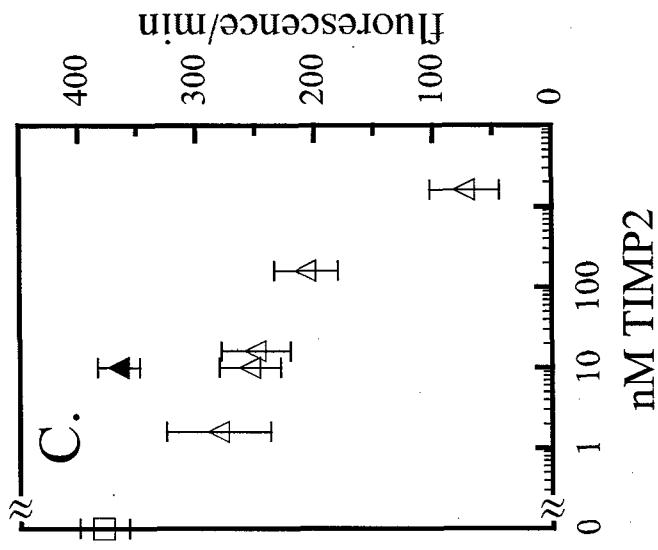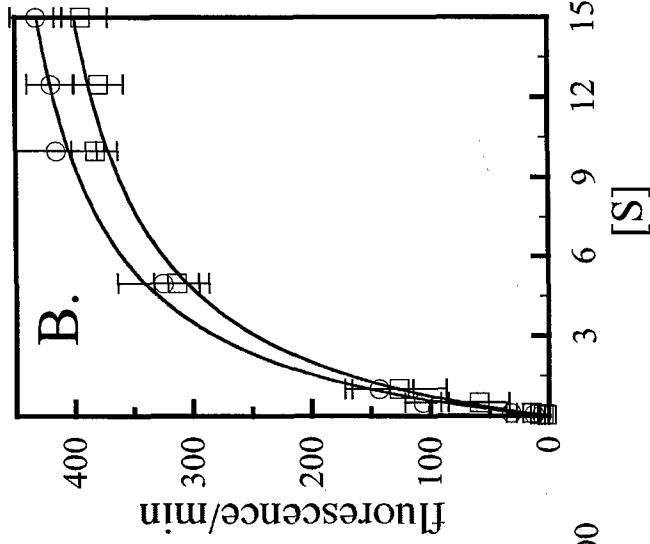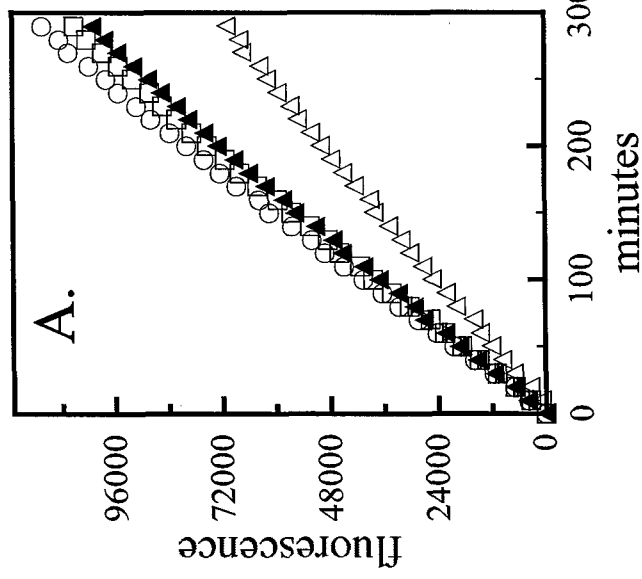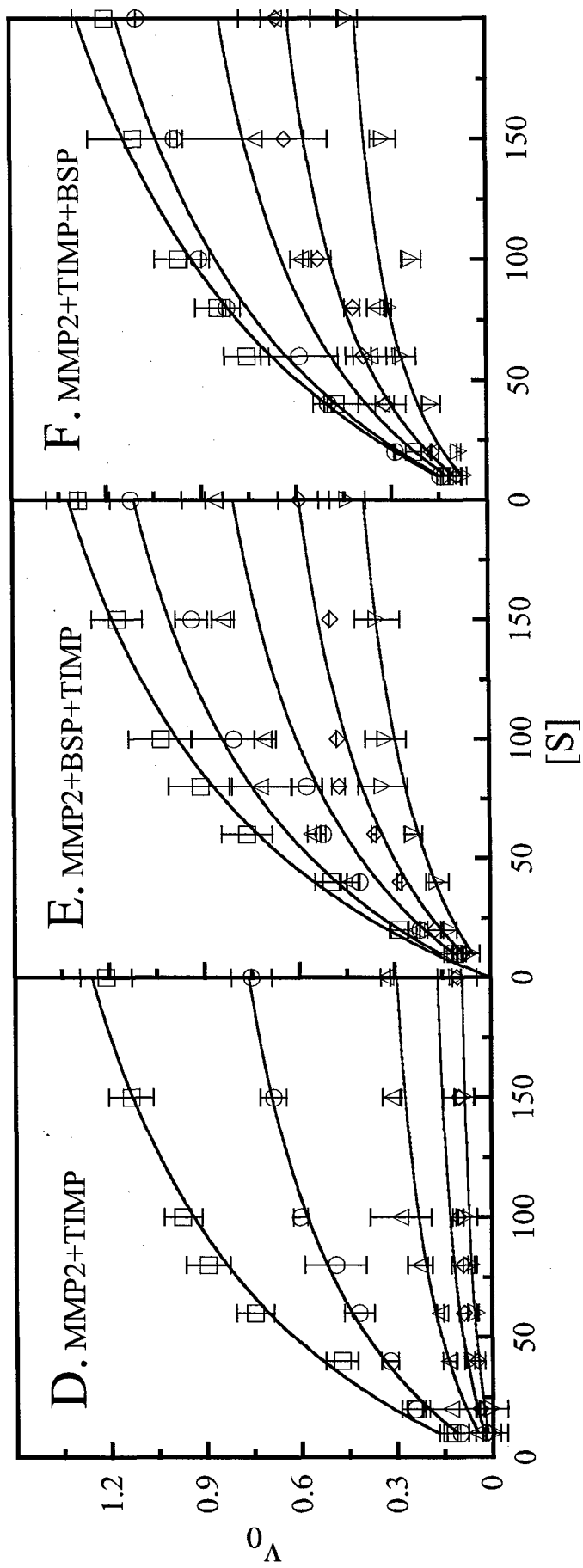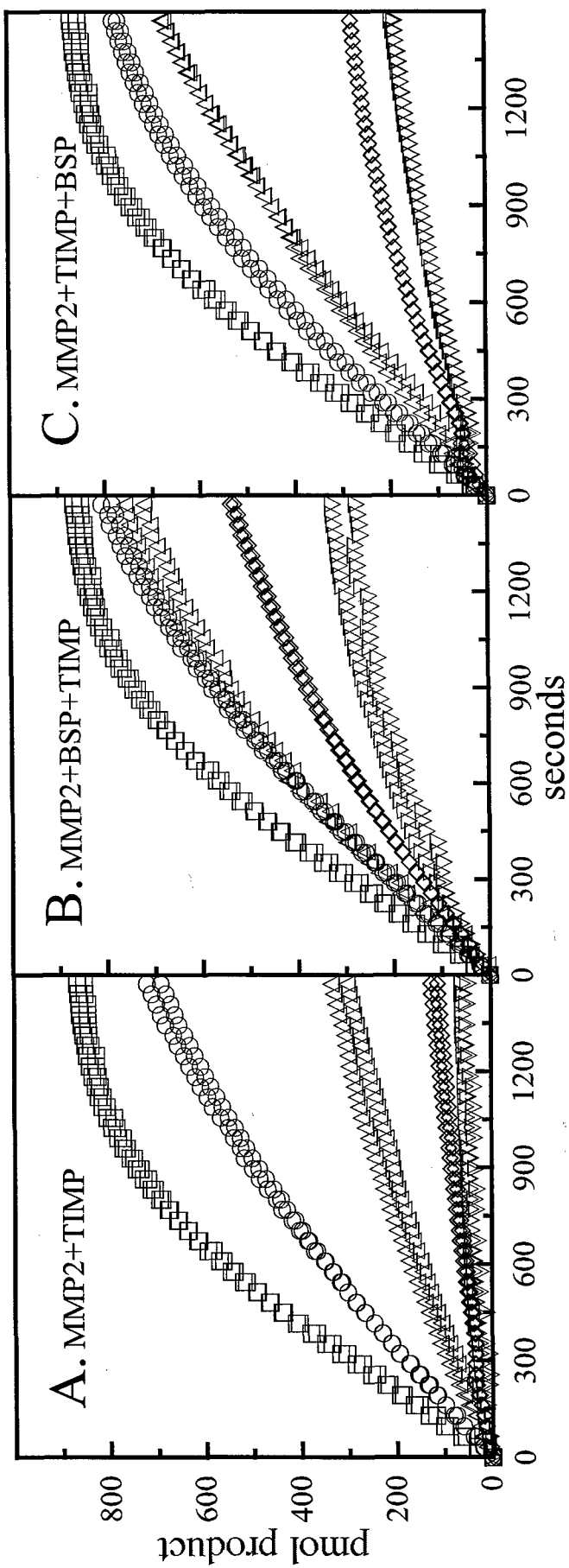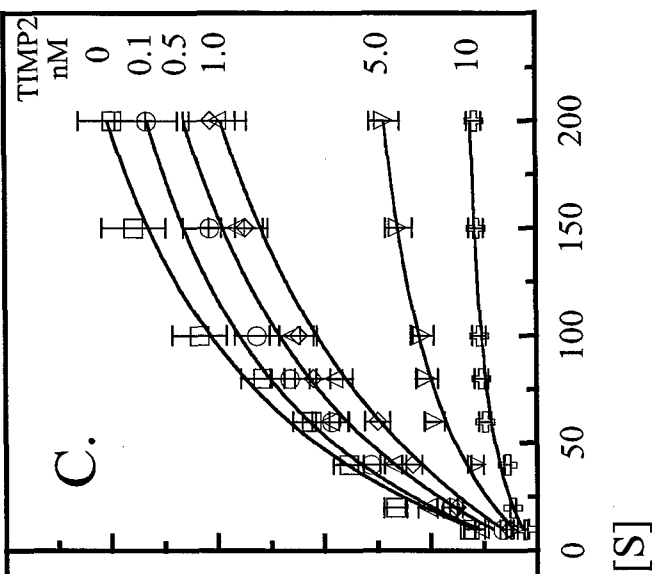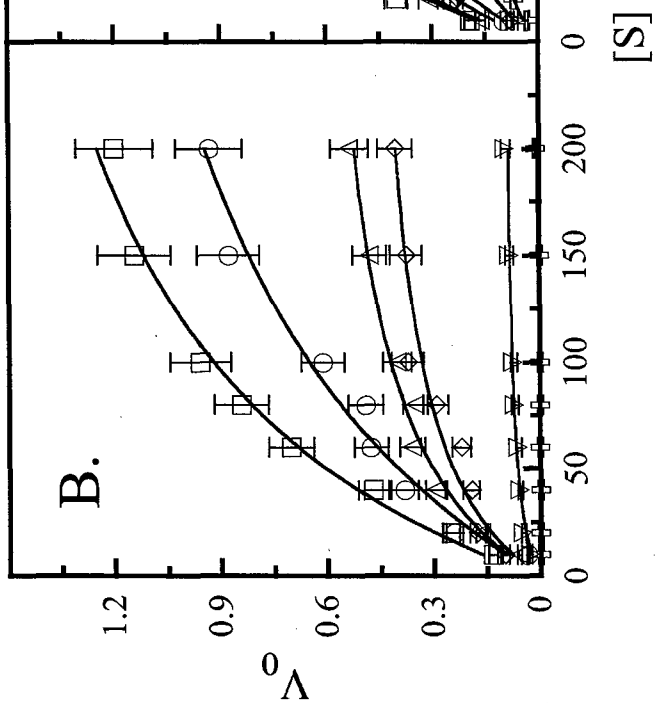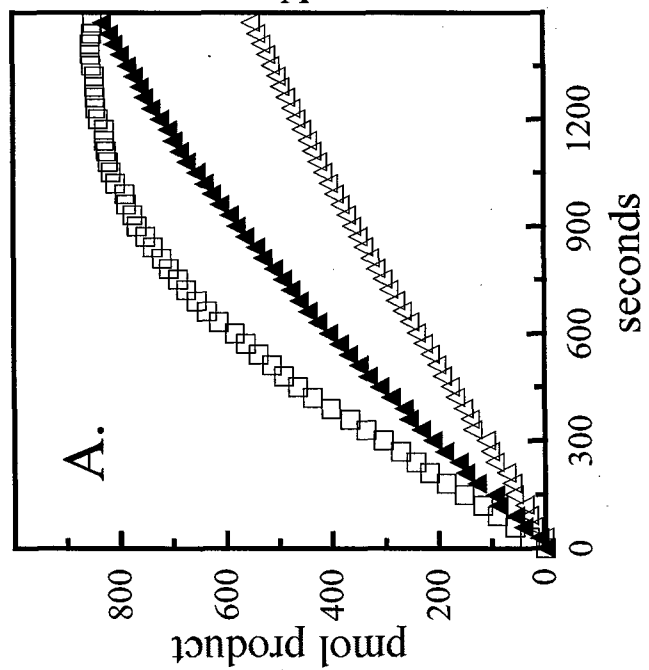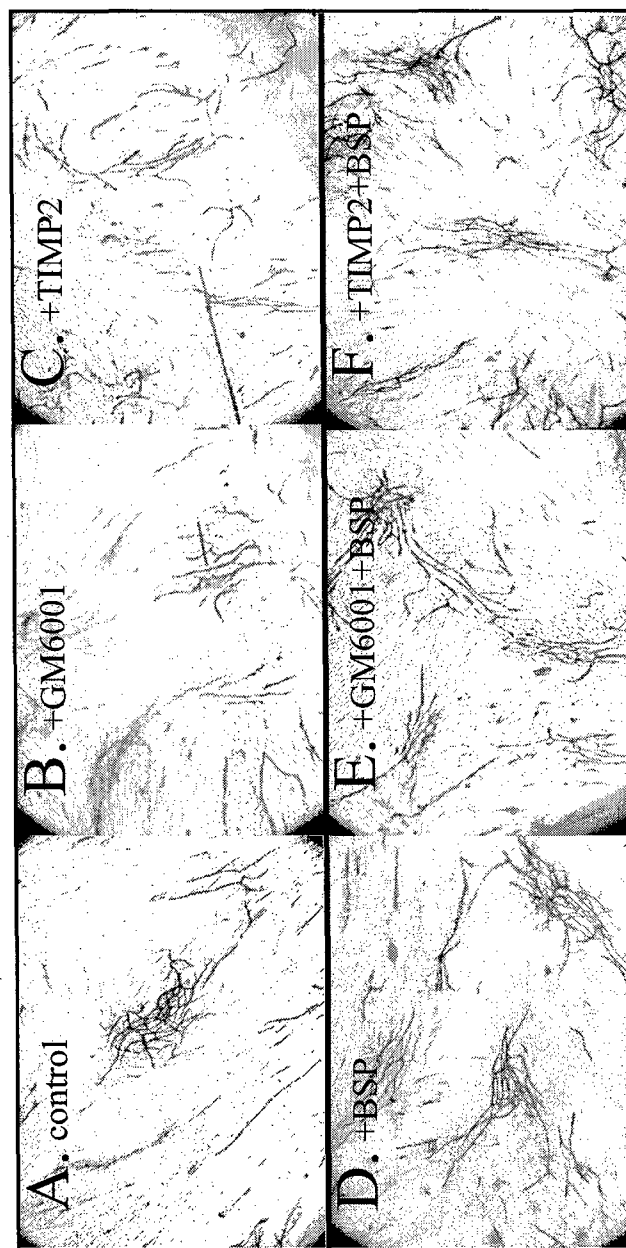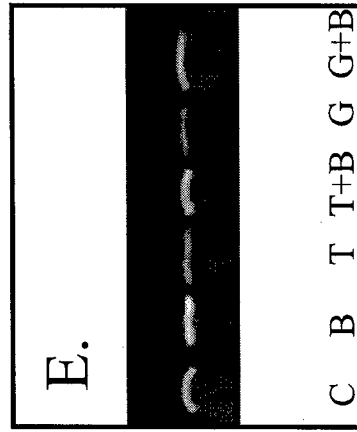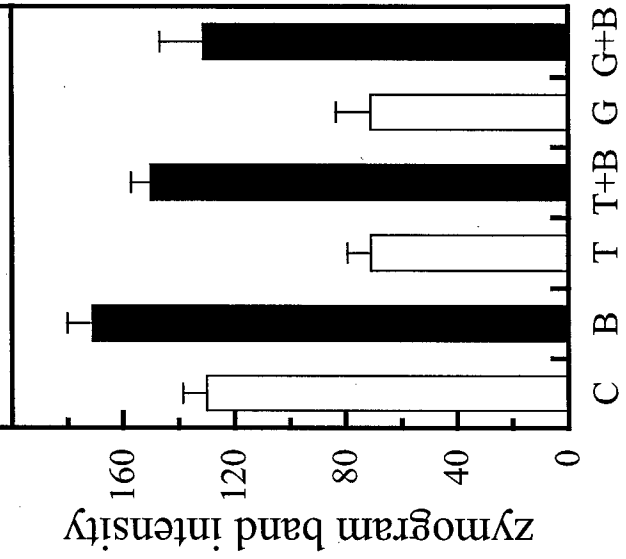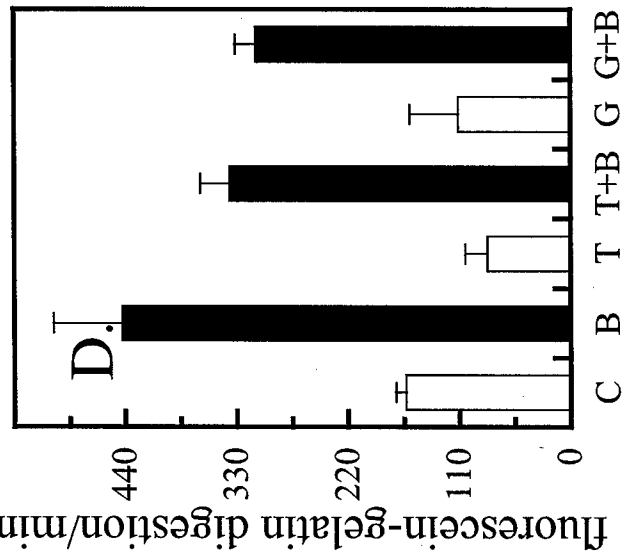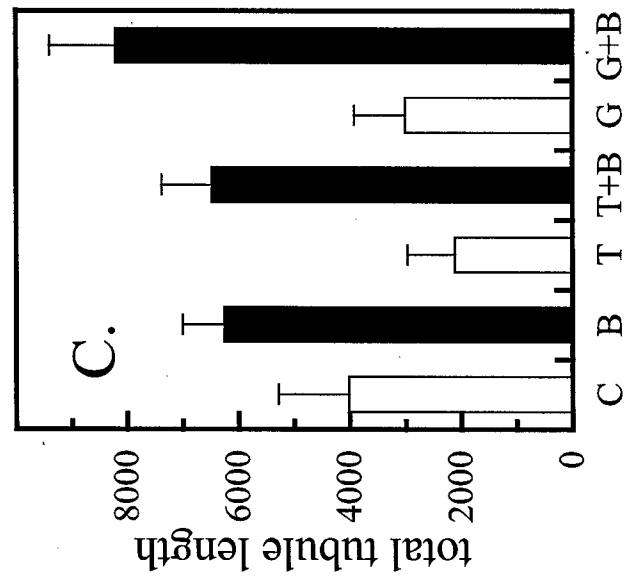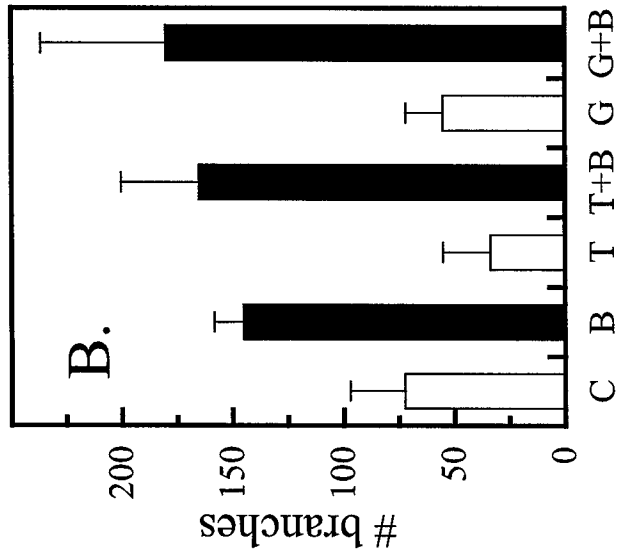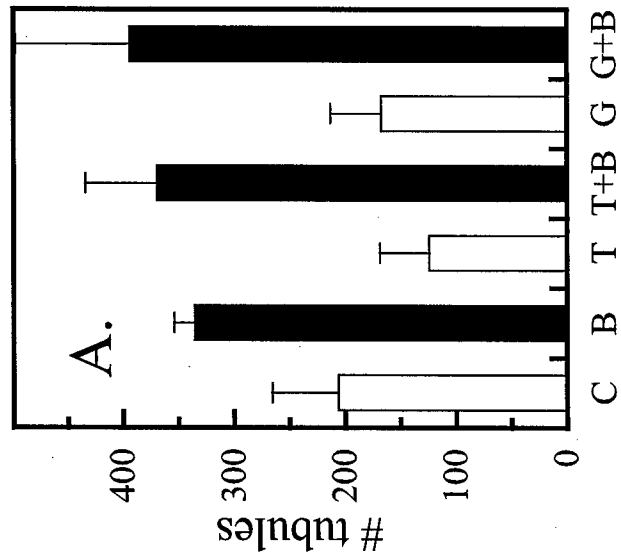
APPENDIX V

Era of Hope 2005 Department of Defense Breast Cancer Research Program Meeting. June 8th – 11th, 2005, Philadelphia, PA.

SMALL INTEGRIN BINDING LIGAND N-LINKED GLYCOPROTEINS (SIBLINGS) BIND AND ACTIVATE MATRIX METALLOPROTEINASES.

Alka Jain[*], Larry W. Fisher[#], and Neal S. Fedarko[*]
[*] Division of Geriatric Medicine, Department of Medicine, Johns Hopkins University,
[#] National Institutes of Health, DHHS, Bethesda, MD.

Matrix metalloproteinases (MMPs) are critical for development, wound healing, and for the progression of cancer. MMPs are generally accepted to be secreted in a latent form and to be activated only upon removal of their inhibitory propeptides. We have been studying a gene family we term SIBLINGs (for Small Integrin-Binding Ligand N-linked Glycoproteins) that are induced by certain neoplasms. Members of the SIBLING family include bone sialoprotein (BSP), osteopontin (OPN), dentin matrix protein (DMP1), dentin sialophosphoprotein, and matrix extracellular phosphoglycoprotein. Our published work has shown that BSP and OPN are extended and flexible in solution (such lack of ordered structure is shared by a number proteins that have multiple binding partners). SIBLINGs can bind integrins including αVβ3 via their RGD sequence. OPN and DMP1 can also bind CD44 (via an amino terminal domain). SIBLINGs can bind to complement Factor H and sequester it to the cell surface thereby regulating complement-mediated cell lysis. More recently we have investigated the ability of SIBLINGs to bind to and modulate the activity of specific MMPs.

Three members of the SIBLING family (BSP, OPN and DMP1) were able to specifically bind (Kd≈nM) three different MMPs. BSP specifically bound to pro- and active MMP-2, while OPN bound to pro- and active MMP-3, and DMP1 bound pro- and active MMP-9. Binding was demonstrated by: 1) co-purification of the pairs through nondenaturing chromatographic columns; 2) solution phase intrinsic fluorescence binding studies; and 3) showing that BSP and OPN affinity columns can be used to purify MMP-2 and MMP-3, respectively, from media containing several MMPs. Binding of SIBLING to their corresponding proMMPs was associated with structural changes as indicated by: 1) fluorescent quenching during SIBLING binding titration (indicating a change in the microenvironment of the MMP's tryptophans); 2) increased susceptibility of proMMP-SIBLING pairs to plasmin digestion; 3) increased enzymatic activity of the pro-MMPs upon binding their specific SIBLING partner; 4) reduced ability of specific low molecular weight inhibitors to block SIBLING + MMP complexes; and 5) restoration of activity to TIMP-inhibited MMPs by the corresponding SIBLING.

SIBLING expression has been correlated with cancer progression and severity and it is interesting to consider that these proteins may be locally activating their corresponding proteases in vivo. Perhaps most significantly (from a clinical standpoint) SIBLINGs were found to restore activity to propeptide-free MMPs whose activity had been blocked by both natural and synthetic inhibitors. SIBLINGs are induced by neoplasms in vivo and their modulation of MMP activity might contribute to the relative lack of efficacy seen in the recent clinical trials of MMP inhibitors.

APPENDIX VI

Era of Hope 2005 Department of Defense Breast Cancer Research Program Meeting. June 8th – 11th, 2005, Philadelphia, PA.

SMALL INTEGRIN BINDING LIGAND N-LINKED GLYCOPROTEIN (SIBLING) GENE FAMILY EXPRESSION IN BREAST CANCER.

Alka Jain[*], Larry W. Fisher[#], and Neal S. Fedarko[*]
[*] Department of Medicine, Johns Hopkins University, Baltimore, MD 21224 and [#]National Institutes of Health, DHHS, Bethesda, MD.

We have recently shown that members of the SIBLING (Small Integrin Binding Ligand N-linked Glycoprotein) gene family have the capacity to bind and modulate the activity of matrix metalloproteinases (MMPs). MMPs play critical roles in tumor progression and metastasis. A systematic study of SIBLING and MMP expression by tumors was undertaken. The expression levels of five SIBLING gene family members - bone sialoprotein (BSP), osteopontin (OPN), dentin matrix protein (DMP1), matrix extracellular phosphoglycoprotein (MEPE), and dentin sialophosphoprotein (DSPP) as well as certain MMPs were determined using a cancer profiling array that contained normalized cDNA from both tumor and corresponding normal tissues from 53 individual patients.

Significantly elevated SIBLING family expression was observed in breast cancer where all SIBLINGs but MEPE were increased. Given the observed binding and activation specificity seen with SIBLINGs and their partner MMPs (BSP with MMP-2, OPN with MMP-3, and DMP1 with MMP-9, it was reasonable to postulate that SIBLINGs and their paired MMPs might exhibit correlated expression levels. When the levels of SIBLING and matched MMP expressed by individual tumors were analyzed by regression analysis, significant correlation was seen for the expression of BSP and MMP-2 ($r^2 = 0.40$, $p \leq 0.0001$) and OPN pairing with MMP-3 ($r^2 = 0.28$, $p \leq 0.0001$). SIBLING expression levels in breast cancer tissue were segregated by subtypes of either ductal or lobular tumors and the average values of each group compared. SIBLING mRNA levels were significantly higher in the ductal cancer groups, while the levels in the lobular group were intermediate between normal and ductal levels. The ductal versus lobular subtypes correspond to disease entities that differ in tumor size, shape, dissemination and proliferation rates.

The association of SIBLING expression levels with tumor progression was investigated by stratifying breast cancer tumors into TNM stages, which reflect tumor size (T), lymph node involvement (N), and metastatic state (M). The sequence of tumors ranged from those with no nodal involvement or metastasis state (N0M0), but that increased in size (from T1 to T2 to T3) as well as N1M0 tumors that increased in size. For BSP, OPN, DMP1 and DSPP significant differences were observed for the expression pattern as a function of tumor progression when analyzed by nonparametric ANOVA. Regression analysis of SIBLING values and TNM stage yielded significant correlation for all four SIBLINGs. SIBLING expression correlated with tumor stages associated with changing size and lymph node involvement. These results suggest SIBLINGs possess biological plausibility to be playing a role in early disease progression in breast cancer.

SMALL INTEGRIN BINDING LIGAND N-LINKED GLYCOPROTEINS MODULATE MATRIX METALLOPROTEINASES AND ANGIOGENESIS.

N. Fedarko[*], L.W. Fisher[#], A. Jain[*].
[*] Department of Medicine, Johns Hopkins University, Baltimore, MD 21224 and [#]National Institutes of Health, DHHS, Bethesda, MD.

Tumor progression involves modulation of cell adhesion, differentiation, division, apoptosis, angiogenesis as well as migration and metastasis. We have been studying a gene family we term SIBLINGs (for Small Integrin-Binding Ligand N-linked Glycoproteins) that are induced in breast cancer and have the capacity to bind to and modulate the activity of matrix metalloproteinases (MMPs). Members of the SIBLING family include bone sialoprotein (BSP), osteopontin (OPN), dentin matrix protein (DMP1), dentin sialophosphoprotein, and matrix extracellular phosphoglycoprotein.

It is our hypothesis that SIBLINGs promote cancer progression through neoplastic expression of SIBLINGs that bind to and modulate the activity of specific MMPs. MMPs play multiple roles in tumor progression including: angiogenesis; processing and presentation of certain growth factors; and metastasis. We have tested the hypothesis with both in vitro and in vivo models.

Angiogenesis was investigated in vitro using human umbilical vein endothelial cells that proliferate, migrate, and form a network of anastomosing tubules resembling a capillary bed. BSP, OPN and DMP1 stimulated tubule formation and increased the length and branching of the tubules equal to or greater than the positive control, basic fibroblast growth factor. The KAE variants of OPN and BSP (whose integrin-binding RGD sequence had been mutated to the inactive tripeptide, KAE) exhibited less tubule formation. Incubation of cells with synthetic, low molecular weight inhibitors of MMPs significantly reduced tubule formation, while the inclusion of SIBLING with MMP-specific inhibitors restored a degree of tubule formation. Angiogenesis was investigated in vivo using the chick embryo chorioallantoic membrane (CAM) system The CAM is an extra-embryonic membrane formed on day 4 of incubation by fusion of the chorion and the allantois. It has a very thick capillary network that forms a continuous surface in direct contact with the shell. The CAM model was used to test the effect of BSP and OPN on capillary formation A radially arranged "spoke-wheel" pattern was present around BSP, OPN, DMP1 and basic fibroblast growth factor rings, whereas no vascular response was observed in either control (vehicle treated) or mutant KAE-SIBLINGs.

The observed effects of SIBLINGs, as well as their KAE variants, are consistent with SIBLINGs modulating MMP activity. Thus, SIBLINGs have biochemical and biological plausibility to be playing active roles in tumor progression in vivo.